



SOLAR-HYDROGEN POWERED PROTON EXCHANGE MEMBRANE FUEL CELL (PEMFC) MODELING AND SIMULATION

A dissertation submitted to the
Department of Electrical Engineering, University of Moratuwa
In partial fulfillment of the requirements for the
Degree of Master of Science

by
Sekarage Roshan Wickremaarachchi

Supervised by: Prof. Lanka Udawatta
Eng. Anura Wijayapala.

Department of Electrical Engineering
University of Moratuwa
Sri Lanka

2010

94543



Abstract

The main scope of this study provides a research insight on direct solar Hydrogen-proton exchange membrane fuel cell concept and the description of fuel cell operating principles is followed by a modeling and simulation of the current fuel cell technology together with issues concerning Hydrogen fuel. Appropriate applications for current and perceived potential advances of fuel cell technology are discussed.

Fuel cell modeling is helpful for fuel cell developers because it can lead to fuel cell design improvements, as well as, better, and more efficient fuel cells. The model must be robust and accurate and be able to provide solutions to fuel cell problems quickly. A good model should predict fuel cell performance under a wide range of fuel cell operating conditions. Even a modest fuel cell model will have large predictive power. The necessary improvements for fuel cell performance and operation demand better design, materials, and optimization. These issues can only be addressed if realistic mathematical process models are available.

Fuel cells are one of the cleanest and most efficient technologies for generating electricity. Since there is no combustion, there are none of the pollutants commonly produced by boilers and furnaces. For systems designed to consume hydrogen directly, the only products are electricity, water and heat. Fuel cells are an important technology for a potentially wide variety of applications including on-site electric power for households and commercial buildings; supplemental or auxiliary power to support car, truck and aircraft systems; power for personal, mass and commercial transportation; and the modular addition by utilities of new power generation closely tailored to meet growth in power consumption. These applications will be in a large number of industries worldwide.

The theoretical development of the proton exchange membrane fuel cell (PEMFC) is discussed with the areas under electro chemistry, thermal distribution, and pressure. The particular simulations and modeling are discussed by using modeling software.

DECLARATION

The work submitted in this dissertation is the result of my own investigation, except where otherwise stated.

It has not already been accepted for any degree, and is also not being concurrently submitted for any other degree

UOM Verified Signature

 Sekarage Roshan Wickremaarachchi
16 December 2009

tuwa, Sri Lanka.
Electronic Theses & Dissertations
www.ho.mrt.ac.lk

We/I endorse the declaration by the candidate.

UOM Verified Signature

Prof.Lanka Udawatta

Eng. Anura wijayapala.

CONTENTS

Declaration	i
Abstract	iv
Acknowledgement (optional)	v
List of Figures	vi
List of Tables	viii
List of Principal abbreviations	ix
1. Introduction	1
1.1 Motivation	2
1.2 Goals/Scope of the Fuel cell Concept	4
1.3 World energy demand	5
1.4 Vision of H ₂ Clean energy economy based on renewable in Combinations	7
1.5 What is Hydrogen Fuel	8
1.6 Physical and Chemical properties of H ₂	8
1.7 How is H ₂ produced	9
1.7.1 Reformation of natural Gas	9
1.7.2 Bio mass Gasification	9
1.7.3 Coal Gasification	9
1.7.4 Carbon Black and Hydrogen Process	10
1.7.5 Electrolysis of Water	10
1.8 PEM based Electrolyzer	10
1.9 History of FC	11
1.10 Hydrogen Fuelled PEM fuel cell applications	12
1.10.1 Transportation	13
1.10.2 under water applications	15
1.10.3 Distributed power generation	15
1.10.4 Residential Power	15
1.10.5 Portable power	16
2. Regenerative Fuel cell Systems explained	17
2.1 Introduction to the PEMFC	17
2.2 Types of Fuel cells	19
2.1.1 Polymer Exchange membrane Fuel Cell (PEMFC)	19
2.1.2 Alkaline Fuel Cell (AFC)	19
2.1.3 Phosphoric Acid Fuel Cell (PAFC)	20
2.1.4 Solid Oxide Fuel Cell (SOFC)	20
2.1.5 Molten Carbonate Fuel Cell (MCFC)	20
2.1.6 Direct Methanol Fuel Cell (DMFC)	17
2.3 Structure of the Fuel cell	21
2.3.1 Electrode Layer	21
2.3.2 Gas diffusion Layer	21
2.3.3 Catalyst Layer	21
2.3.4 Bipolar Plates	21

2.4 Structure of the polymer electrolyte	22
2.5 Water Management in the PEMFC	24
2.5.1 Over View of the Problem	24
2.5.2 Air flow and water evaporation	24
2.6 Operating Pressure of FC	26
2.6.1 Outline of the Problem	26
3. Theoretical Development of Fuel cell Electro-Chemistry	27
3.1 Mathematical model of Fuel cell in the literature	27
3.1.1 Creating Mathematical Models	29
3.2 Fuel cell electrochemistry	31
3.2.1 Introduction	31
3.2.2 Basic electro kinetic Concepts	31
3.2.3 The voltage loss for the polarization curve	32
3.2.4 Modeling the catalyst Layer	35
3.2.5 The ohmic voltage loss	40
4. Modeling of PEM Fuel cell Heat and Pressure	42
4.1 Fuel cell thermodynamics	42
4.1.1 Entropy of Hydrogen oxygen and water in the PEM fuel cell	42
4.2 Heat transfer of Fuel cell	43
4.3 Energy balance for Fuel Cell Layers	44
4.4 Modeling the temperature in the Interior layer and Gas diffusion layer.	48
4.5 Pressure Drop in Flow Channels	50
5. PEM Fuel cell Special Features	52
5.1 Compression between batteries and fuel cells for Photovoltaic system backups	52
5.2 Efficiency and hydrogen consumption efficiency	53
5.3 Efficiency and fuel cell voltage	55
5.4 Why is the efficiency of PEMFC not 100%	56
5.6 Implementation of PEMFC system	55
5.6.1 Solar hydrogen Fuel cell system for a Home	55
5.6.2 PEMFC stack principle	58
5.6.2 Solar Hydrogen Fuel cell Basic model	59
5.6.3 Fuel cell Concept Model vehicle	60
6. Conclusions	62
References	66
Appendix A GDL (gas diffusion layer) Modeling	68
Appendix B Useful Fuel Cell Equations	73
Appendix C modeling and simulation MatLab Programs	75

Acknowledgement

The undergraduate and postgraduate studies at Anna University in India and Katubedda University in Srilanka respectively were a specific condition for me to proceed with an useful research study of this type. Similarly the course materials of the study program were also helpful to make a successful access to this research study in Industrial Automation.

Most importantly, Close supervision and guidance enriched the movement in positive direction in line with the research proposal from the very start, without any complication although the said research study, to a certain extent was a difficult task. But because of the regular instructions and guidences of supervisor; Professor Lanka Uduwatta and Eng.Anura Wijepala. It was possible for me to overcome the confronted barriers without any much effort.

In this direction, Professor. Lanak Udawatta and Eng.Anura Wijepala offered some unlimited discussions and sessions without considering the time factor, which in return created some friendly environment to sort out the relevant studies for the research.

Faculty of Engineering of University of Moratuwa, is categorically responsible for this academic research study. Contributions offered such like communication over the issues, unconditional access to any clarification, and instant guidance by the Electrical Engineering department are not that simple as far as the completion part of this research study is concerned.

This study demanded many sources and relevant material which were readily available firstly in library of Katubedda University which paved direction to mark the area of research proposal.

Lastly, I should thank many individuals, friends and colleagues who have not been mentioned here personally in making this educational process a success. May be I could not have made it without your supports.

List of Figures

Figure	Page	
1.1	Illustrates wind, solar and hydroelectric power.	3
1.2	Energy Consumption	5
1.3	Primary energy demand by region,(% AAGR is for 1980–2030)	6
1.4	World electricity generation by fuel	6
1.5	Percent average annual growth rate (%AAGR)	7
1.6	Hydrogen Production Pathways	9
1.7	Electrical power from renewable energy sources.	10
1.8	A simplified diagram of the PEM electrolyzer	11
1.9	The principle of an electrolyzer.	11
1.10	Two prototype automobiles powered by fuel cells	13
1.11	Fuel cell bicycle	13
1.12	Fuel cell air craft	13
1.13	Assemble alkaline fuel cells for Apollo space craft	14
1.14	Fuel cell Boat	14
1.15	Fuel cell powered mining vehicle	14
1.16	A fuel-cell distributed power plant	15
1.17	A fuel-cell power plant for residential applications	16
1.18	Fuel cell portable applications	16
2.1	Structure of Fuel Cell	18
2.2	Fuel Cell Structural reactions	19
2.3	The construction of anode/electrolyte/cathode assembly	21
2.4	Compacted Single cell PEMFC	22
2.5	Structure of polyethylene	22
2.6	Structure of PTFE	23
2.7	structure of a sulphonated fluoroethylene	23
2.8	The structure of Nafion-type membrane materials	23
2.9	The different water movements to, within, and from the electrolyte of a PEM fuel cell	25
2.10	Simple motor driven air compressor and PEM fuel cell.	26
3.1	Parameters that must be solved for in a mathematical model	28
3.2	Model-building sequence	30
3.3	Fuel cell electrochemical reactions at the electrolyte and electrode	31
3.4	A Polarization curve generated in MATLAB	34
3.4	B Power curve generated in MATLAB	34
3.5.	A Cell current as a function of effectiveness factor	38
3.5.	B Butler-Volmer activation losses	38
3.5.	C Polarization curve	39
3.5.	D Superficial flux density of Hydrogen	39

3.6	Ohmic loss as a function of fuel cell area	41
4.1	Hydrogen and Oxygen entropies as a function of temperature	43
4.2	Stack illustration for heat flow study	44
4.3	Fuel cell layer as a control volume	45
4.4	Temperature plots for $t = 60, 300,$ and 1000 sec using 7 slices per layer	47
4.5	The simplified geometry of GDL	48
4.6	3D Plot of Temperature in Interior layer	49
4.7	Temperature in Gas Diffusion Layer	49
5.1	The overall losses In PEMFC system	56
5.2	Solar hydrogen Fuel cell system for a Home	57
5.3	Fuel cell basic model	59
5.4	Fuel cell Concept car	60



University of Moratuwa, Sri Lanka.
 Electronic Theses & Dissertations
www.lib.mrt.ac.lk

List of Tables

Table	Page
1.1 Hydrogen density	8
1.2 Hydrogen Properties	8
1.3 Hydrogen density compared to other fuels	8
1.4 History of Fuel cell Development	12
3.1 Comparison of Recent Mathematical Models	29
3.2 Parameters for derivation	35
4.1 Material Properties Used for Heat Transfer Calculations	46
5.1 Efficiency and hydrogen consumption	53
5.2 Efficiency limits for PEMFC	55
5.3 The properties of the Fuel cell	57
5.4 Cost analysis of the Solar-Hydrogen FC system for a Home	58
5.5 PEMFC Experimental data	59



Electronic Theses & Dissertations
www.lib.mrt.ac.lk

List of Principal Abbreviations

DMFC	Direct methanol fuel cell
EMF	Electromotive force
HHV	Higher heating value
LHV	Lower heating value
MCFC	Molten carbonate (electrolyte) fuel cell
MEA	Membrane electrode assembly
MOSFET	Metal oxide semiconductor field-effect transistor
NASA	National Aeronautics and Space Administration
PAFC	Phosphoric acid (electrolyte) fuel cell
PEM	Proton exchange membrane or polymer electrolyte membrane – different names for the same thing which fortunately have the same abbreviation
PEMFC	Proton exchange membrane fuel cell or polymer electrolyte membrane fuel cell
PTFE	Polytetrafluoroethylene
SOFC	Solid oxide fuel cell
CB&H	Carbon Black & Hydrogen Process
GE	General Electric
AFC	Alkaline Fuel Cells
GDL	Gas Diffusion Layer
PV	Photovoltaic

University of Moratuwa, Sri Lanka.
Electronic Theses & Dissertations
www.lib.mrt.ac.lk

Chapter 1

Introduction

Hydrogen and Fuel cells are set to become the latest power solution of the future. The interest in hydrogen and fuel cells has increased during the past decade due to the fact that the use of fossil fuels for power has resulted in many negative consequences. Some of these include severe pollution, extensive mining of the world's resources and political control and domination of countries that have extensive resources. A new power source is needed that is energy efficient, has low pollutant emissions, and has an unlimited supply of fuel. Hydrogen and fuel cells are now closer to commercialization than ever, and they have the ability to fulfill all of the global power needs while meeting the efficacy and environmental expectations.

In today's energy supply system, electricity, gasoline, diesel fuel, and natural gas serve as energy carriers. These carriers are made by the conversion of primary energy sources, such as coal, petroleum, underground methane, and nuclear energy, into an energy form that is easily transported and delivered in a usable form to industrial, commercial, residential, and transportation end users. The sustainable energy supply system of the future features electricity and hydrogen as the dominant energy carriers [1]. Hydrogen would be produced from a very diverse base of primary energy feed stocks using the resources and processes that are most economical or consciously preferred. Methods to produce hydrogen from natural gas are well developed and account for over 95% of all hydrogen produced and 48% globally[2]. It is anticipated that hydrogen from natural gas can serve as a foundation to the world transition to a hydrogen energy economy.c.lk

Fuel cell technology is a new concept which is still under the research and developments. In such a situation scientists and developers are struggling to overcome the issues with fuel cells. PEM Fuel cell modeling is helpful for fuel cell developers because it can lead to fuel cell design improvements, as well as cheaper, better, and more efficient fuel cells. Electro chemical and thermal modeling in PEMFC is very essential for further development of FC technology. Fluid dynamic system is already modeled in previous researches.[3].The model must be robust and accurate and be able to provide solutions to fuel cell problems quickly. Electro chemical modeling can be found in previous researches for direct methanol fuel cell [4]. A good model should predict fuel cell performance under a wide range of fuel cell operating conditions. Even a modest fuel cell model will have large predictive power. A few important parameters to include in a fuel cell model are the cell, fuel and oxidant temperatures, the fuel or oxidant pressures, the cell potential, and the weight fraction of each reactant. The necessary improvements for fuel cell performance and operation demand better design, materials, and optimization. These issues can only be addressed if realistic mathematical process models are available. There are many published models for PEM fuel cells in the literature, but it is often a daunting task for a newcomer to the field to begin understanding the complexity of the current models.

1.1 Motivation

Fossil fuels are limited in supply, and are located in select regions throughout the world. This leads to regional conflicts and wars which threaten peace. The limited supply and large demand will cause the cost of fossil fuels to continue to increase. Therefore, the end of low cost oil is rapidly approaching. Fossil fuels are currently needed in order to sustain our current living conditions. However, by using them, people, plants and animals are suffering from the side effects of these fuels. Waste products from these fuels heat the earth's atmosphere and pollute the earth's air, water and ground. This results in decreased living conditions for all species of the earth. There are both economic and environmental reasons for developing alternative energy technologies.

A strong interest in alternative energy sources first occurred in the 1970's when crude oil was suddenly in short supply. Even though there still seemed to be plenty of fossil fuels left to mine it awakened the world to the fact that the supplies are limited and eventually will run out. During the past decade, there has been an increased interest in environmentally friendly and more efficient power production. This interest has rapidly expanded research in alternative fuels and power sources [5]. The reliance upon the combustion of fossil fuels has resulted in severe air pollution and extensive mining of the world's oil resources. In addition to being hazardous to our ecosystem, and the health of many species, the pollution is also changing the atmosphere of the world. This trend is called global warming, and will continue to become worse due to the increase in the combustion of fossil fuels for electricity due to the growing world population.

The world needs a power source that has low pollutant emissions, is energy-efficient, and has an unlimited supply of fuel for a rising world population. Many alternative energy technologies have been researched and developed. These include solar, wind, hydroelectric power, bio energy, geothermal energy as well as many others. Solar cells use the sun to generate electricity, wind power is obtained from the kinetic energy of the wind and bio energy is extracted from plants. There are also renewable energies that extract gas from biological waste and harness energy from ocean waves. Each of these alternative energy sources has its advantages and disadvantages and all are in varying stages of development.

It is advantageous for our earth and all of the species that inhabit it to be conscious of the energy that we are using. The Renewable Energy explores all of the basic renewable energy technologies such as wind, solar, electrolyzes and PEM fuel cell with a hydrogen storage system. This demonstrates how renewable energy can be transformed and utilized. These types of energy can be naturally replenished by our environment.

Today energy is used for three purposes, electricity, heat and movement (transportation). Most of the world's energy comes from fossil fuels like coal, oil and natural gas. Other sources like nuclear power and different renewable sources also supplies energy. Modern world is looking for a renewable energy system due to following facts.



Figures 1.1- Illustrate wind, solar and hydroelectric power.

1. Pollution:

The burning of fossil fuels pollutes. CO₂ is the most threatening emission creating the so called greenhouse effect causing global warming. Other emissions from fossil fuels like SO₂, NO_x, CO, PAH, Benzene, HC and more, also result in local pollution causing, smog, acid rain and affecting human health, especially in large cities.

2. Oil depletion:

Oil is the most important resource, fuelling our freedom to transport ourselves easily. Oil therefore is very valuable for those countries that produce it, and an increasing cost for those not. However, oil is not an inexhaustible resource. Several countries are facing higher cost of imported oil thus relying more on non domestic resources. At the same time oil production is about to peak, meaning that production will soon keep falling. To keep up the global progress and prosperity a change to a more sustainable and clean energy system is needed. A hydrogen and fuel cell holds the potential to create this future. Hydrogen is one of the most promising fuels in the future energy mix. There is no alternative fuel option available with the same advantages.

3. Clean:

When produced from renewable energy sources, hydrogen is the cleanest fuel we have at our disposal. When used in a combustion engine, hydrogen burns to produce only water vapor. The heat generated in this reaction is sufficient to produce levels of nitrogenous emissions that can be kept extremely low. When used in a fuel cell, hydrogen combines with oxygen to form water vapor. This reaction takes place at lower temperatures and so the only waste product from hydrogen fuelled fuel cell is water vapor. It is pure H₂O, safe enough to drink!

4. Safe:

Hydrogen is a fuel, and like any fuel it has high energy content. Its inherent safety is neither much greater nor much less than that of natural gas, gasoline or LPG for example. As long as appropriate safety procedures are followed, as they should with any fuel, hydrogen is indeed a safe fuel. Remember that hydrogen has been produced, transported and used in industry for over 100 years.

5. Multiple Sources:

One of hydrogen's greatest advantages as a fuel is that there are many ways to produce it, using both renewable and traditional energy sources.

6. Energy Security:

The relevance of hydrogen to energy security is that it can offer energy independence. Using hydrogen in conjunction with fuel cells empowers countries to invest in a sustainable energy infrastructure that is matched with their energy production capabilities and demands. In association with distributed generation, hydrogen fuel enables individual homes and communities to manage their own energy supply. This reduces dependence on energy infrastructures such as large-scale power stations, national grids, and long distance pipelines. This large scale infrastructure can be costly to secure, and expensive to maintain.

7. Environmental:

The long term environmental benefits of using hydrogen as a fuel are enormous. Hydrogen fuel produces few pollutants when burnt, and none at all when used in a fuel cell. Hydrogen is a carbon free fuel, and when produced using renewable energy, the whole energy system can become carbon neutral, or even carbon free. So, hydrogen fuel can contribute to reducing Green House Gas emissions and can reduce the production of many toxic pollutants.

8. Economic:

Hydrogen has been produced and used by industry for over a hundred years. The technology required to deploy wide scale availability of hydrogen fuel is available today. The speed to which these technologies are deployed will depend on the availability of vehicles that use hydrogen fuel. These vehicles are presently only produced in small numbers and as a result are inherently costly to manufacture. To aid with the transition to hydrogen and fuel cell vehicles, these technologies need to be able to integrate and compete with existing technologies which have had the benefit of many years of mass manufacturing and distribution.

1.2 Scope of the Fuel cell concept

The main scope in this provides a research on Hydrogen and proton exchange membrane fuel cell concept. A description of fuel cell operating principles is followed by a Modeling and Simulation of the current fuel cell technology together with issues concerning Hydrogen fuel. Appropriate applications for current and perceived potential advances of fuel cell technology are discussed. Current energy technologies in world, include fossil fuels such as coal, oil, gas, as well as the heat engine and batteries. Coal, oil and gas are foreseen to be in short supply in the near future, as the world population grows rapidly and the amount of fuel used increases. Some of the disadvantages of fossil fuels include: The major concept of this research to introduce renewable and sustainable energy solution to fulfill the following difficulties which arise from the fossil and rest fuels.

1. Non-renewable:

Fossil fuels are non-renewable resources that take millions of years to form. Therefore, once the reserves are depleted, there is no way to obtain more.

2. Pollution:

Carbon dioxide is emitted by fossils fuels which are the main contributor to the greenhouse effect. Coal gives off both carbon dioxide and sulphur dioxide and sulphur trioxide, which creates acid rain. The acid rain can lead to the destruction of forests, and the erosion of rock

and masonry structures. Crude oil has toxic chemicals that cause air pollution when combusted.

3. Destruction of land:

The mining of coal results in the destruction of land.

4. Dangerous:

The mining of coal is considered one of the most dangerous jobs in the world.

5. Plant location:

In order to burn enough fossil fuels to provide energy for the grid, trainloads of fuel are needed on a regular basis. Therefore, this means that the plants should be near fossil fuel reserves.

6. Oil spills:

Oil spills occur, and cause pollution and environmental hazards. They result in catastrophic effects on marine life for many years.

7. Politics:

Many of the countries that have oil reserves are politically unstable. Nations that do not have reserves and have oil dependence may seek to influence politics of those countries for their own advantage.

1.3 World's energy demand

The use of fossil fuels increased rapidly during the twentieth century, and has quadrupled since the 1970s. The global population consumes petroleum products at a rate 100,000 times greater than the rate that they are formed [2, 5]. China is currently the third largest consumer of oil, however, if a Chinese citizen consumed oil at the same rate as an American citizen, China would need 90 million barrels of oil per day to sustain its needs [2]. According to [5], the typical amount of oil produced in one day is about 80 million barrels.

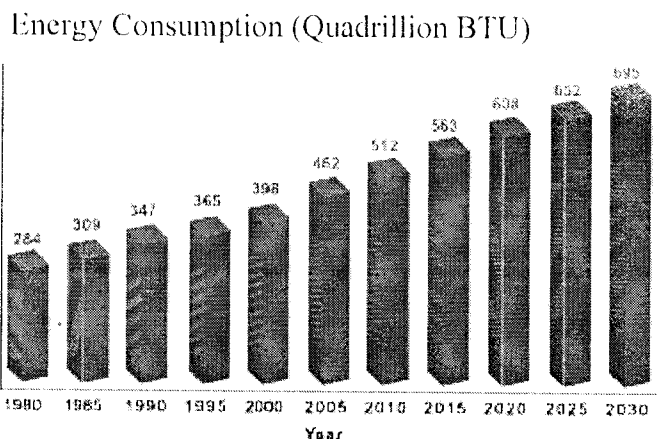


Figure 1.2- Energy Consumption

This figure shows the current and projected energy consumption from 1980–2030 [5]. International energy consumption is estimated to increase by 2.0 percent per year from 2003 to 2030. Total worldwide energy use grows from 421 quadrillion British thermal units (BTU) in 2003 to 563 quadrillion BTU in 2015 and 722 quadrillion BTU in 2030.

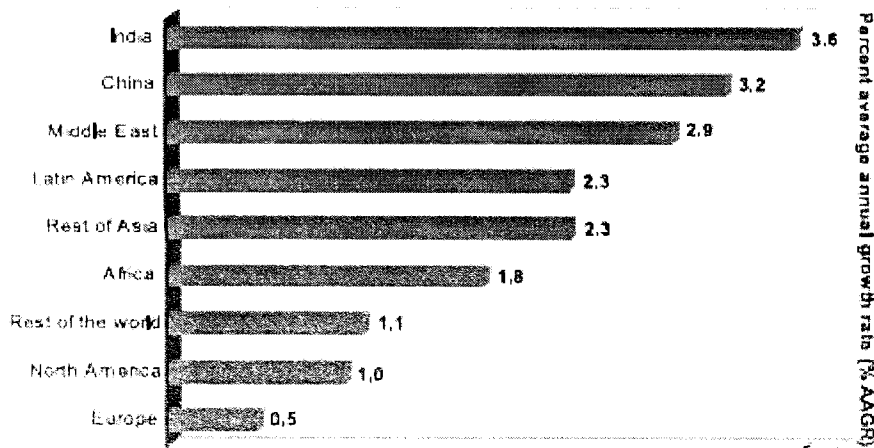


Figure 1.3- Primary energy demand by region, (% AAGR is for 1980–2030)

The most rapid growth in energy demand from 2003 to 2030 is projected for Asia, (including China and India), Central and South America, Africa, the Middle East, and Eurasia [6]. The energy requirements for these nations are increasing by 5.0 percent per year on average. The energy demand by region is shown in Figure 1.3. In every country, there are groups that support fossil fuel taxes in order to reduce the consumption of fossil fuels. There are also groups that are advocates of alternative energy technologies. Many experts are encouraging the reduction of fossil fuel use for industrialized countries, and are promoting the building of their infrastructure to adopt sustainable, renewable sources of power. Approximately 43% of the global population use oil as their primary means of obtaining energy. Natural gas follows with 15%, waste and combustible renewable account for 13%, coal has 8%, and alternative sources of energy (including geothermal, hydro and solar) the remaining 3% as illustrated in Figure 1.4.

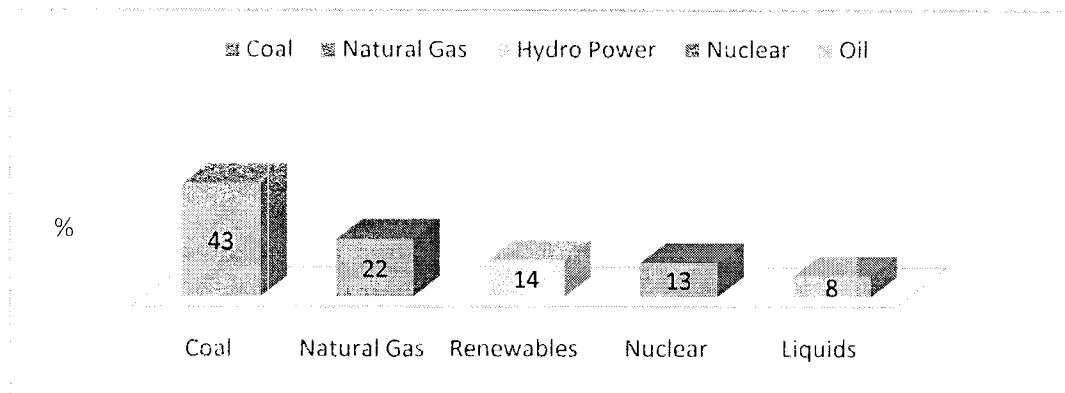


Figure 1.4- World electricity generation by fuel

During the 18th and 19th century, coal was the primary fuel used during the Industrial Revolution. After automobiles and household electricity became popular, oil became the primary fuel during the twentieth century. However, during the last few years, coal has become the fastest growing fossil fuel due to the increased consumption of fossil fuels in China. Although the renewable forms of energy currently have a small percentage of the total energy consumption, they have the highest average annual growth rate (AAGR) compared with all other energy forms as shown in Figure 1-5.

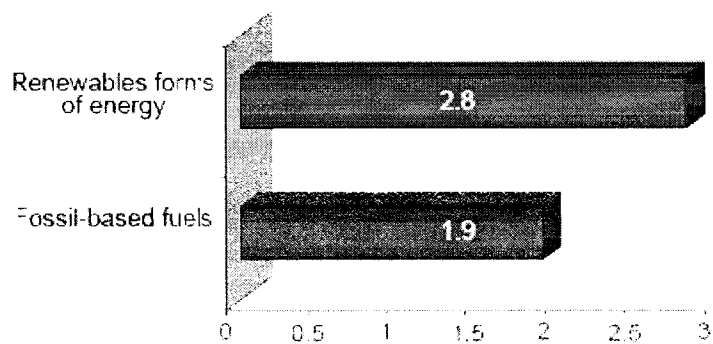


Figure 1.5- Percent average annual growth rate (%AAGR)

1.4 Vision of Hydrogen Clean Energy Economy Based on Renewable in Combination

Most of the current energy needs in the world are being met by fossil fuels. These fuels are easily obtained, stored, and transported because of the large amount of money that has been used to create, build, and maintain the system. Due to the current fuel distribution system, technology has advanced at a faster pace during the last two centuries than in all of recorded history. Despite all the advantages fossil fuels have provided for our society, it has also had negative effects on the environment, some of which likely has yet to be seen. Some of these harmful effects include air pollution due to acid rain emissions, water and soil pollution due to spills and leaks, and carbon dioxide accumulation in the atmosphere. These pollutants have the potential to warm the global atmosphere and kill many species.

In addition to the negative environmental consequences of using these fuels, there is a finite supply of fossil fuels that will inevitably force the use of another form of energy. The demand for energy will also continuously increase due to the constant increase of the global population. The future energy economy will consist of many renewable energy technologies used in combination. As far as fuels are concerned, hydrogen is one of the most powerful fuels. This is most evident with NASA space ships. The primary fuel that is used is hydrogen. Hydrogen is the most abundant element in the universe; however, it does not exist in its pure form on earth. Therefore, it has to be extracted from common fuel types or water. The process that is used most frequently for extracting hydrogen is by steam reforming natural gas. It can also be extracted from coal, nuclear power, bio fuels or even waste products.

Hydrogen can also be produced without fossil fuels through the process of electrolysis. Renewable forms of energy such as photovoltaic cells, wind, hydro and geothermal are increasingly being used to produce electricity. This electricity can be used for electrolysis, which splits water into hydrogen and oxygen. The hydrogen can be used, or stored to generate electricity.

In order to successfully have a society based upon renewable energy, there has to be a way to store energy because renewable energy is intermittent. Solar and wind energy are both excellent methods of obtaining energy from natural resources, however, the levels of sunshine, and the intensity of wind varies. When these sources are not available electricity cannot be generated. When a large amount of energy is being produced, hydrogen can be created from water. The hydrogen can then be stored for later use. Fuel cells have already been used for decades for stationary use for business and residential use. Portable electronics such as laptops, cameras and cellular phones can last 10 to 20 times longer by using hydrogen. All of the major automakers have already invested heavily in hydrogen

fuel cell technology vehicles. Although the cost of renewable energy systems is still very high, technological breakthroughs and larger quantities produced are dramatically reducing costs every year.

1.5 What is hydrogen fuel

Hydrogen was discovered in 1766 by the English chemist and physicist H. Cavendish. Hydrogen is the first element in the periodic table, consisting of one proton and one electron making it the smallest and lightest of all elements. Hydrogen reacts with many different materials and is one of the most abundant elements in the universe, 90% of the atoms in the known universe are hydrogen. Hydrogen therefore can be produced from a various types of sources. The most important source is water, which can be split into hydrogen and oxygen by electrolysis. These can be combined again in a fuel cell, creating power, heat and water as the only emission.

Hydrogen is the simplest and most common element in the universe [4]. It is a colorless, odorless, and tasteless gas that has the highest energy content per unit of weight of any known fuel. Hydrogen is very chemically active and rarely stands alone as an element. It usually exists in combination with other elements, such as oxygen in water, carbon in methane, and in trace elements as organic compounds. Hydrogen therefore must be broken from its bonds with other elements in order to be used as a fuel. There are numerous processes that can be used to break these bonds.

1.6 Physical and Chemical properties of hydrogen

Table 1.1- Hydrogen Density

Gas (m3)	Liquid (litre)	Weight (kg)
1	1,163	0,0898
0,856	1	0,0709
12,126	14,104	1

Table 1.2- Hydrogen Properties (nm³ at 981 mbar and 15 degrees Celsius)

Data	Value
Density	0,08988 kg/nm ³
Upper heating value	12,745 MJ/nm ³
Lower heating value	10,783 MJ/nm ³
Ignition energy	0,02 MJ
Ignition temperature	520 degrees Celsius
Lower ignition level (gas concentration in air)	4,1 Vol.%
Upper ignition level (gas concentration in air)	72,5 Vol.%
Flame rate	2,7 m/s

Table 1.3- Hydrogen density compared to other fuels

	Hydrogen	Gasoline	Diesel	Natural gas	Methanol
Density (kg/L)	0,0000898	0,702	0,855	0,00071	0,799
Density (kg/m ³)	0,0898	702	855	0,71	799
Energy density (MJ/kg)	120	42,7	41,9	50,4	19,9
Energy density (MJ/L)	0,01006	31,2	36,5	00,036	15,9
Energy density (MJ/m ³)	10,783	31200	36500	36,1	18000
Energy density (kWh/kg)	33,3	11,86	11,64	14	5,53
Energy density (kWh/m ³)	2,79	8666,67	10138,88	10,02	4420

1.7 How is hydrogen produced

One of the benefits of hydrogen fuel is that it can be produced from a diverse array of potential feed stocks, including water, fossil fuels and organic matter. Described below are the most common and best understood hydrogen production pathways. Each of these pathways has its own pros and cons that should be considered in terms of cost, emissions, feasibility, scale, and logistics.

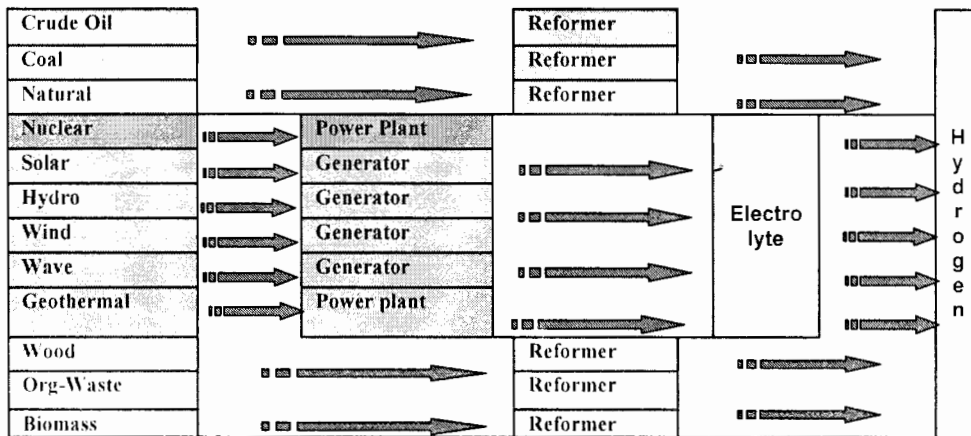


Figure 1.6- Hydrogen Production Pathways

1.7.1 Reformation of Natural Gas

In this process, natural gas (for example methane, propane, or ethane) is combined with high temperature steam (700-1000°C) where it reacts in presence of a catalyst, thereby breaking the bonds of the natural gas and creating hydrogen, carbon monoxide, and carbon dioxide. Steam reformation of natural gas is currently the most common method of bulk hydrogen production. It is also one of the best understood and least expensive methods. Steam reformation currently accounts for approximately 80% of global hydrogen production. This method of hydrogen production is dependent on a potentially limited and volatile natural gas supply. The process results in moderate emissions of CO₂.

1.7.2 Biomass Gasification

In this process, biomass such as forestry byproducts, straw, municipal solid waste or sewage is heated at high temperatures in a reactor where the bonds in the molecules forming the biomass are broken. This creates gas consisting mainly of hydrogen, carbon monoxide, and methane (CH₄). Using the same steam reformation process described above, the methane is converted into hydrogen and carbon dioxide. Carbon dioxide emissions from biomass gasification do not contribute to a net increase in greenhouse gas emissions. Biomass gasification is currently one of the most advanced and least expensive methods of producing hydrogen from renewable resources.

1.7.3 Coal Gasification

The basic process of coal gasification begins with converting the coal into a gaseous state by heating the coal in a reactor at very high temperatures. The gaseous coal is then treated with steam and oxygen and the result is the formation of hydrogen gas, carbon monoxide, and carbon dioxide. Coal gasification is the oldest method of hydrogen production. This method of production becomes economically viable if CO₂ is sequestered and used to recover methane trapped in un-minable coal beds. It is almost twice as expensive to

produce hydrogen from coal as from natural gas due to the ratio of hydrogen to carbon, which in natural gas is 4:1 and in carbon is 0.8:1.

1.7.4 Carbon Black & Hydrogen Process

The only inputs in the CB&H process are electric power and hydrocarbons. In the CB&H process carbon based raw materials ranging from natural gas to heavy oils are heated in a high temperature reactor. A plasma burner, utilizing recycled hydrogen from the process, splits the hydrocarbons. The products then go through a cooling and filtering system to separate the carbon black from the hydrogen. The first commercial CB&H plant went online in 1999. No emissions result from this process; one hundred percent of the raw materials are used, and two valuable products, carbon black and hydrogen, are produced. CB&H replaces the traditional process for producing carbon black, (used primarily in tire production) which is extremely polluting.

1.7.5 Electrolysis of Water

Electrolysis of water involves passing an electric current through water, thereby splitting the water molecules into their basic elements of hydrogen and oxygen. Hydrogen gas rises from the negative cathode and oxygen gas collects at the positive anode. After steam reformation of natural gas, this is the most common method of hydrogen production and is very well understood. Hydrogen produced using electrolysis has the potential to be completely emissions free if the electricity used is generated from clean, renewable sources such as wind and solar as shown in figure 1.6. Large amounts of electricity are required during electrolysis, making it one of the most energy intensive methods of hydrogen production. If the electricity used during electrolysis is generated from dirty sources, such as coal, oil, or even natural gas, the greenhouse gas emissions will be comparatively high.

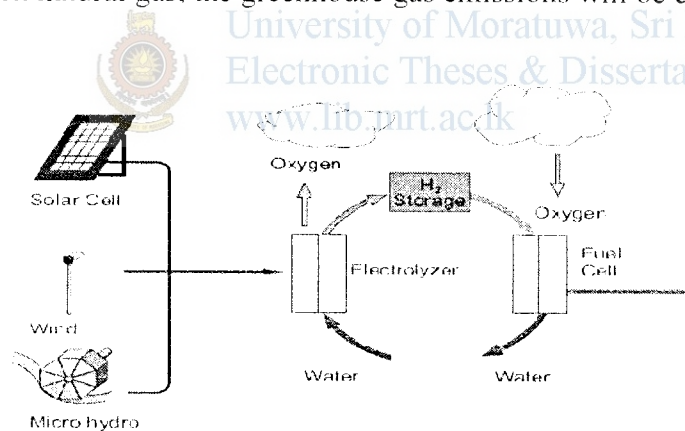


Figure 1.7- Electrical power from renewable energy sources.

1.8 PEM Based Electrolyzes

The polymer electrolyte membrane (PEM) based electrolyzer is very popular, and many modern electrolyzers are built with PEM technology. The PEM electrolyzer uses the same type of electrolyte that is used for a PEM fuel cell [9]. The electrolyte is a thin, solid ion-conducting membrane is used instead of the aqueous solution. These electrolyzers use a bipolar design, and can be made to operate at high differential pressures across the membrane. The reactions are as follows: The basic structure of a PEM-based electrolyzer is shown in Figure 1.8.



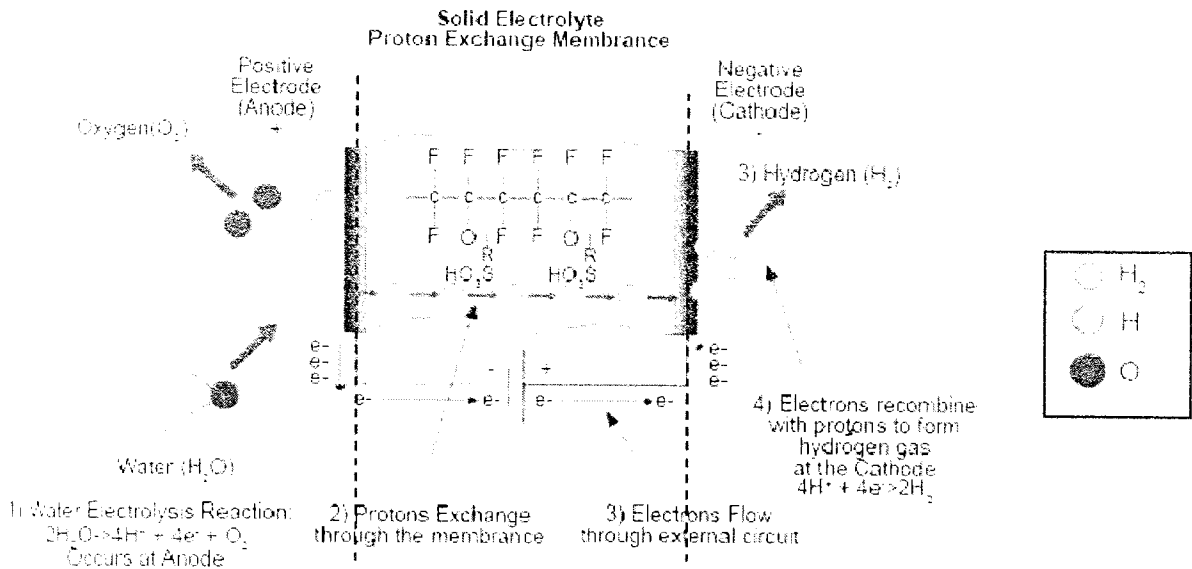
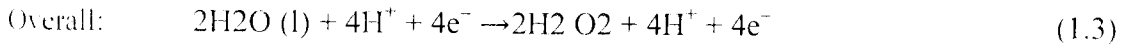


Figure 1.8- A simplified diagram of the PEM electrolyzer

1.9 History of Fuel cell

Whereas the 19th Century was the century of the steam engine and the 20th Century was the century of the internal combustion engine, it is likely that the 21st Century will be the century of the fuel cell. Fuel cells are now on the verge of being introduced commercially, revolutionizing the way we presently produce power. Fuel cells can use hydrogen as a fuel, offering the prospect of supplying the world with clean, sustainable electrical power.

The first demonstration of a fuel cell was by William Grove in 1839[9]. Real developments in fuel cells first happened for space applications in the 1960's. Since the 80's and until now much development in fuel cells has been focused on use for transportation, combined heat and power production and power supply in portable products. Fuel cells convert the chemical energy in a fuel, mostly hydrogen, into electricity and heat without any noise and mechanical movement. The only emission of the reaction in the fuel cell is pure water. A fuel cell is like a battery with the only difference that it will continue to provide power as long a fuel is provided.

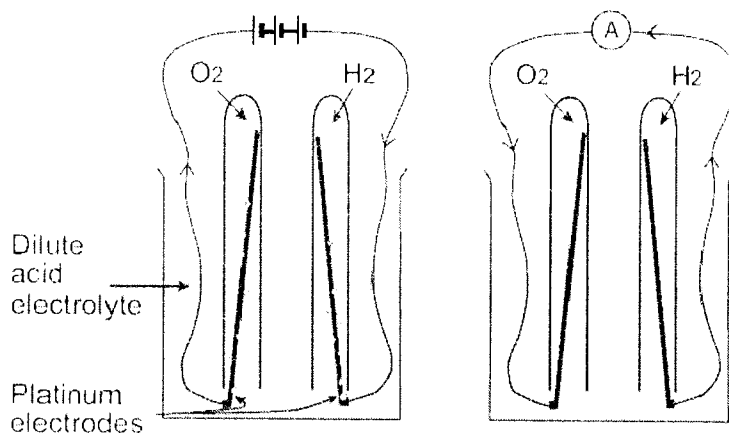


Figure 1.9- The principle of an electrolyzer, shown left; of a fuel cell, shown right.

Sir William Grove (1811-96), a British lawyer and amateur scientist developed the first fuel cell in 1839. The principle was discovered by accident during an electrolysis experiment. When Sir William disconnected the battery from the electrolyzer and connected the two electrodes together, he observed a current flowing in the opposite direction, consuming the gases of hydrogen and oxygen. He called this device a 'gas battery'. His gas battery consisted of platinum electrodes placed in test tubes of hydrogen and oxygen, immersed in a bath of dilute sulphuric acid. It generated voltages of about one volt. In 1842 Grove connected a number of gas batteries together in series to form a 'gas chain'. He used the electricity produced from the gas chain to power an electrolyzer, splitting water into hydrogen and oxygen. However, due to problems of corrosion of the electrodes and instability of the materials, Grove's fuel cell was not practical. As a result, there was little research and further development of fuel cells for many years to follow.

Table 1.4- History of Fuel cell Development

1800	W.Nicholson and A. Carlisle described the process of using electricity to break water
1836	William Grove fuel cell demonstration
1889	Separate terms: L. Mond and C. Wright and C. Thompson/experiments L.Cailleteon and L.Colardeau performed various fuel cell
1893	F. Ostwald described roles of fuel cell components
1896	W.Jacques constructed a carbon battery
Early 1900	E.Baur and Students conducted experiments on high temperature devices
1960	T. Grubb and L. Niedrach invented PEMFC technology at GE
1990-present	Worldwide extensive fuel cell research on all fuel cell types.

1.10 Hydrogen-fueled PEM Fuel Cell Applications

There are many PEM fuel cell manufacturers at varying stages of development and commercialization of their products. At least five of these manufacturers appear to be targeting the backup power markets. Recently, some of these manufacturers have tested their products in field applications, yet; few are testing in the federal sector, which is the focus of this review. Fuel cells can be configured to provide power completely independent of the grid, use the grid as backup power or provide backup power to a grid connected system should the grid fail. The latter is the typical configuration for backup power. Several federal sites are involved with testing the ability of PEM fuel cell systems to keep critical loads operational during power outages. Primarily, the applications are stationary and often the sites already employ a backup power technology that they are considering replacing or supplementing the existing backup power source with another technology to extend the periods of runtime.

1.10.1 Transportation

1. Cars

The California Low Emission Vehicle Program, administered by the California Air Resources Board (CARB), has been a large incentive for automobile manufacturers to actively pursue fuel cell development. This program requires that beginning in 2003, ten percent of passenger cars delivered for sale in California from medium or large sized manufacturers must be Zero Emission Vehicles, called ZEVs. Automobiles powered by fuel cells meet these requirements, as the only output of a hydrogen fuel cell is pure water. The NECAR 5 (Figure 1.10) is the latest prototype fuel cell automobile by DaimlerChrysler.



Figure 1.10- Two prototype automobiles powered by fuel cells, the NECAR 5 and JEEP

2. Scooters and Bicycles

Manhattan Scientifics and German subsidiary Novars have developed a number of fuel cell powered bicycles and scooters. A prototype Hydrocycle™ powered by a 670W Novars PEMFC was unveiled in 2000. The same technology has also been showcased by Aprilia, which unveiled a version of the Hydrocycle™ at the Bologna Motor Show in December 2000.



Figure 1.11-Fuel cell bicycle

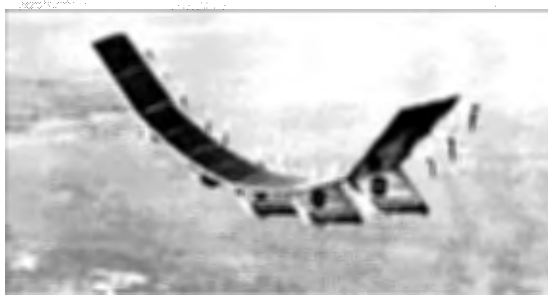


Figure 1.12-Fuel cell air craft

3. Aero environment

Aero environment will use regenerative PEMFCs to provide night-time power for its solar-powered NASA-funded Helios long duration aircraft, pictured above (Fig 1.12). Photovoltaic panels will power electric motors and electrolyze water during the day, and at night the fuel cell will power the motors by converting the hydrogen and oxygen back into water. Test flights of a fuel cell Helios are planned for 2003.

4. Space

The first fuel cells in space were 1kW solid polymer (PEMFC) type units manufactured by General Electric, which were used in eight NASA Gemini missions from 1965. UTC Fuel Cells (a division of United Technologies Corporation) has developed and manufactured

alkaline fuel cells for NASA since the 1960s. These have been used in the Apollo, Apollo-Soyuz, Skylab and Space Shuttle programs.

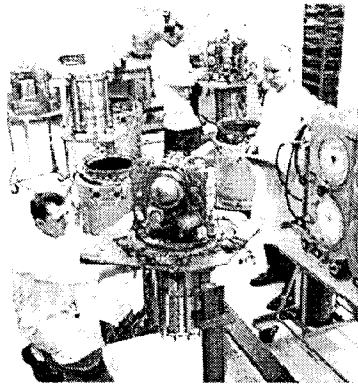


Figure 1.13- Assembly of alkaline fuel cells for Apollo spacecraft, 1964

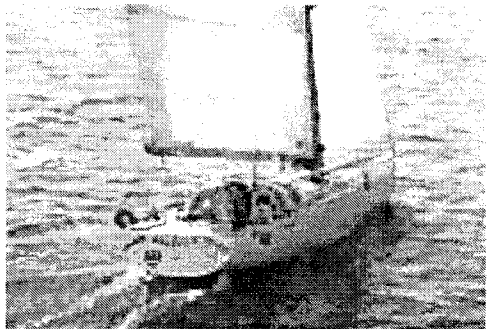


Figure 1.14 -Fuel cell Boat

5. Marine

HaveBlue (USA) is developing hydrogen based power and propulsion systems for ocean going yachts. These will extract hydrogen from water using renewable power technologies, which can then be fed to a fuel cell or other suitable power plant to power an electric motor or supply onboard energy needs.

6. Mining

At present, most mining vehicles use diesel engines. Fuel cells have several advantages over diesel power in mining applications, including lower emissions (which simplify ventilation requirements in a mine) and lower noise levels. Fuel cell Propulsion Institute (FCPI) has developed the world's first fuel cell powered locomotive, a mining and tunneling haulage vehicle, pictured below. Powered a by 17kW Nuvera Fuel Cells PEMFC unit fuelled by hydrogen stored.

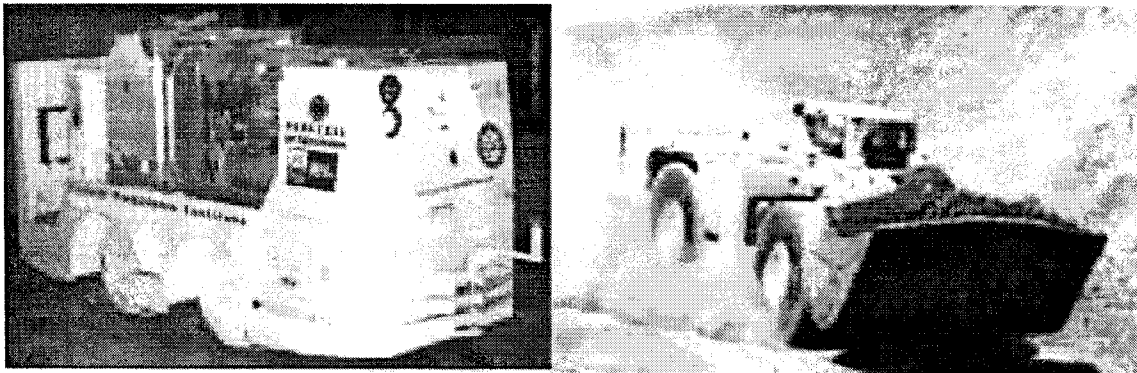


Figure 1.15- Fuel cell powered mining vehicle

7. Railways

Railway Technical Research Institute, which is now involved in a Japanese government funded project to develop alternatives to on-board railway diesel engines. In 2002 this project was supplied four Hydrogen Power 7kW PEM fuel cell systems, for integration into prototype railway power applications.

1.10.2 Underwater Applications

The first fuel cell system to be used underwater was developed by Allis-Chalmers in 1964 for testing by the Electric Boat Corp. This self-contained system was fuelled by hydrazine-oxygen. It supplied 1.5kWe at sea water pressure. Fuel Cell Technologies Ltd has developed and successfully deployed a number of Autonomous Underwater Vehicles (AUVs) powered by hydrogen fuel cell systems, which provide power for much longer than battery systems.

1.10.3 Distributed power generation

Distributed or “decentralized” power plants, contrasted with centralized power plants, are plants located close to the consumer, with the capability of providing both heat and electrical power (a combination known as “cogeneration”). Heat, the by-product of electrical power generation, is transferred from the fuel cell to a heat exchanger. The overall efficiency of a cogeneration system can be in excess of 80 percent, comparatively high compared to a system producing electricity alone. Using fuel cell power plants obviates the need for an electrical grid. This unit, produced by Ballard Power provides 250 kilowatts heat and electricity which is enough power for an industry, a school or a community of up to 50 homes (Photo courtesy of Ballard Power).

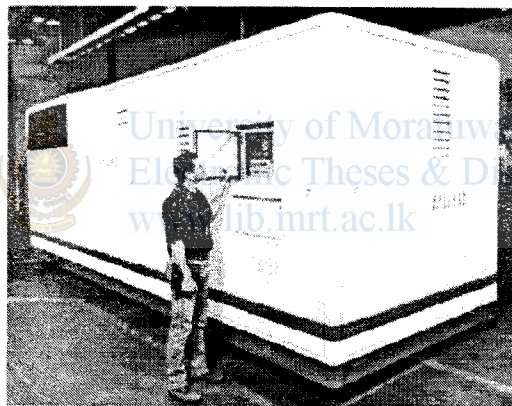


Figure 1.16- A fuel-cell distributed power plant.

1.10.4 Residential Power

Fuel cell power plants are also being developed by several manufacturers to provide electricity and heat to single family homes. Fuelled by either natural gas or propane, these plants will be able to supply base load power or all of the electricity required by a modern day home. Ballard Power has developed a one kilowatt fuel cell designed to supply both base load electrical power as well as heat to a dwelling. The electrical efficiency of this fuel cell system is rated at 42% and the heat efficiency is rated at 43%. Therefore the combined cogeneration efficiency of the system can be as high as 85%.



Figure 1.17- A fuel-cell power plant for residential applications

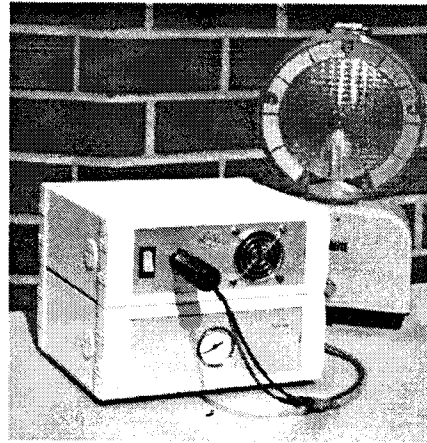


Figure 1.18 Fuel cell portable applications

1.10.5 Portable Power

Several manufacturers are also developing fuel cell power supplies for portable applications, providing a few watts up to several kilowatts of electricity (Fig.5.9). Fuelled by stored natural gas, propane, methanol or hydrogen gas, portable fuel cells may one day replace both gasoline and diesel engine generators for portable applications as well as conventional batteries for uses such as remote lighting, laptop computers and mobile phones.



University of Moratuwa, Sri Lanka.
Electronic Theses & Dissertations
www.lib.mrt.ac.lk

Chapter 2

Regenerative Fuel Cell Systems Explained

2.1 Introduction to PEMFC

In the early 1960s, General Electric (GE) also made a significant breakthrough in fuel cell technology. Through the work of Thomas Grubb and Leonard Niedrach, they invented and developed the first polymer electrolyte membrane (PEM) fuel cell. It was initially developed under a program with the US Navy's Bureau of Ships and U.S. Army Signal Corps to supply portable power for personnel in the field. Attracted by the possibility of using GE's PEM fuel cell on the Apollo missions, NASA tested its potential to provide auxiliary power onboard its Gemini spacecraft.

The Gemini space program consisted of 12 flights in preparation for the Apollo missions to the moon. For lunar flights, a longer power source was required than could be provided by batteries, which had been used on previous space flights. Unfortunately, the GE fuel cell, model PB2, encountered technical difficulties prior to launch, including the leakage of oxygen through the membrane[9]. As a result the Gemini missions 1 to 4 flew on batteries instead. The GE fuel cell was redesigned and a new model, the P3, successfully operated on the Gemini flights 6 to 12. The Gemini fuel cell power plant consisted of two fuel cell battery. GE redesigned their PEM cell, and the new model P3, despite malfunctions and poor performance on Gemini 5, served adequately for the remaining Gemini flights. Project Apollo mission planners; however, chose to use alkali fuel cells for both the command and lunar modules, as did designers of the Space Shuttle a decade later.

GE continued working on PEM cells and in the mid-1970s developed PEM water electrolysis technology for undersea life support, leading to the US Navy Oxygen Generating Plant. The British Royal Navy adopted this technology in early 1980s for their submarine fleet. Other groups also began looking at PEM cells. In the late 1980s and early 1990s, Los Alamos National Lab and Texas A&M University experimented with ways to reduce the amount of platinum required for PEM cells. Recently PEM developers added the weatherproofing material Gore-Tex to their cells to strengthen the electrolyte.

Polymer electrolyte membrane (PEM) fuel cells are the most popular type of fuel cell, and traditionally use hydrogen as the fuel. PEM fuel cells also have many other fuel options, which range from hydrogen to ethanol to biomass-derived materials. These fuels can either be directly fed into the fuel cell, or sent to a reformer to extract pure hydrogen, which is then directly fed to the fuel cell. Proton exchange membrane (PEM) fuel cells work with a polymer electrolyte in the form of a thin, permeable sheet. This membrane is small and light, and it works at low temperatures (about 80 degrees C, or about 175 degrees F). Other electrolytes require temperatures as high as 1,000 degrees C. To speed the reaction a platinum catalyst is used on both sides of the membrane. Hydrogen atoms are stripped of their electrons, or "ionized," at the anode, and the positively charged protons diffuse through one side of the porous membrane and migrate toward the cathode.

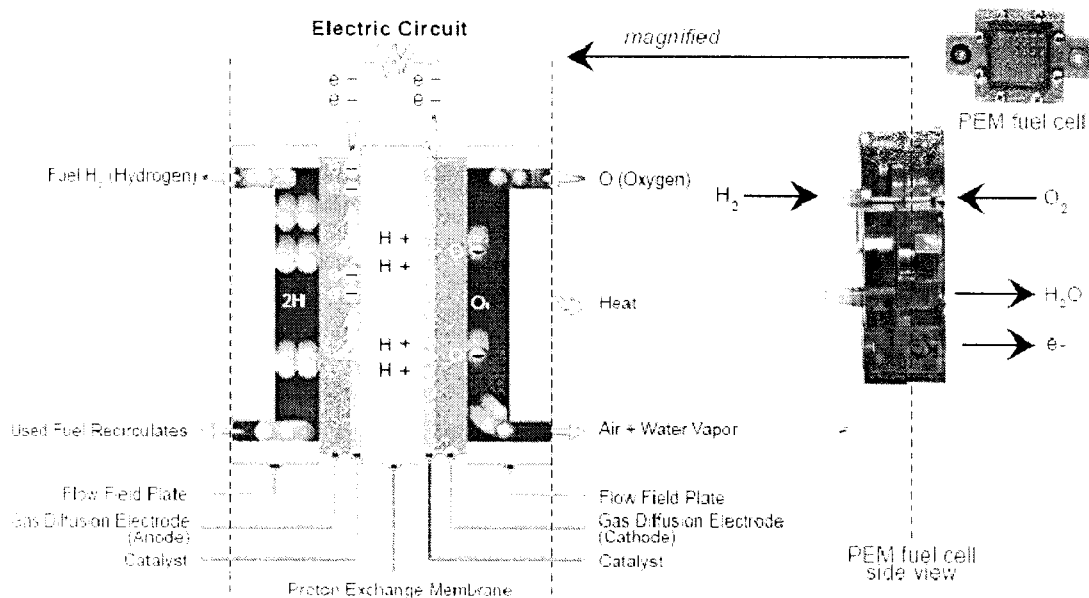


Figure 2.1- Structure of Fuel cell

The electrons pass from the anode to the cathode through an exterior circuit and provide electric power along the way. At the cathode, the electrons, hydrogen protons and oxygen from the air combine to form water. For this fuel cell to work, the proton exchange membrane electrolyte must allow hydrogen protons to pass through but prohibit the passage of electrons and heavier gases.

Efficiency for a PEM cell reaches about 40 to 50 percent. An external reformer is required to convert fuels such as methanol or gasoline to hydrogen. Currently, demonstration units of 50 kilowatt (kw) capacity are operating and units producing up to 250kw are under development. Proton exchange membrane fuel cells, also known as polymer electrolyte membrane fuel cells (PEMFC), are a type of fuel cell being developed for transport applications as well as for stationary and portable applications. Their distinguishing features include lower temperature and pressure ranges and a special polymer electrolyte membrane. The newly formed protons permeate through the polymer electrolyte membrane to the cathode side. The electrons travel along an external load circuit to the cathode side of the MEA, thus creating the current output of the fuel cell. Meanwhile, a stream of oxygen is delivered to the cathode side of the MEA. At the cathode side oxygen molecules react with the protons permeating through the polymer electrolyte membrane and the electrons arriving through the external circuit to form water molecules.

Fuel cells will be an integral part of the future hydrogen economy. Fuel cells have the ability to fulfill all of our global power needs while being highly efficient and a low polluting technology. There are six main types of fuel cells. The type most commonly used for transportation and portable applications is the polymer electrolyte membrane (PEM) fuel cell.

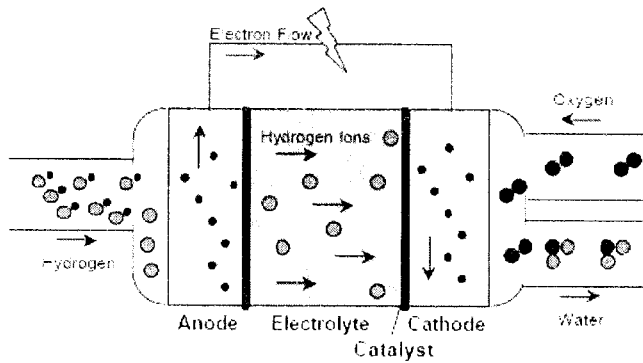


Figure 2.2- Fuel Cell Structural reactions

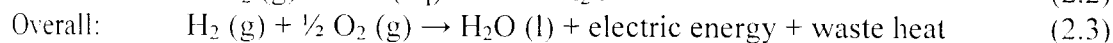
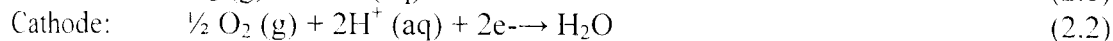
PEM fuel cells predominantly use hydrogen as the fuel, but also have the ability to use other types of fuel as well including ethanol and biomass derived materials. PEM fuel cells operate at temperatures between 20° and 80 °C, which enable a startup time comparable to the internal combustion engine. PEM fuel cells are able to obtain net power densities of over 1 kW/liter, which makes them competitive with the internal combustion engine for transportation applications. There are numerous advantages and challenges for PEM fuel cells.

2.2 Types of Fuel Cells

Many types of fuel cells are currently being researched. The six primary types of fuel cells are differentiated from one another on the basis of the electrolytes and/or fuel used with that particular type of fuel cell. The operating temperature and size of fuel cells are often the determining factor is which fuel cell will be used for specific applications. Fuel cell types include the following.

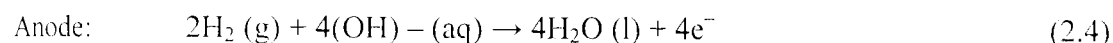
2.2.1 Polymer Exchange Membrane Fuel Cell (PEMFC)

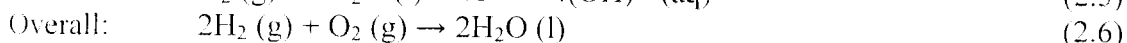
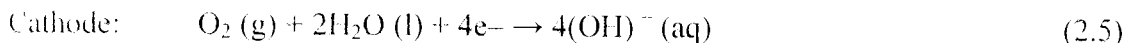
The polymer electrolyte membrane (also called proton exchange membrane or PEM) fuel cell delivers high-power density while providing low weight, cost, and volume. A PEM fuel cell consists of a negatively charged electrode (anode), a positively charged electrode (cathode), and an electrolyte membrane. Hydrogen is used on the anode side, and oxygen is utilized on the cathode. Protons are transported from the anode to the cathode through the electrolyte membrane and the electrons are carried over an external circuit load. A typical PEM fuel cell has the following reactions:



2.2.2 Alkaline Fuel Cells (AFCs)

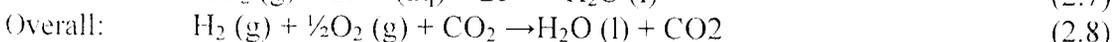
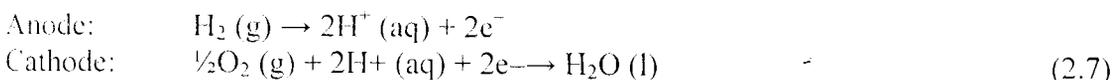
Alkaline fuel cells (AFCs) have been used by NASA on space missions and can achieve power-generating efficiencies of up to 70 percent. The operating temperature of these cells range between 150 to 200 °C (about 300 to 400 °F). An aqueous solution of alkaline potassium hydroxide soaked in a matrix act as the electrolyte. Alkaline fuel cells typically have a cell output from 300 watts to 5 kW. The chemical reactions that occur in this cell are:





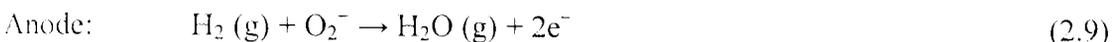
2.2.3 Phosphoric Acid Fuel Cell (PAFC)

The phosphoric acid fuel cell (PAFC) is one of the few commercially available fuel cells. Several hundred fuel cell systems have been installed all over the world. Most of the PAFC plants that have been built are in the 50 to 200 kW capacity range, but large plants of 1 MW and 5 MW have been built. The largest plant operated to date achieved 11 MW of grid-quality alternating current (AC) power. PAFCs are very efficient fuel cells, generating electricity at more than 40 percent efficiency. Operating temperatures are in the range of 300 to 400 °F (150 to 200 °C).



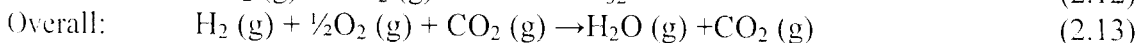
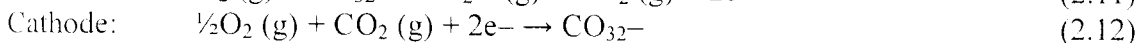
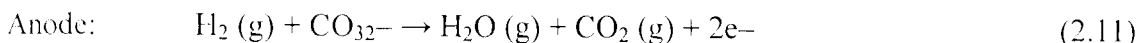
2.2.4 Solid Oxide Fuel Cells (SOFCs)

Solid oxide fuel cells (SOFCs) seem promising for large, high-power applications such as industrial and large scale central electricity generating stations. A solid oxide system is usually constructed of a hard ceramic material consisting of solid zirconium oxide and a small amount of Yttria, instead of a liquid electrolyte. The operating temperatures can reach 1,800 °F or 1000 °C.



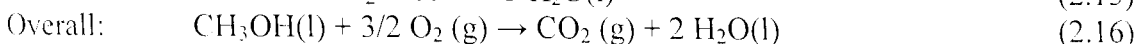
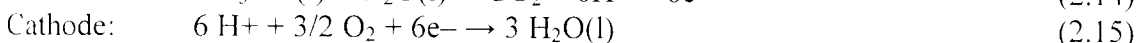
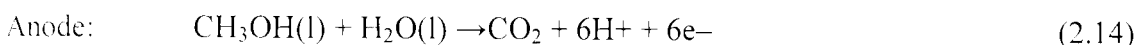
2.2.5 Molten-Carbonate Fuel Cells (MCFCs)

Molten carbonate fuel cells are another fuel cell technology that has been successfully demonstrated in several locations throughout the world. The high operating temperature offers a significant advantage because it enables a higher efficiency and the flexibility to use more types of fuels and inexpensive catalysts. MCFCs have high fuel-to-electricity efficiencies ranging from 60 to 85 percent with cogeneration, and operate at about 1,200 °F or 650 °C. Overall reactions for the MCFC are:



2.2.6 Direct Methanol Fuel Cells (DMFCs)

The large potential market for fuel cell portable applications has generated a strong interest in a fuel cell that can run directly on methanol. The direct methanol fuel cell (DMFC) uses the same polymer electrolyte membrane as the PEM fuel cell. The fuel for the DMFC, however, is methanol instead of hydrogen. The chemical reactions for this fuel cell are as follows:



2.3 Structure of fuel Cell

2.3.1 Electrolyte Layer

The electrolyte layer is the heart of a fuel cell. It enables the fuel cell to conduct its electrons properly by attracting the protons, and enabling them to travel through the layer while maintaining their proton state. The electrons travel to the external circuit to power the load, and the hydrogen protons travel through the electrolyte until they reach the cathode to combine with oxygen to form water. The electrolyte must be able to conduct ions well; it must present a good enough barrier to not allow other reactants to enter it; it must not conduct electrons; and it has to be easy to integrate into the fuel cell stack as shown in figure 2.3.

2.3.2 Gas Diffusion Layer

The gas diffusion layers (GDL) have two main functions. They must allow gases to pass through them, and be conductive enough to allow electrons to travel through them. These layers also provide a layer to bond the catalyst to, and its structure promotes the removal of water that may get in the way of the reaction. This layer is very thin, with a thickness of 0.25 – 0.40 mm, and a pore size ranging between 4 – 50 microns [9].

2.3.3 Catalyst Layer

The fuel cell reactions occur in the catalyst layer. The anode catalyst layer breaks the hydrogen fuel into protons and electrons, and at the cathode catalyst layer, oxygen combines with the protons to form water. These catalyst layers are often the thinnest layer in the fuel cell (5 to 30 μm), but are often the most complex because they incorporate several types of gases and water and electrochemical reactions. The catalyst layers are usually made of a porous mixture of carbon supported platinum or platinum/ruthenium.

2.3.4 Bipolar Plates

Bipolar plates evenly distribute fuel and oxidant to the cells, and collect the current to power the desired devices. In a fuel cell with a single cell, there are no bipolar plates (only single-sided flow field plates). Yet, in fuel cells with more than one cell, there is usually at least one bipolar plate (flow fields exist on both sides of the plate). Bipolar plates perform many roles in fuel cells. They distribute fuel and oxidant within the cell, separate the individual cells in the stack, collect the current, carry water away from each cell, humidify gases, and keep the cells cool. Bipolar plates also have reactant flow channels on both sides, forming the anode and cathode compartments of the unit cells on the opposing sides of the bipolar plate as in figure 2.4.

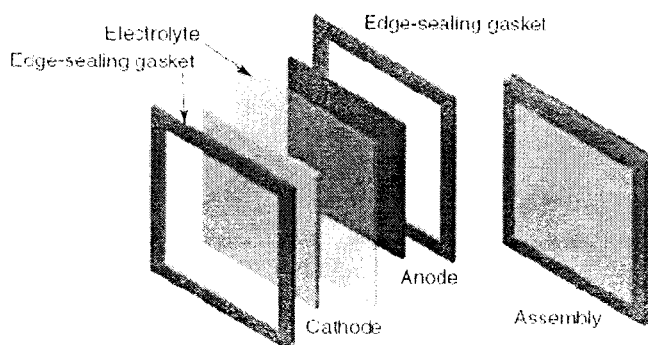


Figure 2.3- The construction of anode/electrolyte/cathode assembly

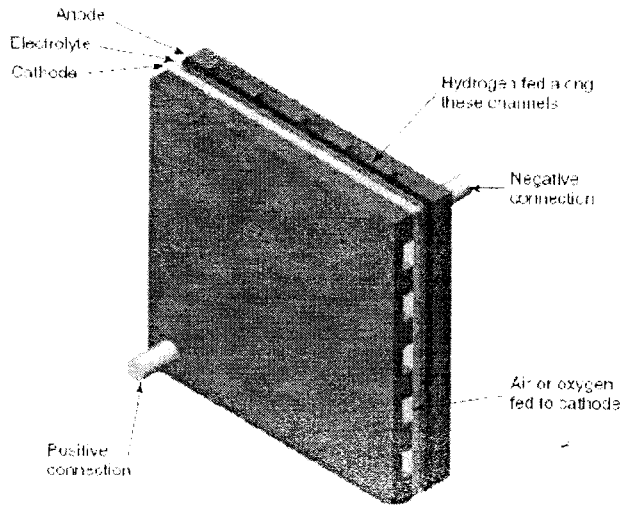


Figure 2.4-Compacted Single cell PEMFC

2.4 Structure of the Polymer Electrolyte

The different companies producing polymer electrolyte membranes have their own special tricks, mostly proprietary. However, a common theme is the use of sulphonated fluoropolymers, usually fluoroethylene. The most well known and well established of these is Nafion (Dupont), which has been developed through several variants since the 1960s. This material is still the electrolyte against which others are judged, and is in a sense an 'industry standard'. Other polymer electrolytes function in a similar way. The construction of the electrolyte material is as follows. The starting point is the basic, simplest to understand, man-made polymer – polyethylene. Its molecular structure based on ethylene is shown in Figure 2.5

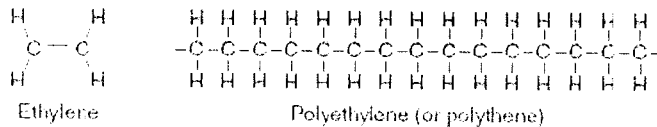


Figure 2.5-Structure of polyethylene.

This basic polymer is modified by substituting fluorine for the hydrogen. This process is applied to many other compounds and is called perfluorination. The 'mer' is called tetrafluoroethylene. The modified polymer, shown in Figure 2.6, is polytetrafluoroethylene, or PTFE. It is also called as Teflon, the registered trademark of ICI. This remarkable material has been very important in the development of fuel cells. The strong bonds between the fluorine and the carbon make it durable and resistant to chemical attack. Another important property is that it is strongly hydrophobic, and so it is used in fuel cell electrodes to drive the product water out of the electrode, and thus it prevents flooding. It is used in this way in phosphoric acid and alkali fuel cells, as well as in PEMFCs. (The same property gives it a host of uses in outdoor clothing and footwear.)

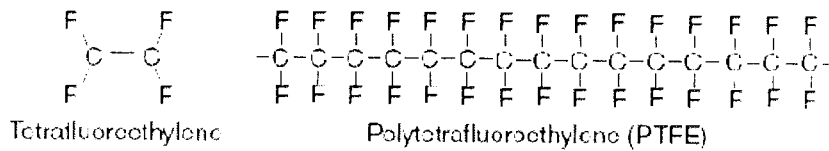


Figure 2.6-Structure of PTFE.

However, to make an electrolyte, a further stage is needed. The basic PTFE polymer is 'sulphonated' a side chain is added, ending with sulphonic acid HSO_3 . Sulphonation of complex molecules is a widely used technique in chemical processing. One possible side chain structure is shown in Figure 2.7. The details vary for different types of Nafion, and with different manufacturers of these membranes.

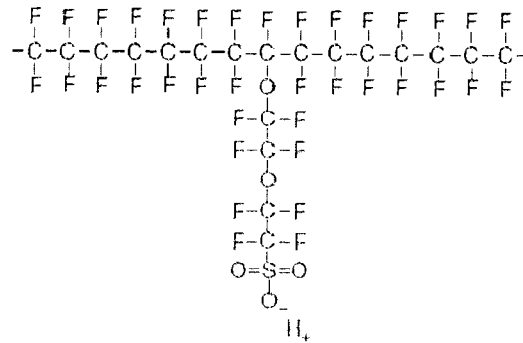


Figure 2.7-structure of a sulphonated fluoroethylene

From the point of view of fuel cell use, the main features of Nafion and other fluorosulphonate ionomers are that,

- They are chemically highly resistant,
- They are strong (mechanically), and so can be made into very thin films, down to $50\mu\text{m}$,
- They are acidic,
- They can absorb large quantities of water,
- If they are well hydrated, the H^+ ions can move quite freely within the material they are good proton conductors.

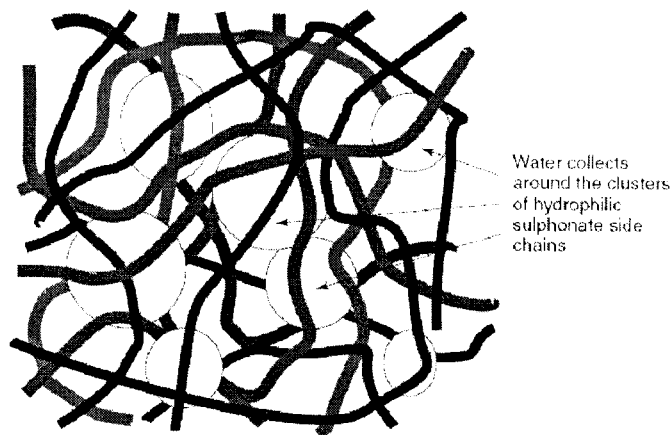


Figure 2.8-The structure of Nafion-type membrane materials.

2.5 Water Management in the PEMFC

2.5.1 Overview of the problem

It will be clear from the description of a proton exchange membrane, that there must be sufficient water content in the polymer electrolyte. The proton conductivity is directly proportional to the water content. However, there must not be so much water that the electrodes that are bonded to the electrolyte flood, blocking the pores in the electrodes or the gas diffusion layer. A balance is therefore needed, which takes care to achieve.

In the PEMFC, water forms at the cathode. In an ideal world, this water would keep the electrolyte at the correct level of hydration. Air would be blown over the cathode, and apart from supplying the necessary oxygen it would dry out any excess water. Because the membrane electrolyte is so thin, water would diffuse from the cathode side to the anode, and throughout the whole electrolyte a suitable state of hydration would be achieved without any special difficulty. This happy situation can sometimes be achieved, but needs a good engineering design to bring to pass.

There are several complications. One is that during the operation of the cell the H⁺ ions moving from the anode to the cathode pull water molecules with them. This process is sometimes called electro-osmotic drag. Typically, between one and five water molecules are 'dragged' for each proton (Zawodzinski et al., 1993 and Ren and Gottesfeld, 2001). This means that, especially at high current densities, the anode side of the electrolyte can become dried out even if the cathode is well hydrated. Another major problem is the drying effect of air at high temperatures. But it suffices to say at this stage that at temperatures of over approximately 60°C, the air will always dry out the electrodes faster than the water is produced by the H₂/O₂ reaction. One common way to solve these problems is to humidify the air, the hydrogen, or both, before they enter the fuel cell.

2.5.2 Airflow and water evaporation

Except in the special case of PEM fuel cells supplied with pure oxygen, it is universally the practice to remove the product water using the air that flows through the cell. The air will also always be fed through the cell at a rate faster than that needed just to supply the necessary oxygen. If it were fed at exactly the 'stoichiometric' rate, then there would be very great concentration losses. This is because the exit air would be completely depleted of oxygen. In practice, the stoichiometry (λ) will be at least 2. In Appendix B, Section B1.2, a very useful equation is derived connecting the air flow rate, the power of a fuel cell and the stoichiometry (equation B-4). Problems arise because the drying effect of air is so non-linear in its relationship to temperature. To understand this, we have to consider the precise meaning and quantitative effects of terms such as relative humidity, water content, and saturated vapor pressure.

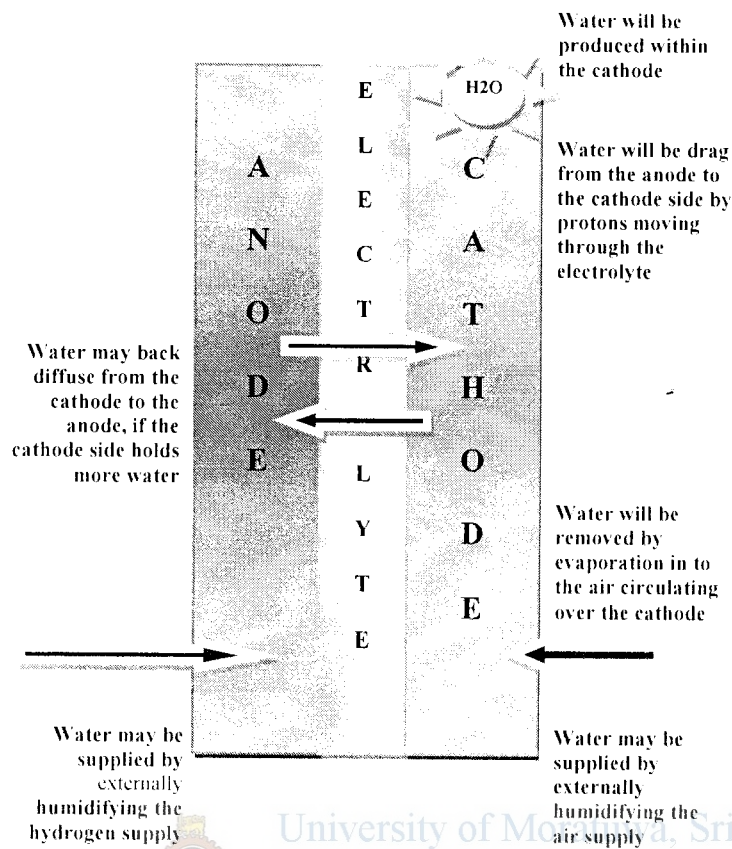


Figure 2.9- The different water movements to, within, and from the electrolyte of a PEM fuel cell

When considering the effect of oxygen concentration, the partial pressures of the various gases that make up air were given. At that point we ignored the fact that air also contains water vapor. We did this because the amount of water vapor in air varies greatly, depending on the temperature, location, weather conditions, and other factors. This quantity is variously known as the humidity ratio, absolute humidity, or specific humidity and is defined as,

Humidity ratio,

$$\omega = m_w / m_a \quad (2.17)$$

Where, "mw" is the mass of water present in the sample of the mixture and "ma" is the mass of dry air. The total mass of the air is $m_w + m_a$.

However, this does not give a very good idea of the drying effect or the 'feel' of the air. Warm air, with quite high water content, can feel very dry, and indeed have a very strong drying effect. When the air cannot hold any more water vapor, it is 'saturated'. Air that has no 'drying effect' that will not be able to hold any more water, could reasonably be said to be 'fully humidified'. This state is achieved when $P_w = P_{sat}$, where P_w is the partial pressure of the water and P_{sat} is the saturated vapor pressure of the water. We define the relative humidity as the ratio of these two pressures: Relative humidity,

$$\phi = P_w / P_{sat} \quad (2.18)$$

2.6 Operating Pressure of FC

2.6.1 Outline of the problem

Although small PEM fuel cells are operated at normal air pressure, larger fuel cells, of 10kW or more, are sometimes operated at higher pressures. The advantages and disadvantages of operating at higher pressure are complex, and the arguments are not at all clear-cut, there is much to be said on both sides. The basic issues around operating at higher pressure are the same as for other engines, such as diesel and petrol internal combustion engines, only with these machines the term used is 'supercharging' or 'turbo charging'. Indeed, the technology for achieving the higher pressures is essentially the same as the purpose of increasing the pressure in an engine is to increase the specific power, to get more power out of the same size engine. Hopefully, the extra cost, size, and weight of the compressing equipment will be less than the cost, size, and weight of simply getting the extra power by making the engine bigger. It is a fact that most diesel engines are operated at above atmospheric pressure they are supercharged using a turbocharger. The hot exhaust gas is used to drive a turbine, which drives a compressor that compresses the inlet air to the engine. The energy used to drive the compressor is thus essentially 'free', and the turbocharger units used are mass-produced, compact, and highly reliable. In this case the advantages clearly outweigh the disadvantages. However, with fuel cells the advantage/disadvantage balance is much closer. Above all, this is because there is little energy in the exit gas of the PEMFC and any compressor has to be driven largely or wholly using the precious electrical power produced by the fuel cell.

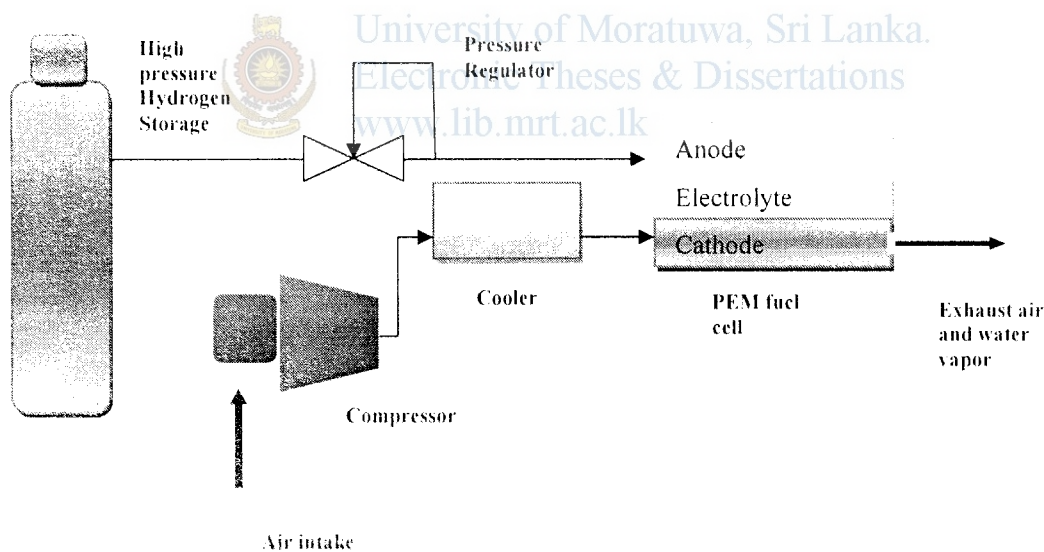


Figure 2.10- Simple motor driven air compressor and PEM fuel cell.

The simplest type of pressurized PEM fuel cell is that in which the hydrogen gas comes from a high-pressure cylinder. Such a system is shown in Figure 2.10. Only the air has to be compressed. The hydrogen gas is coming from a pressurized container, and thus its compression 'comes free'. The hydrogen is fed to the anode in a way called dead-ended; there is no venting or circulation of the gas it is just consumed by the cell. The compressor for the air must be driven by an electric motor, which of course uses up some of the valuable electricity generated by the fuel cell in a worked example; it is shown that the typical power consumption will be about 20% of the fuel cell power for a 100-kW system. Other systems described in the literature[12] report even higher proportions of compressor power consumption.

Theoretical Development of Fuel Cell Electro-Chemistry

3.1 Mathematical Models in the Literature

Fuel cell modeling is helpful for fuel cell developers because it can lead to fuel cell design improvements, as well as, better, and more efficient fuel cells. The model must be robust and accurate and be able to provide solutions to fuel cell problems quickly. A good model should predict fuel cell performance under a wide range of fuel cell operating conditions. Even a modest fuel cell model will have large predictive power.

A few important parameters to include in a fuel cell model are the cell, fuel and oxidant temperatures, the fuel or oxidant pressures, the cell potential, and the weight fraction of each reactant[7][8]. Some of the parameters that must be solved for in a mathematical model are shown in Figure 3.1. The necessary improvements for fuel cell performance and operation demand better design, materials, and optimization. These issues can only be addressed if realistic mathematical process models are available. There are many published models for PEM fuel cells in the literature, but it is often a daunting task for a newcomer to the field to begin understanding the complexity of the current models.

The first column of Table 3.1 shows the number of dimensions the models have in the literature. Most models in the early 1990s were one dimensional, models in the late 1990s to early 2000s were two dimensional, and more recently there have been a few three dimensional models for certain fuel cell components. The second column specifies that the model can be dynamic or steady state. Most published models have steady state voltage characteristics and concentration profiles. The next column of Table 3.1 presents the types of electrode kinetic expressions used. Simple Tafel-type expressions are often employed. Certain researchers use Butler-Volmer-type expressions, and a few other models use more realistic, complex multi step reaction kinetics for the electrochemical reactions. The next column compares the phases used for the anode and cathode structures. It is well known that there are two phases (liquid and gas) that coexist under a variety of operating conditions. Inside the cathode structure, water may condense and block the way for fresh oxygen to reach the catalyst layer.

An important feature of each model is the mass transport descriptions of the anode, cathode, and electrolyte. Several mass transport models are used. Simple Fick diffusion models and effective Fick diffusion models typically use experimentally determined effective transport coefficients instead of Fick diffusivities, and do not account for convective flow contributions. Therefore, many models use Nernst-Planck mass transport expressions that combine Fick's diffusion with convective flow. The convective flow is typically calculated from Darcy's law using different formulations of the hydraulic permeability coefficient. Some models use Schlogl's formulations for convective flow instead of Darcy's law, which also accounts for electro osmotic flow, and can be used for mass transport inside the PEM. A very simple method of incorporating electro osmotic flow in the membrane is by applying the drag coefficient model, which assumes a proportion of water and fuel flow to proton flow. Another popular type of mass transport description is the Maxwell-Stefan formulation for multi component mixtures. This has been used for gas-

phase transport in many models, but this equation would be better used for liquid–vapor–phase mass transport. Very few models use this equation for both phases. Surface diffusion models and models derived from irreversible thermodynamics are seldom used. Mass transport models that use effective transport coefficients and drag coefficients usually only yield a good approximation to experimental data under a limited range of operating conditions.

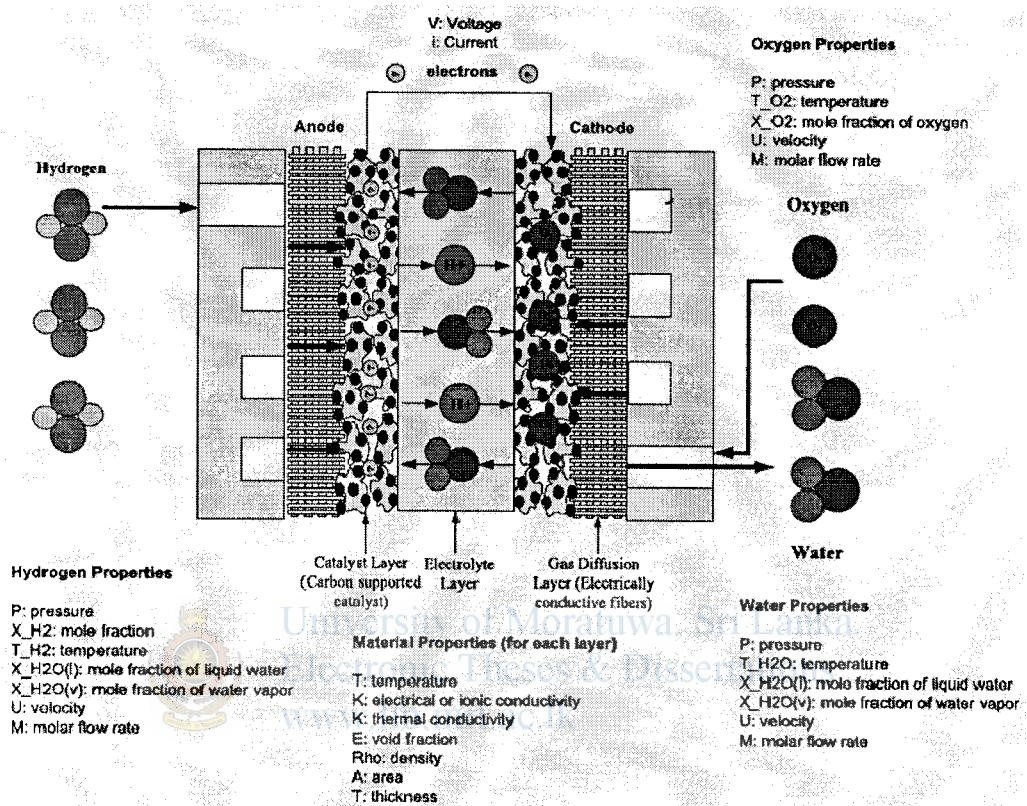


Figure 3.1- Parameters that must be solved for in a mathematical model.

The second to last column of Table 3.1 [8] shows that the swelling of polymer membranes is modeled through empirical or thermodynamic models for PEM fuel cells. Most models assume a fully hydrated PEM. In certain cases, the water uptake is described by an empirical correlation, and in other cases a thermodynamic model is used based upon the change of Gibbs free energy inside the PEM based upon water content. The last column notes whether the published model includes energy balances. Most models assume an isothermal cell operation and therefore have no energy balances included. However, including energy balance equations is an important parameter in fuel cell models because the temperature affects the catalyst reactions and water management in the fuel cell.

A model is only as accurate as its assumptions allow it to be. The assumptions need to be well understood in order to understand the model's limitations and to accurately interpret its results. Common assumptions used in fuel cell modeling are:

- Ideal gas properties
- Incompressible flow
- Laminar flow
- Isotropic and homogeneous electrolyte, electrode, and bipolar material structures
- A negligible ohmic potential drop in components

• Mass and energy transport is modeled from a macro perspective using volume-averaged conservation equations

The concepts presented in this chapter can be applied to all fuel cell types, regardless of the fuel cell geometry. Even simple fuel cell models will provide tremendous insight into determining why a fuel cell system performs well or poorly.

Table 3.1- Comparison of Recent Mathematical Models

No. of Dimensions	Dyn/SS	Anode and Cathode Kinetics	Anode and Cathode Phase	Mass Transport (Anode and Cathode)	Mass Transport (Electrolyte)	Membrane Swelling	Energy Balance
one dimension, two dimension, or three dimension	Dynamic or steady state	Tafel-type expressions, Butler-Volmer, complex kinetics equations	Gas, liquid, combination of gas and liquid	Effective Fick's diffusion, Nernst-Planck, Nernst-Planck, Nernst-Planck, Schlogl, Maxwell-	Nernst-Planck, Schlogl, Nernst-Planck, drag coefficient, Maxwell-Stefan, Effective Fick's diffusion	Empirical or thermodynamic models	Isothermal or full energy balance

3.1.1 Creating Mathematical Models

The basic steps used for creating a mathematical model are the same regardless of the system being modeled[8]. The details vary somewhat from method to method, but an understanding of the common steps, combined with the required method, provides a framework in which the results from almost any method can be interpreted and understood. The basic steps of the model-building process are:

1. Model selection
2. Model fitting
3. Model validation

These three basic steps are used iteratively until an appropriate model for the data has been developed. In the model selection step, plots of the data, process knowledge, and assumptions about the process are used to determine the form of the model to be fit to the data. Then, using the selected model and data, an appropriate model-fitting method is used to estimate the unknown parameters in the model. When the parameter estimates have been made, the model is then carefully assessed to see if the underlying assumptions of the analysis appear reasonable. If the assumptions seem valid, the model can be used to answer the scientific or engineering questions that initiated the modeling effort. If the model validation identifies problems with the current model, however, then the modeling process is repeated using information from the model validation step to select and/or fit an improved model.

3.1.2 Variation on the Basic Steps

The three basic steps of process modeling assume that the data have already been collected and that the same data set can be used to fit all of the candidate models. Although this is often the case in model-building situations, one variation on the basic model-building sequence comes up when additional data are needed to fit a newly hypothesized model based on a model fit to the initial data. In this case, two additional steps experimental design and data collection can be added to the basic sequence between model selection and model-fitting. Figure 3.2[8] shows the basic model-fitting sequence with the integration of the related data collection steps into the model-building process.

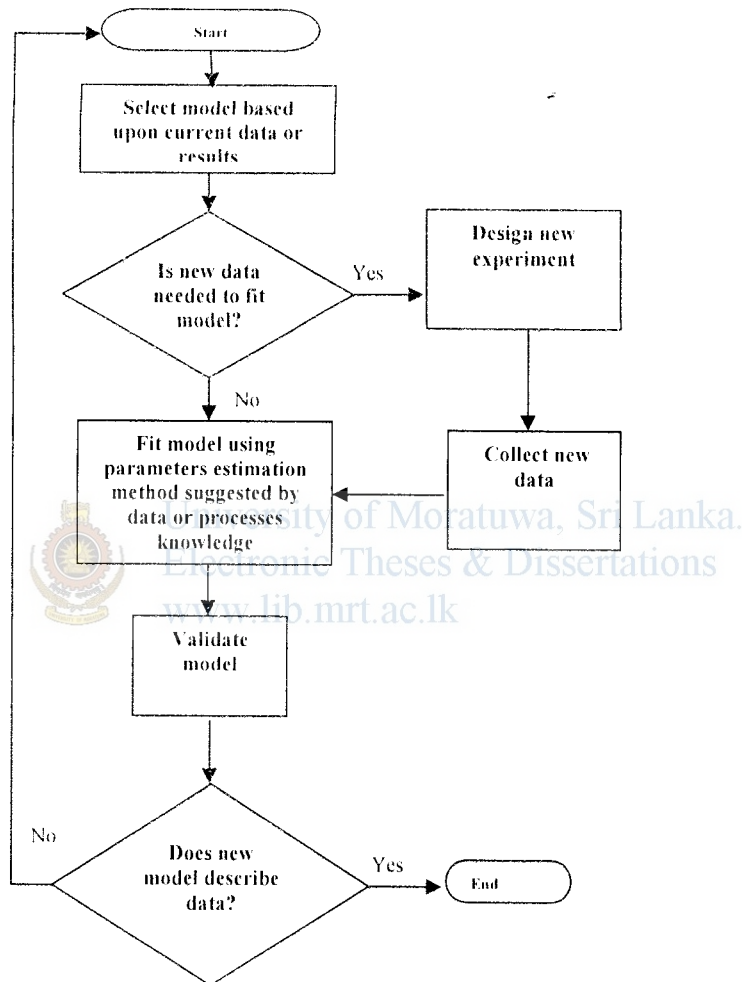


Figure 3.2- Model-building sequence

Considering the model selection and fitting before collecting the initial data is also a good idea. Without data in hand, a hypothesis about what the data will look like is needed in order to guess what the initial model should be. Hypothesizing the outcome of an experiment is not always possible, but efforts made in the earliest stages of a project often maximize the efficiency of the whole model-building process and result in the best possible models for the process. The remainder of this research is devoted to the background theory and modeling of the fuel cell layers to help one to better understand the fuel cell system, and to create an accurate overall fuel cell model.

3.2 Fuel Cell Electrochemistry

3.2.1 Introduction

This section covers the electrochemistry needed in order to predict or model basic electrode kinetics, activation over potential, currents, and potentials in a fuel cell. It is essential to understand the underlying reaction process occurring at the anode and cathode when modeling fuel cells. The electrochemical reactions control the rate of power generation, and are the cause of activation voltage losses. A lot of progress has been made in the area of electrode kinetics, but there is still a lot of work that needs to be developed in order to fully understand the actual complex anode and cathode kinetics.

3.2.2 Basic Electro kinetic Concepts

All electrochemical processes involve the transfer of electrons between an electrode and a chemical species with a change in Gibbs free energy. Electrochemical reaction occurs at the interface between the electrode and the electrolyte, as shown in Figure 3.3

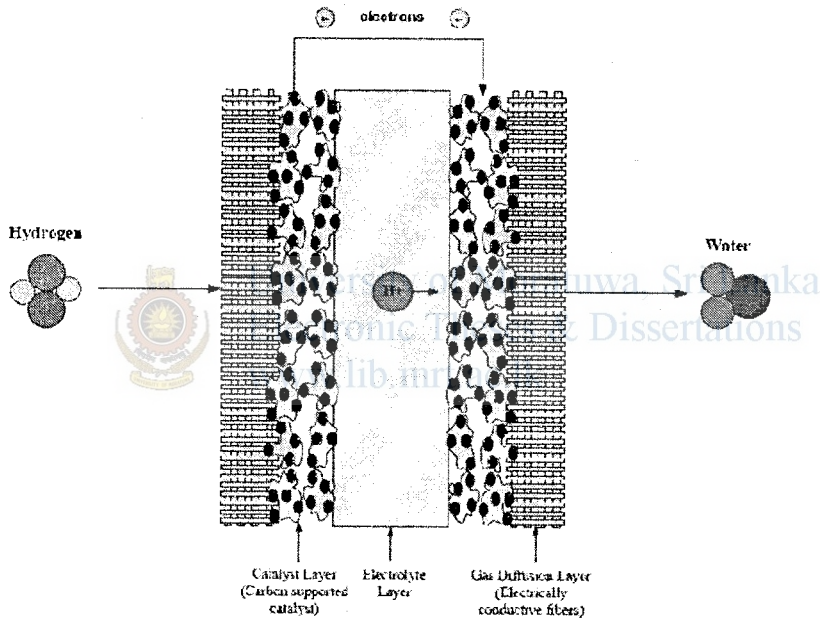


Figure 3.3- Fuel cell electrochemical reactions at the electrolyte and electrode.

The overall PEM fuel cell reactions do not seem overly complicated; the actual reactions proceed through many steps and intermediate species. For example, for the anodic reaction, the following elementary reactions are important.



The first reaction is a dissociative chemisorption step known as a Tafel reaction, and the second reaction is a charge transfer “Volmer” reaction. It suggests that the hydrogen first absorbs on the electrode surface, and then dissociates into the H atoms. Second Equation actually produces the proton and electron. The first reaction takes into consideration that the reacting species must first be absorbed on the electrode surface before the chemical reaction can occur. The rate of the electrode reaction may be influenced by the diverse

adsorbed species and the number of vacant sites. The surface coverage can be defined as the fraction of the electrode surface covered by adsorbed species.

$$\theta = \frac{C_{i,ad}}{C_{i,ad} + C_s} \quad (3.3)$$

where "ad" is the species that is adsorbed on the electrode surface, and "s" is the concentration. $C_{i,ad}$ is at the saturation of the electrode surface. The reaction rate equations can be written more descriptively to include the metal adsorption sites (M):



Therefore, the expression for the rate of reaction can be written as follows

where $(1 - \theta)$ is the metal surface not covered by adsorbed hydrogen. The equations presented in this section begin to illustrate some of the factors involved with the electrochemical reactions occurring at the electrode/electrolyte interface.

3.2.3 The Voltage Losses for a Polarization Curve

Understanding the reactions at the fuel cell anode and cathode is critical when modeling fuel cells. This shows the basic electrochemistry needed to predict electrode kinetics, activation losses, currents, and potentials in a fuel cell. The electrochemical reactions control the rate of power generation and are the main cause of activation voltage losses. The activation over voltage is the voltage loss due to overcoming the catalyst activation barrier in order to convert products into reactants. The equations presented in this, help to predict how fast the reactants are converted into electric current, and how much energy loss occurs during the actual electrochemical reaction.

The first step in creating the polarization curve is to calculate the Nernst voltage and voltage losses. To calculate the Nernst voltage for this example, the partial pressures of water, hydrogen, and oxygen will be used. First calculate the saturation pressure of water:

The partial pressure of hydrogen

$$p_{H_2} = \frac{p_{H_2}^0}{1 + \theta} \quad (3.8)$$

The partial pressure of oxygen

$$p_{O_2} = \frac{p_{O_2}^0}{1 + \theta} \quad (3.9)$$

The activation losses are estimated using the Tafel equation:

$$V_{act} = -b * \log\left(\frac{i}{i_0}\right) \quad \text{where } b = \frac{R * T}{2 * \alpha * F} \quad (3.10)$$

R is the gas constant, T is the temperature (K), F is Faraday's constant and α is the charge transfer coefficient. The ohmic losses are estimated using Ohm's law:

$$V_{ohmic} = -(i * r) \quad (3.11)$$

The mass transport (or concentration losses) can be calculated using the following equation:

$$V_{conc} = \alpha_{phal} * i^k * \ln\left(1 - \frac{i}{i_L}\right) \quad (3.12)$$

To insure that there are no negative values calculated for V_{conc} for the MATLAB program, the mass transport losses will only be calculated if

$$1 - \left(\frac{i}{i_L}\right) > 0 \quad (3.13)$$

else $V_{conc} = 0$.

The Nernst voltage can be calculated using the following equation:

$$E_{Nerst} = -\frac{G_{f,liq}}{2 * F} - \frac{R * T_k}{2 * F} * \ln\left(\frac{P_{H_2O}}{P_{H_2} * P_{O_2}^{1/2}}\right) \quad (3.14)$$

Since all of the voltage losses had a (-) in front of each equation, the actual voltage is the addition of the Nernst voltage plus the voltage losses:

$$V = E_{Nerst} + V_{act} + V_{ohmic} + V_{conc} \quad (3.15)$$

Example 3.1: A 25-cm² active area hydrogen-air fuel cell stack has 20 cells, and operates at a temperature of 60 °C. Both the hydrogen and air are fed to the fuel cell at a pressure of 3 atm. Create the polarization and fuel cell power curve for this fuel cell stack. (Appendix C-C-1). Some useful parameters for creating the polarization curve are:

The transfer coefficient, α , is 0.5, the exchange current density, i_0 , is $10^{-6.912}$ A/cm², the limiting current density, i_L , is 1.4 A/cm², the amplification constant (α_1) is 0.085, the Gibbs function in liquid form, $G_{f,liq}$, is -228,170 J/mol, the constant for mass transport, k, is 1.1, and the internal resistance, R, is 0.19 Ω cm².

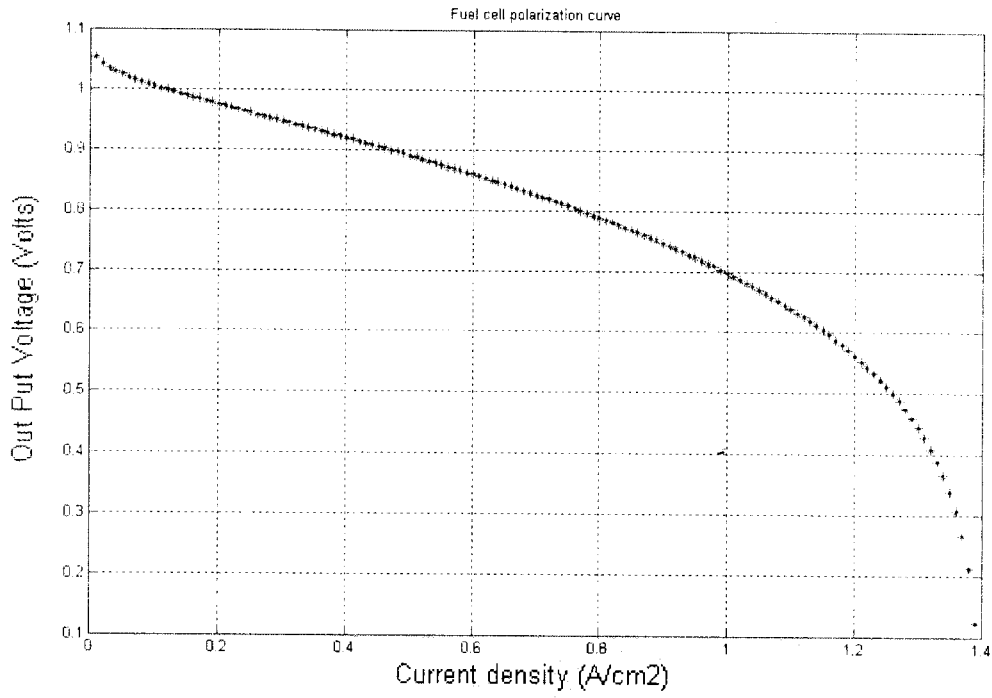


Figure 3.4.A Polarization curve generated in for Example 3.1

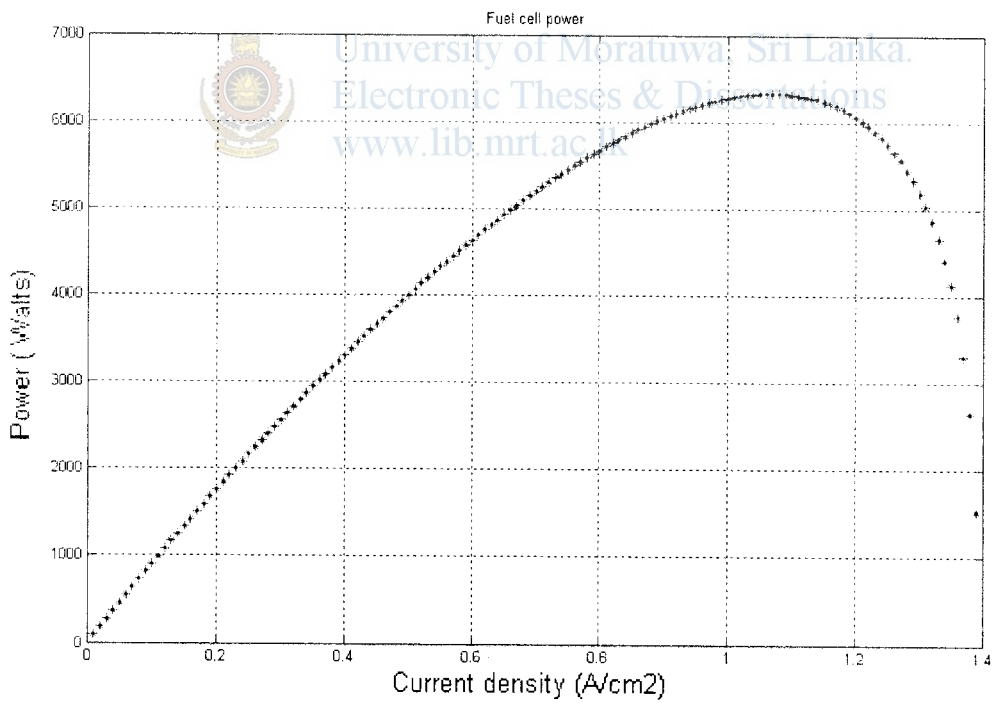


Figure 3.4.B Power curve generated in for Example 3.1

3.2.4 Modeling the Catalyst Layer

Model the PEM fuel cell anode and cathode catalyst layer using the equations for porous catalysts introduced in this section [7][8]. Creation of expressions for the anode and cathode activation losses, liquid water rate of reaction, and hydrogen rate of reaction with the following plots are shown: All of the parameters required for this derivation are listed in Table 3.2.

- (1) Current density versus the effectiveness factor,
- (2) Current density versus activation losses,
- (3) Current density versus voltage (polarization curve)
- (4) Current density versus the hydrogen flux density.

Modeling the catalyst layer is very complex because it has properties of all of the other fuel cell layers combined. Some of the important phenomena that need to be included in a rigorous catalyst layer model include mass, energy, and charge balances along with a relation that accounts for the contact between the porous GDL and polymer membrane layer. In addition, knowing how the catalyst agglomerates are distributed along the GDL is a challenge. The kinetics equations are the most important when modeling the catalyst layer. Commonly used equations are the Tafel and the Butler-Volmer equations (Appendix C-2).

Table 3.2- Parameters for derivation

<i>Parameter</i>	<i>Value</i>
Temperature	348.15 K
O2 permeation in agglomerate	1.5e-11
H2 permeation in agglomerate	2e-11
Agglomerate radius in anode and cathode	110e-5
Total gas pressure	1 atm
Hydrogen pressure	1 atm
Air pressure	1 atm
Saturation	0.6e-12
Anode transfer coefficient	1
Cathode transfer coefficient	0.9
Constant ohmic resistance	0.02 ohm-cm2
Limiting current density	1.4 A/cm2
Mass transport constant	1.1
Amplification constant	0.085
Gibbs function in liquid form	228,170 J/mol
Electrode-specific interfacial area	10,000
Current density	1 to 1.2 A/cm2

The first step is to calculate the Nernst voltage and voltage losses. To calculate the Nernst voltage for this example, the partial pressures of water, hydrogen, and oxygen will be used. First calculate the saturation pressure of water:

$$\log P_{H_2O} = -2.1794 + 0.02953 \times T_c - 9.1837 \times 10^{-5} \times T_c^2 + 1.4454 \times 10^{-7} \times T_c^3 \quad (3.16)$$

The partial pressure of hydrogen:

$$P_{H_2} = 0.5 \times (P_{H_2} / \exp(1.653 \times i / (T_K^{1.334}))) - P_{H_2O} \quad (3.17)$$

The partial pressure of oxygen:

$$P_{O_2} = (P_{Air} / \exp(4.192 \times i / (T_K^{1.334}))) - P_{H_2O} \quad (3.18)$$

The voltage losses will now be calculated. The activation losses are estimated using the Butler-Volmer equation. For the anode:

$$\nabla. i_2 = a_{1,2}(1 - S)i_{anode} \quad (3.19)$$

$$i_{anode} = \left[\frac{P_{H_2}}{P_{ref_{H_2}}} \exp\left(\frac{\alpha_a F}{RT}(\phi_1 - \phi_2)\right) - \exp\left(\frac{\alpha_c F}{RT}(\phi_1 - \phi_2)\right) \right] \quad (3.20)$$

For the cathode:

$$\nabla. i_2 = a_{1,2}(1 - S)i_{cathode} \quad (3.21)$$

$$i_{cathode} = \left[\frac{P_{O_2}}{P_{ref_{O_2}}} \exp\left(\frac{-\alpha_c F}{RT}(\phi_1 - \phi_2 - E_r)\right) \right] \quad (3.22)$$

The ohmic losses (see Chapter 4) are estimated using Ohm's law:

$$V_{conc} = \alpha_{phal} \times i^k \times \ln\left[1 - \frac{i}{i_l}\right] \quad (3.23)$$

To insure that there are no negative values calculated for V_{conc} for the MATLAB program, the mass transport losses will only be calculated if ,

$$\left[1 - \frac{i}{i_l}\right] > 0 \quad (3.24)$$

else $V_{conc} = 0$.

The Nernst voltage can be calculated using the following equation:

$$E_{Nernst} = -\frac{G_{f,liq}}{2 \times F} - \frac{R \times T_k}{2 \times F} \times \ln\left(\frac{P_{H_2O}}{P_{H_2} \times P^{1/2}_{O_2}}\right) \quad (3.25)$$

Since all of the voltage losses had a (-) in front of each equation, the actual voltage is the addition of the Nernst voltage plus the voltage losses:

$$V = E_{Nernst} + V_{act} + V_{ohmic} + V_{conc} \quad (3.26)$$

The hydrogen oxidation reaction rate at the anode can be written as:

$$\nabla. i_2 = a_{1,2}i_{h,1-2}E \quad (3.27)$$

$$\nabla \cdot N_{H_2,G} = -\frac{1}{2F} a_{1,2}(1-S)i_{anode}E \quad (3.28)$$

$$i_{anode} = \left[\frac{P_{H_2}}{P_{ref_{H_2}}} \exp\left(\frac{\alpha_a F}{RT}(\phi_1 - \phi_2)\right) - \exp\left(\frac{\alpha_c F}{RT}(\phi_1 - \phi_2)\right) \right] \quad (3.29)$$

The liquid water cathode catalyst reaction can be written as:

$$\nabla \cdot N_{H_2O,L} = -\frac{1}{4F} a_{1,2}(1-S)i_{cathode}E \quad (3.30)$$

$$i_{cathode} = \left[\frac{P_{O_2}}{P_{ref_{O_2}}} \exp\left(\frac{-\alpha_c F}{RT}(\phi_1 - \phi_2 - E_r)\right) \right] \quad (3.31)$$

Where the effectiveness factor is:

$$E = \frac{1}{3\phi^2} (3\phi \coth(3\phi) - 1) \quad (3.32)$$

The Thiele modulus is expressed by:

$$\phi = \zeta \frac{k'}{D_{O_2,agg}^{eff}} \quad (3.33)$$

The kinetic portion of the Thiele modulus is:

$$k' = \frac{\alpha_{1,2} i_{o,orr}}{4F c_{O_2}^{ref}} \exp\left(-\frac{\alpha_c}{RT}(\eta_{cathode})\right) \quad (3.34)$$

One of the main challenges in modeling the catalyst layer is finding reliable parameters. The reference exchange current density, the transfer coefficients, and the reaction order are all dependent on the rate determining step(s) of the complex electrochemical reaction, as well as the electrode microstructure.

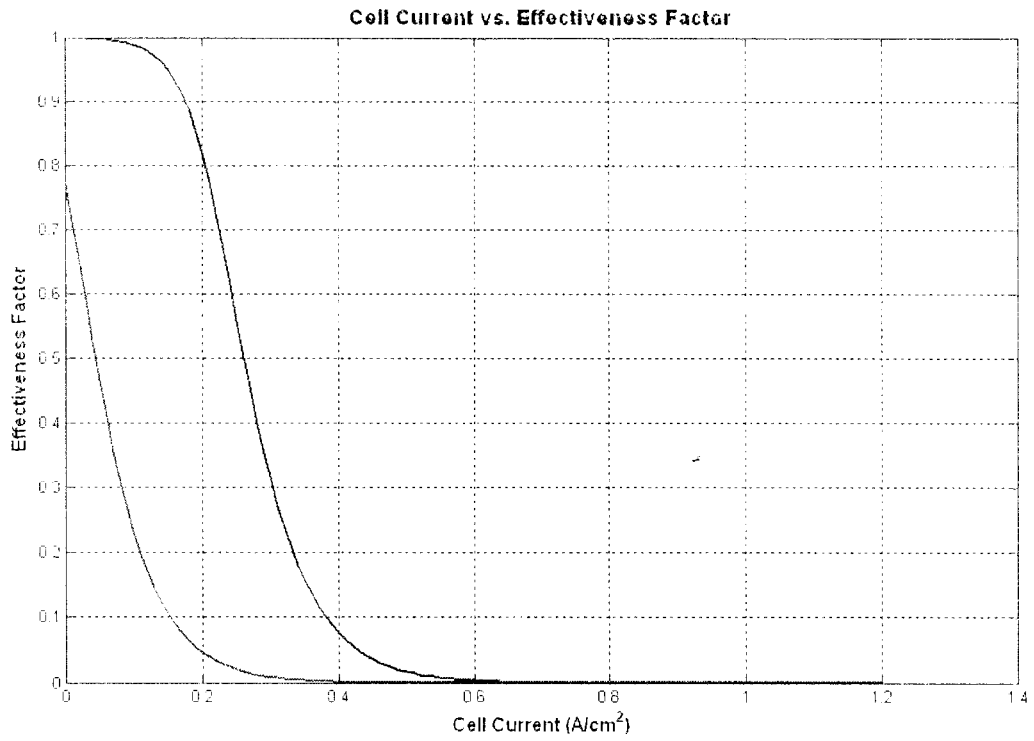


Figure 3.5.A- Cell current as a function of effectiveness factor.

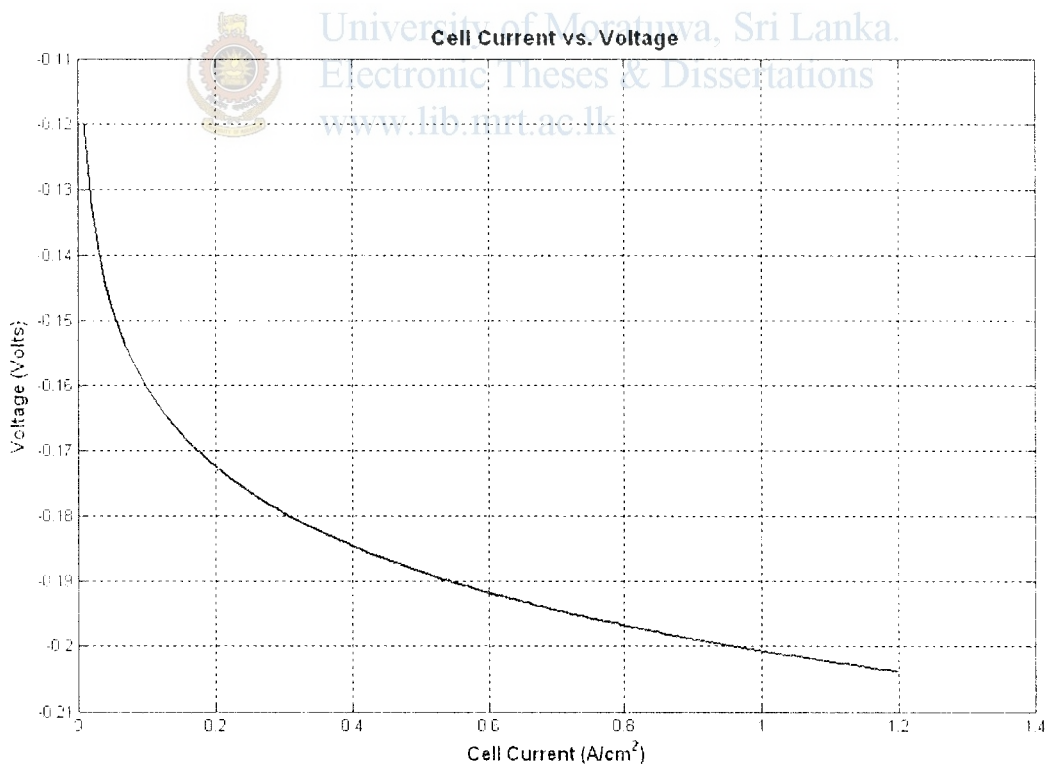


Figure 3.5.B- Butler-Volmer activation losses.

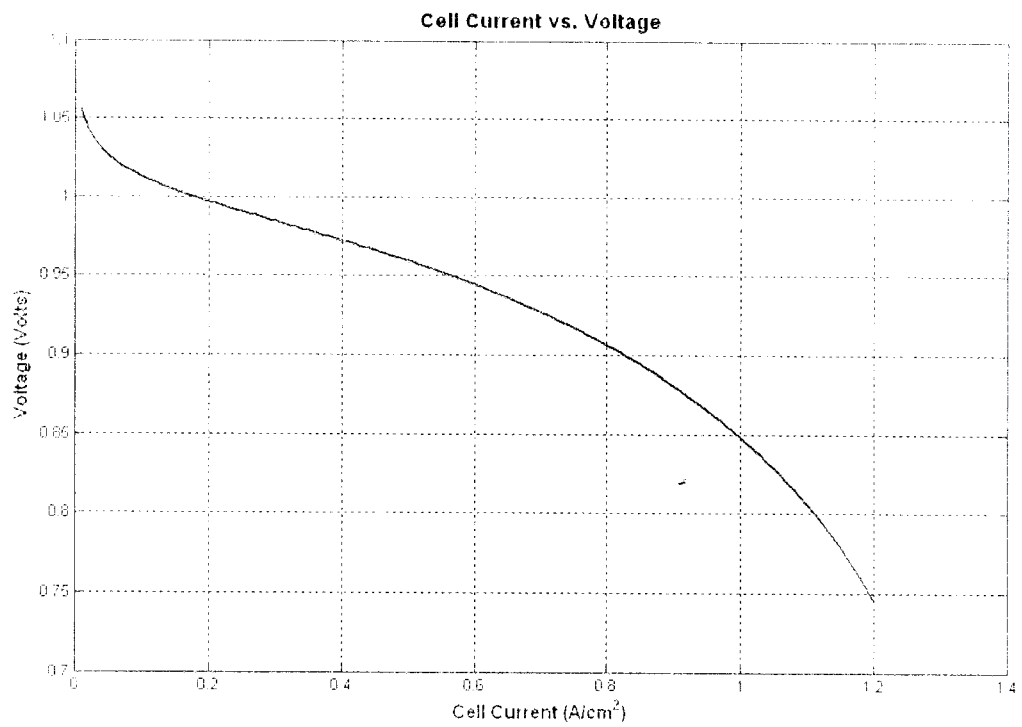


Figure 3.5.C - Polarization curve

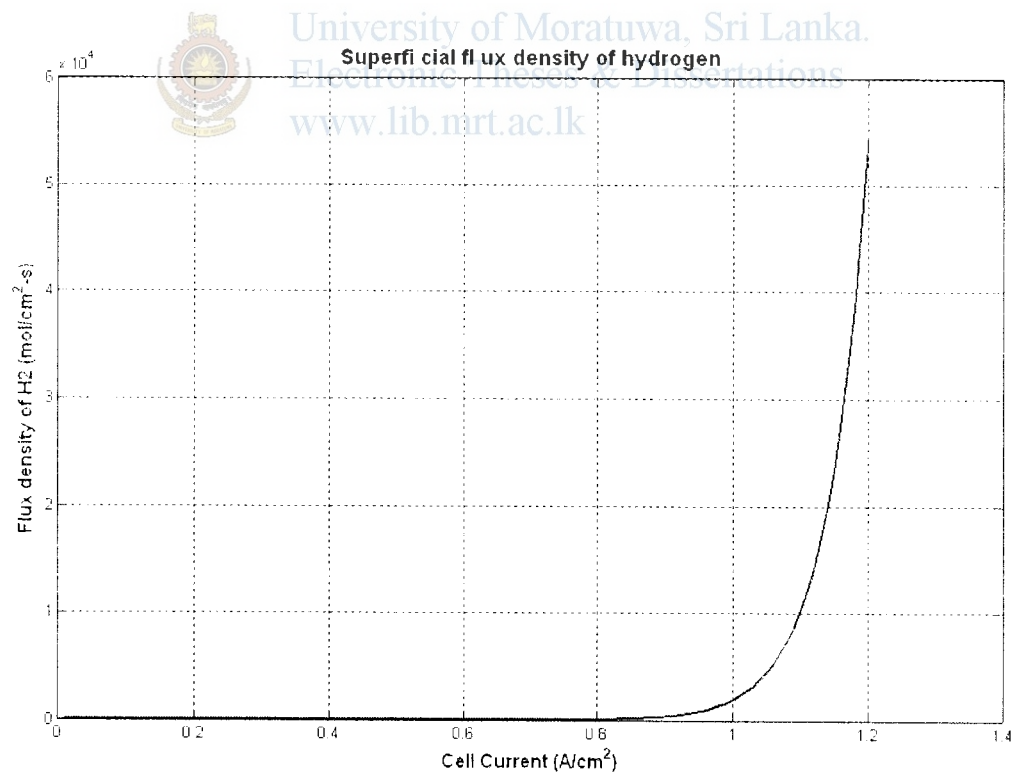


Figure 3.5.D-Superficial flux density of hydrogen.

3.2.5 Calculating the Ohmic Voltage Loss

Every material has an intrinsic resistance to charge flow. The material's natural resistance to charge flow causes ohmic polarization, which results in a loss in cell voltage (Appendix C-C-3). All fuel cell components contribute to the total electrical resistance in the fuel cell, including the electrolyte, the catalyst layer, the gas diffusion layer, bipolar plates, interface contacts, and terminal connections. The reduction in voltage is called "ohmic loss," and includes the electronic (R_{elec}) and ionic (R_{ionic}) contributions to fuel cell resistance. This can be written as:

$$U_{ohmic} = iR_{ohmic} = i(R_{elec} + R_{ionic}) \quad (3.35)$$

R_{ionic} dominates the reaction in Equation because ionic transport is more difficult than electronic charge transport. R_{ionic} represents the ionic resistance of the electrolyte, and R_{elec} includes the total electrical resistance of all other conductive components, including the bipolar plates, cell interconnects, and contacts.

The electrical resistance of the fuel cell components is often expressed in the literature as conductance (σ), which is the reciprocal of resistance:

$$\sigma = 1 / R_{ohmic} \quad (3.36)$$

where the total cell resistance (R_{ohmic}) is the sum of the electronic and ionic resistance. Resistance is characteristic of the size, shape, and properties of the material, as expressed by

$$R = \frac{L_{cond}}{\sigma A_{cond}} \quad (3.37)$$

L_{cond} is the length (cm) of the conductor, A_{cond} is the cross-sectional area (cm²) of the conductor, " σ " is the electrical conductivity (ohm⁻¹ cm⁻¹). The current density, j , (A/cm²), can be defined as

$$j = I / A_{cell} \quad (3.38)$$

$$j = N_{carriers} * q * N_{drift} = s \xi$$

A_{cell} is the active area of the fuel cell, $N_{carriers}$ is the number of charge carriers (carriers/cm³), " q " is the charge on each carrier ($1.6 * 10^{-19}$ C), V_{drift} is the average drift velocity (cm/s) where the charge carriers move ξ is the electric field. The general equation for conductivity is:

$$\sigma = nq \frac{v}{\xi} \quad (3.39)$$

The term v/ξ can be defined as the mobility, u_i . A more specific equation for material conductivity can be characterized by two major factors: the number of carriers available, and the mobility of those carriers in the material, which can be written as:

$$\sigma_i = (|Z_i| * F) * C_i * u_i \quad (3.40)$$

where c_i is the number of moles of charge carriers per unit volume, u_i is the mobility of the charge carriers within the material, z_i is the charge number (valence electrons) for the carrier, and F is Faraday's constant.

Fuel cell performance will improve if the fuel cell resistance is decreased. The fuel cell resistance changes with area. When studying ohmic losses, it is helpful to compare

resistances on a per-area basis using current density. Ohmic losses can be calculated from current density using

$$(3.41)$$

Where ASR_{ohmic} is area-specific resistance of the fuel cell.

Since the ohmic over potential for the fuel cell is mainly due to ionic resistance in the electrolyte, this can be expressed as

$$\text{---} \text{---} \text{---} \quad (3.42)$$

Where “ l ” is the length or thickness of the material. The first term in applies to the anode, the second to the electrolyte, and the third to the cathode. In the bipolar plates, the “land area” can vary depending upon flow channel area. As the land area is decreased, the contact resistance increases since the land area is the term in the denominator of the contact resistance:

$$\text{---} \quad (3.43)$$

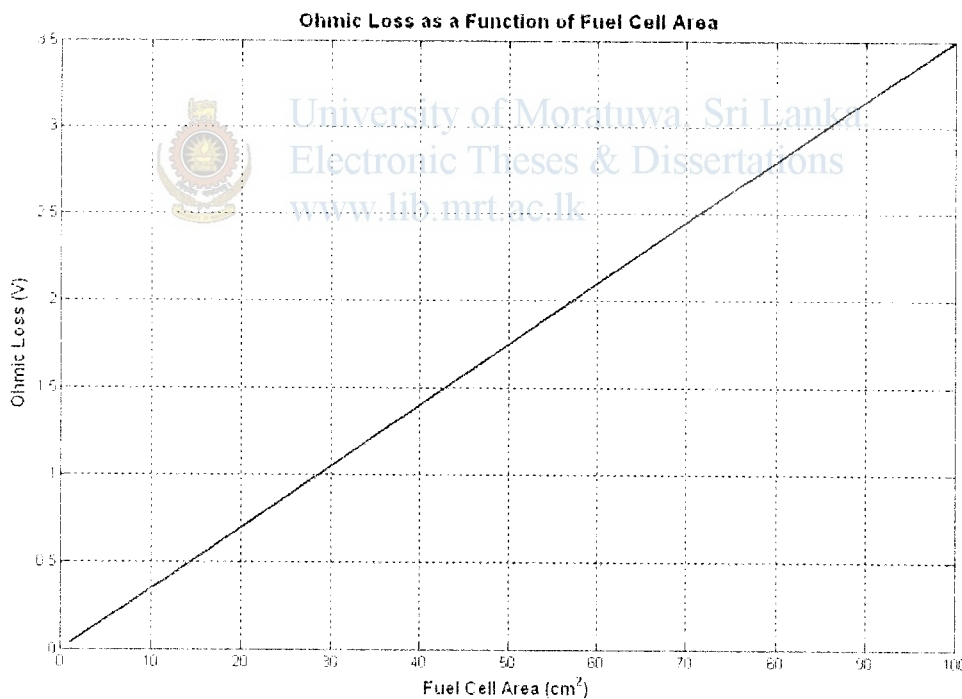


Figure 3.6- Ohmic loss as a function of fuel cell area.

Modeling of PEM Fuel Cell Heat and Pressure

4.1 Fuel Cell Thermodynamics

Thermodynamics is the study of energy changing from one state to another. The predictions that can be made using thermodynamic equations are essential for understanding and modeling fuel cell performance since fuel cells transform chemical energy into electrical energy. Basic thermodynamic concepts allow one to predict states of the fuel cell system, such as potential, temperature, pressure, volume, and moles in a fuel cell.

4.1.1 Entropy of H₂, O₂, and Water in the PEM fuel cell

1. Entropy

Entropy can be defined loosely as the amount of “disorder” in a system, and can be expressed as:

$$S_2 - S_1 = \left[\int_1^2 \frac{\delta Q}{T} \right]_{\text{int rev}} \quad (4.1)$$

This is valid for any reversible process that links two states. Entropy is calculated in the same way that enthalpy was calculated using the properties v , u , and h . When dealing with two-phase liquid-vapor mixtures as in fuel cells, the specific entropy can be calculated in the same manner as enthalpy:

$$S = (1 - X)S_f + XS_g = S_f + X(S_g - S_f) \quad (4.2)$$

Like enthalpy, the values for v , u , and h vary only slightly with changes in pressure at a fixed temperature; therefore, the following can be assumed for most engineering calculations:

$$S(T, p) \approx s_f(T) \quad (4.3)$$

When a pure, compressible system undergoes an internally reversible process in the absence of gravity and overall system motion, an energy balance can be written as:

$$\delta Q_{\text{int rev}} = dU + \delta W_{\text{int rev}} \quad (4.4)$$

In a simple compressible system, the work can be defined as:

$$\delta W_{\text{int rev}} = p \cdot dV \quad (4.5)$$

Substituting previous two equations, one obtains:

$$Tds = dU - pdV = dh - Vdp \quad (4.6)$$

When the ideal gas model is used, the specific entropy depends only upon temperature and can be derived from above Equation, therefore:

(4.7)

(4.8)

Determination of the absolute entropy of H_2 , O_2 , and water (H_2O) at the pressure of 1 atm at a temperature of 300 to 1000 K using increments of 50, using following equations. Plotting of the hydrogen and oxygen enthalpy as a function of temperature by Calculation of the absolute enthalpy for the vapor and liquid form if applicable. The MATLAB code can be used to plot the hydrogen and oxygen Enthalpy as a function of temperature: (Appendix C-C-4)

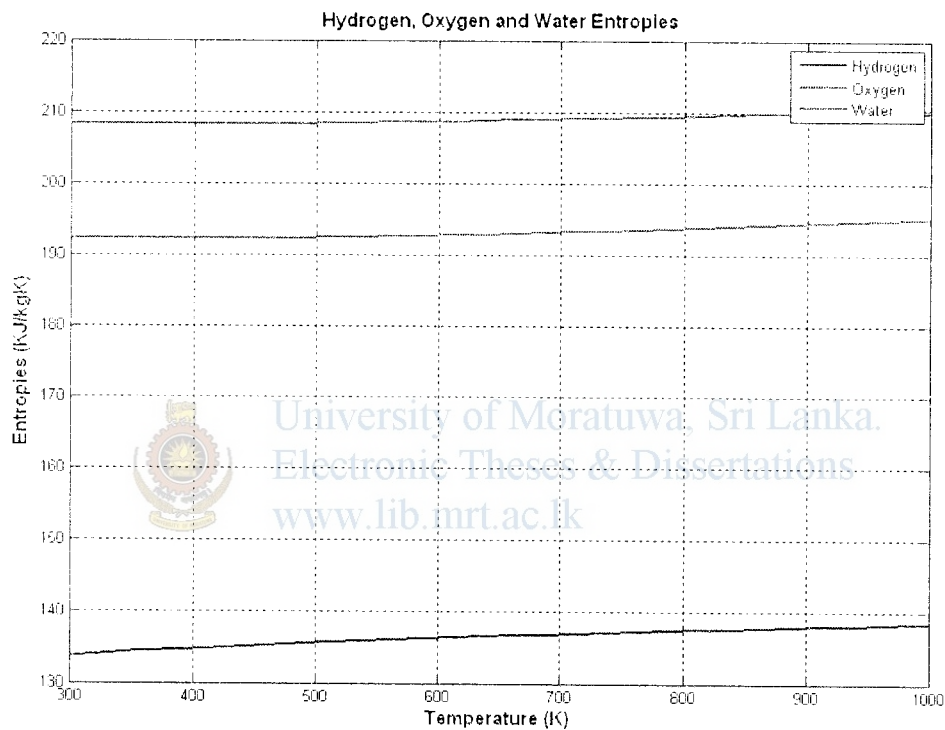


Figure 4.1- Hydrogen and oxygen entropies as a function of temperature.

4.2 Heat Transfer of Fuel cell

Temperature in a fuel cell is not always uniform, even when there is a constant mass flow rate in the channels. Uneven fuel cell stack temperatures are due to a result of water phase change, coolant temperature, air convection, the trapping of water, and heat produced by the catalyst layer. In order to precisely predict temperature-dependent parameters and rates of reaction and species transport, the heat distribution throughout the stack needs to be determined accurately [11] [12]. The determination of the heat distribution in a fuel cell stack is to perform energy balances on the system. The total energy balance around the fuel cell is based upon the power produced, the fuel cell reactions, and the heat loss that occurs in a fuel cell. Convective heat transfer occurs between the solid surface and the gas streams, and conductive heat transfer occurs in the solid and/or porous structures. The reactants, products, and electricity generated are the basic components to consider in modeling basic heat transfer in a fuel cell, as shown in Figure 4.2.

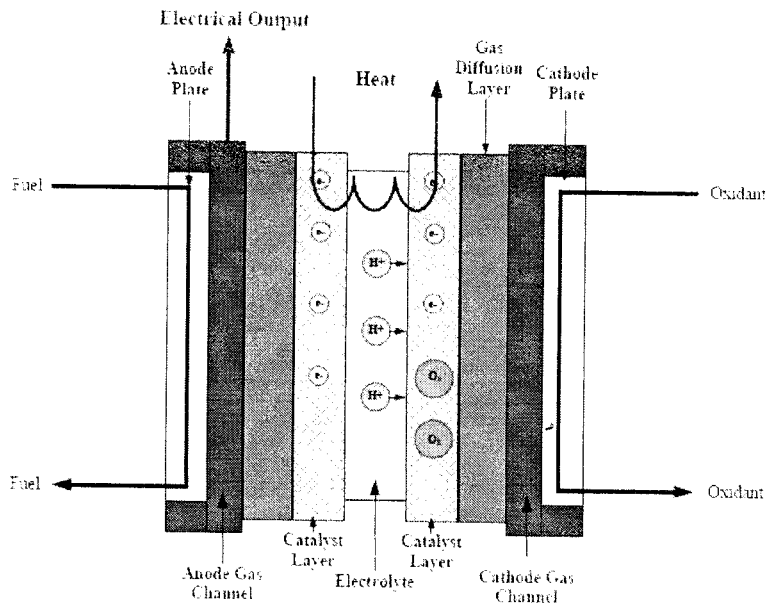


Figure 4.2- Stack illustration for heat flow study

The general energy balance states that the enthalpy of the reactants entering the cell equals the enthalpy of the products leaving the cell plus the sum of the heat generated by the power output, and the rate of heat loss to the surroundings. The basic heat transfer calculations will aid in predicting the temperatures and heat in overall fuel cell stack and stack components. The rate of heat transfer in the x-direction through a finite cross-sectional area, A , is known as Fourier's law, and can be expressed as:

$$(4.9)$$

Where k is the thermal conductivity, $W/(m \cdot K)$.

4.3 Energy Balances for Fuel Cell Layers

Energy balances can be defined around each of the fuel cell layers to enable the study of the diffusion of heat through a particular layer as a function of time or position. Figure 3.9 shows an example of a fuel cell layer as a control volume. This section describes the mode of heat diffusion in each layer, and calculates the energy balances for the end plate, gasket, contact, flow field, GDL, catalyst, and membrane layers [11]. The end plate is typically made of a metal or polymer material, and is used to uniformly transmit the compressive forces to the fuel cell stack. The end plate must be mechanically sturdy enough to support the fuel cell stack, and be able to uniformly distribute the compression forces to all of the major surfaces of each layer within the fuel cell stack. Depending upon the stack design, there also may be contact and gasket layers in the fuel cell stack. The gasket layers help to prevent gas leaks and improve stack compression. The contact layers or current collectors are used to collect electrons from the bipolar plate and gas diffusion layer (GDL). Since there is typically no gas or liquid flows in the end plates, gaskets, or contact layers, conduction is the only mode of heat transfer. One side of each of these layers is exposed to an insulating material (or the ambient environment), and the other side is exposed to a conductive current collector plate or insulating material.

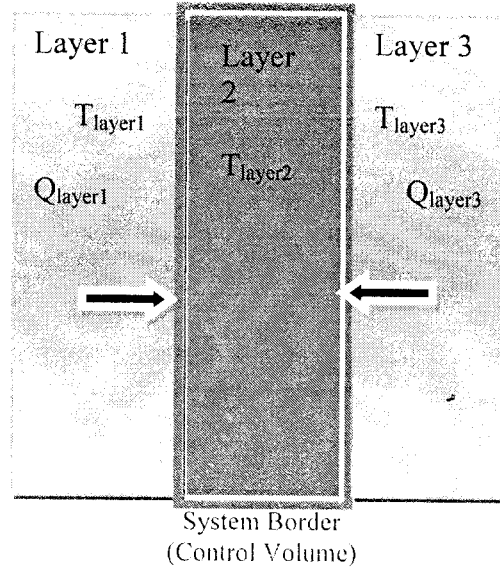


Figure 4.3- fuel cell layer as a control volume

The general energy balance for the end plate, contact, and GDL layers can be written as:

$$(\rho_{\text{Layer2}} A_{\text{Layer2}} t_{\text{layer2}} c_{p\text{Layer2}}) \frac{dT_{\text{Layer2}}}{dt} = Q_{\text{Layer1}} + Q_{\text{Layer3}} \quad (4.10)$$

Where, ρ_{Layer2} is the density of Layer2, A_{Layer2} is the area of Layer2, $c_{p\text{Layer2}}$ is the specific heat capacity of Layer2, Q_{Layer1} is the heat flow from Layer1, and Q_{Layer3} is the heat flow from Layer3.

The derivative on the left side is the rate of change of control volume temperature (dT_{Layer2}/dt). The heat flow from Layer1 to Layer2 is:

$$Q_{\text{Layer1}} = U_{\text{Layer1}} A (T_{\text{Layer1}} - T_{\text{Layer2}}) \quad (4.11)$$

Where, U_{Layer1} is the overall heat transfer coefficient for Layer1, A is the area of the layer, and T is the temperature of the layer. The heat flow from Layer3 to Layer2 can be expressed as:

$$Q_{\text{Layer3}} = U_{\text{Layer3}} A (T_{\text{Layer3}} - T_{\text{Layer2}}) \quad (4.12)$$

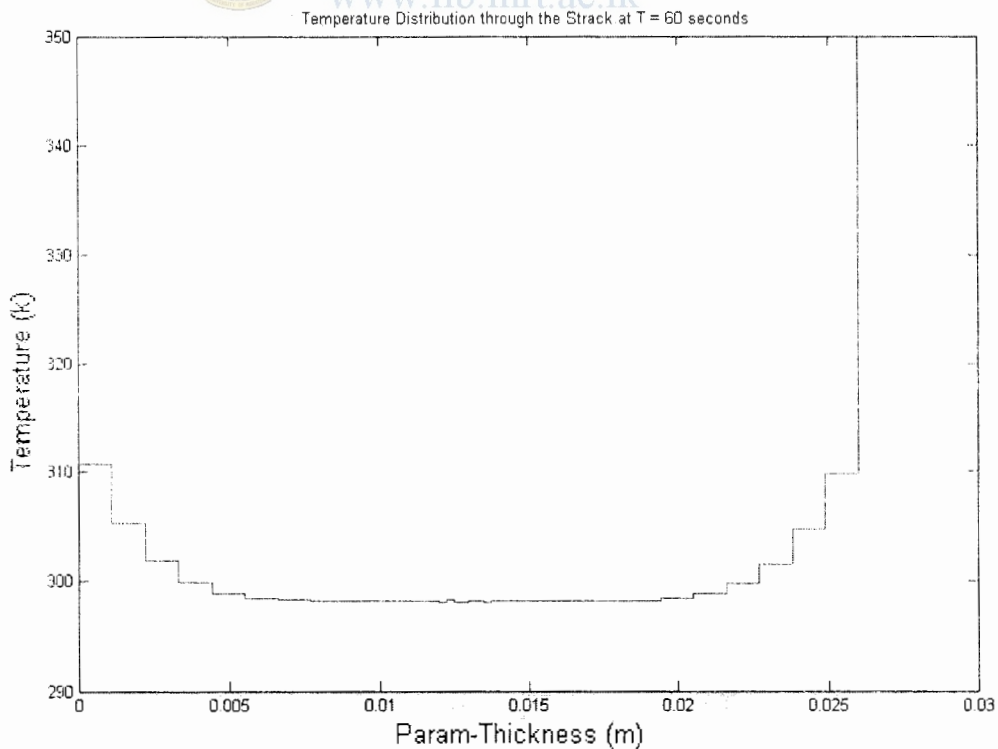
The overall heat transfer coefficient for the heat coming from Layer1 and layer 3

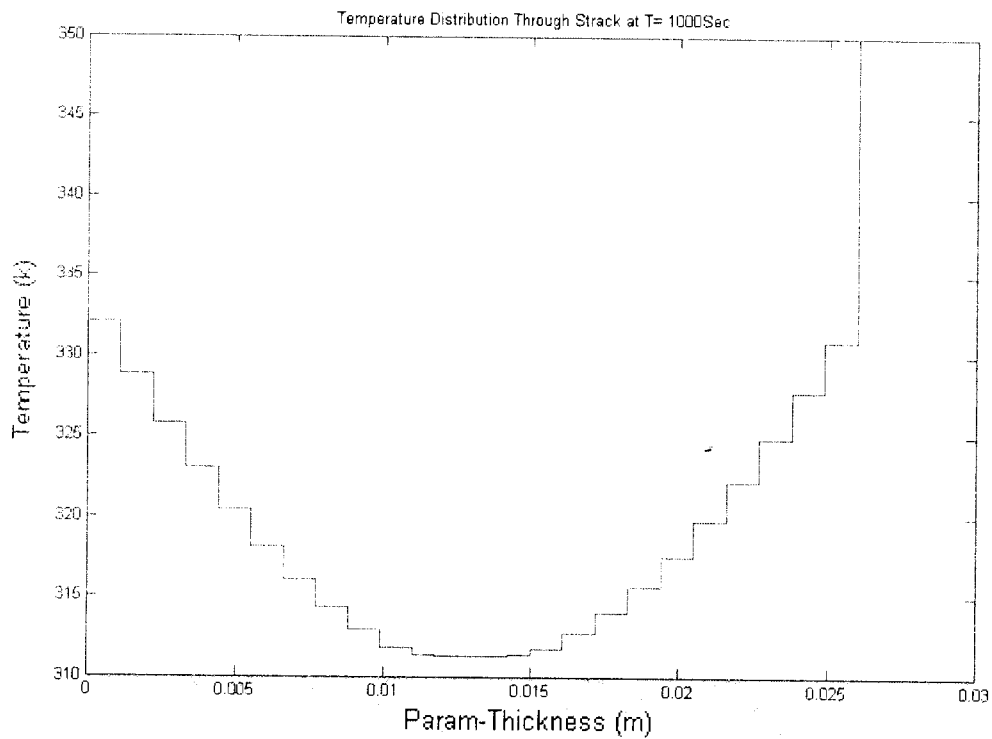
$$U_{\text{Layer1}} = \frac{1}{\frac{t_{\text{Layer2}}}{k_{\text{Layer2}}} + \frac{t_{\text{Layer1}}}{k_{\text{Layer1}}}} \quad U_{\text{Layer3}} = \frac{1}{\frac{t_{\text{Layer3}}}{k_{\text{Layer3}}} + \frac{t_{\text{Layer2}}}{k_{\text{Layer2}}}} \quad (4.13)$$

Table 4.1- Material Properties Used for Heat Transfer Calculations

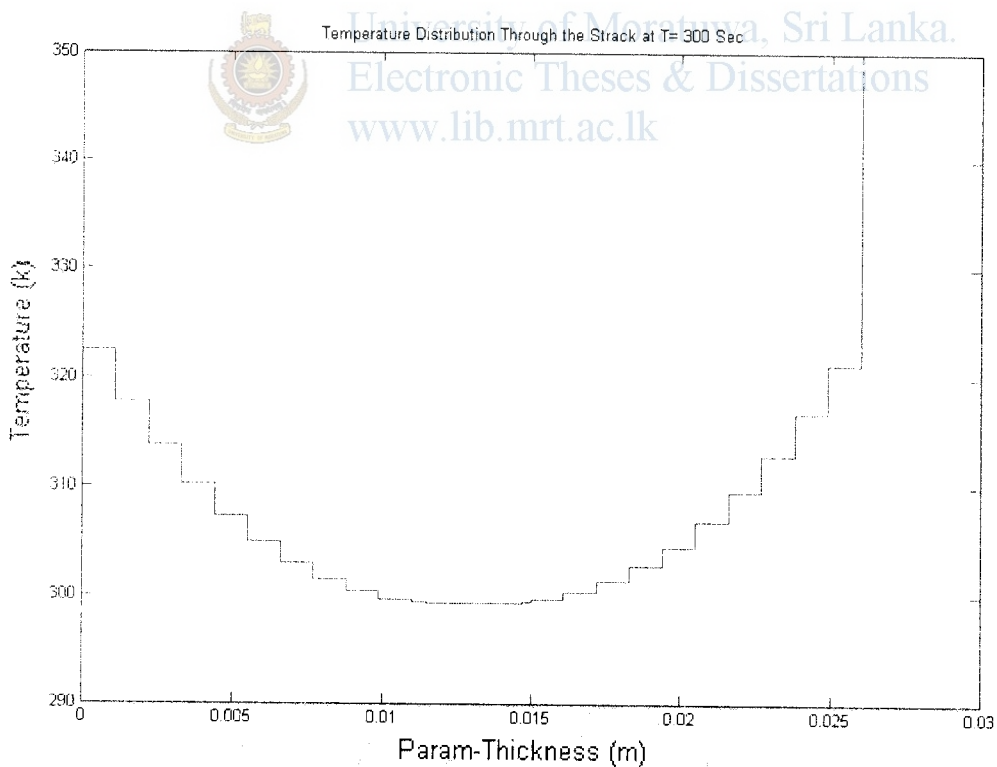
Fuel Cell Layer	Material	Thickness (m)	Area (m ²)	Density (kg/m ³)	Thermal Conductivity (W/m-K)	Specific Heat Capacity (J/kg-K)
End plate	Polycarbonate	0.01	0.0064	1300	0.2	1200
Gasket	Conductive rubber	0.001	0.001704	1400	1.26	1000
Flow field plate	Stainless steel	0.0005	0.003385	8000	65	500
MEA	Carbon cloth/ Pt/C/Nafion	0.001	0.0016	1300	26	864
Flow field plate	Stainless steel	0.0005	0.003385	8000	65	500
Gasket	Conductive rubber	0.001	0.001704	1400	1.26	1000
End plate	Polycarbonate	0.01	0.0064	1300	0.2	1200

Modeling example: A PEM hydrogen/air single cell fuel cell stack operates at an initial temperature of 298.15 K. There are seven layers in the stack: two polycarbonate end plates, two rubber gaskets, stainless steel flow field plates, and an MEA. The necessary material properties for heat transfer calculations for each layer are shown in Table 4.1. Using the equations in Section 3.3.3, plotting of the conductive heat transfer through the stack at 60 sec, 300 sec, and 1000 sec with one and 10 nodes per layer is shown in figure 4.4. Neglect heat generation and losses from thermal resistance, electrochemical reactions, and mass flows through the fuel cell. (Appendix C-C-5). when t=60 sec





When t =300 sec



When t= 1000 sec

Figure 4.4-Temperature plots for t = 60, 300, and 1000 sec using 7 slices per layer.

4.4 Modeling the Temperature in the Interior Layer and Modeling the Gas Diffusion Layer

This section presents the derivations and modeling for the cathode GDL of the fuel cell created by Beuscher et al [8]. The models are derived from multiphase flow in porous media from the hydro geological literature. The differences between the GDL layer and the modeling of unsaturated soils are that the GDL is hydrophobic and soil is hydrophilic, the pore size distributions are different, and the GDL is a non homogeneous weave of carbon fibers. Despite these differences, the hydro geological models are quite useful for fuel cell GDL modeling. However, it sometimes may be difficult to use these models since many properties such as the temperatures, phases, pressure, and the velocity of the species in and surrounding the GDL are unknown parameters while the fuel cell is operating.

The simplified geometry is shown in Figure 4.5. The dashed lines at the top of Figure 4.5 illustrate the portion of the channel where the gas is flowing through. The bottom of the diagram is the catalyst side where heat and water are added to the system, and gas is absorbed. On the upper channel sides, gas is added, and heat and water are removed. Since half of the upper boundary is the solid cathode material, and half is open channel, the boundary conditions are mixed. The portion where there is no flux into the cathode has Neumann boundary conditions, and the portion where there is no liquid water in the channels has Dirichlet boundary conditions. The GDL in Figure 4.5 is $4d$ units long, and h units high. The aspect ratio is the perturbation parameter, and can be defined as $\epsilon = h/d \ll 1$. The lower surface abuts the cathode catalyst layer, and the upper surface is cathode. The channels can be at different pressures, and all quantities are assumed to be steady-state. The three-dimensional plot in MATLAB for the temperature of the interior layer using the equations derived in Appendix A and C-C-6 and the simulation result is shown in figure 4.6 and 4.7.

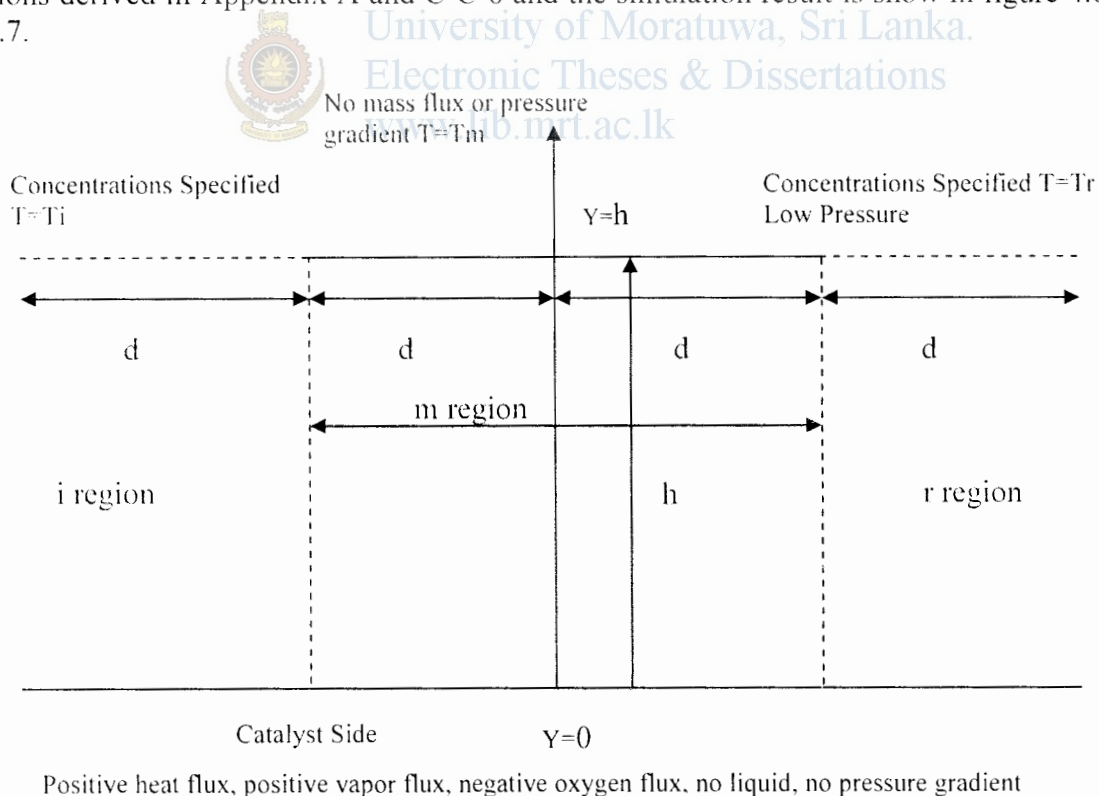


Figure 4.5-The simplified geometry of GDL.

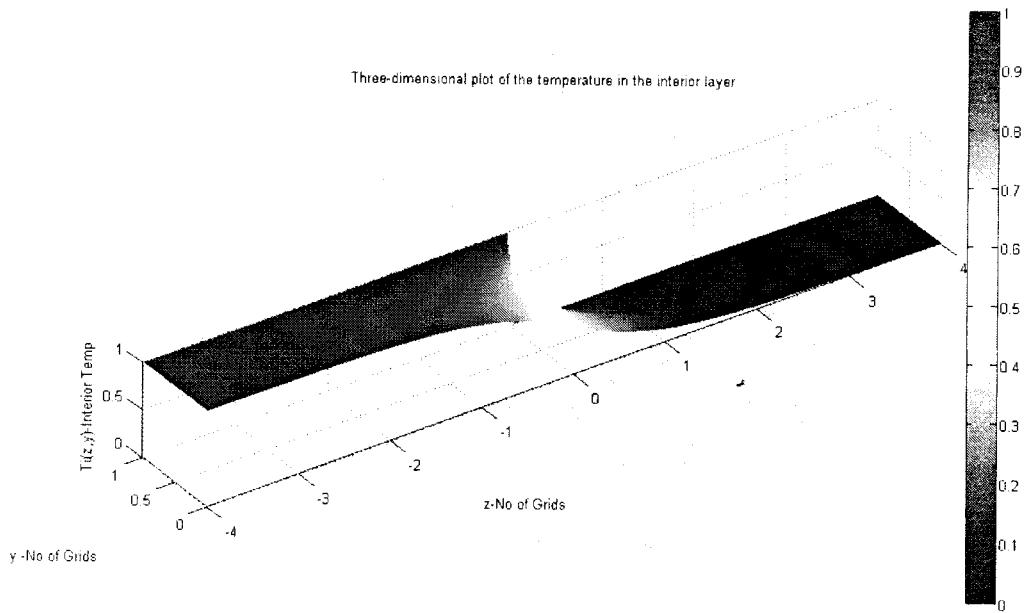


Figure 4.6-3D plot of Temperature variance in Interior Layer

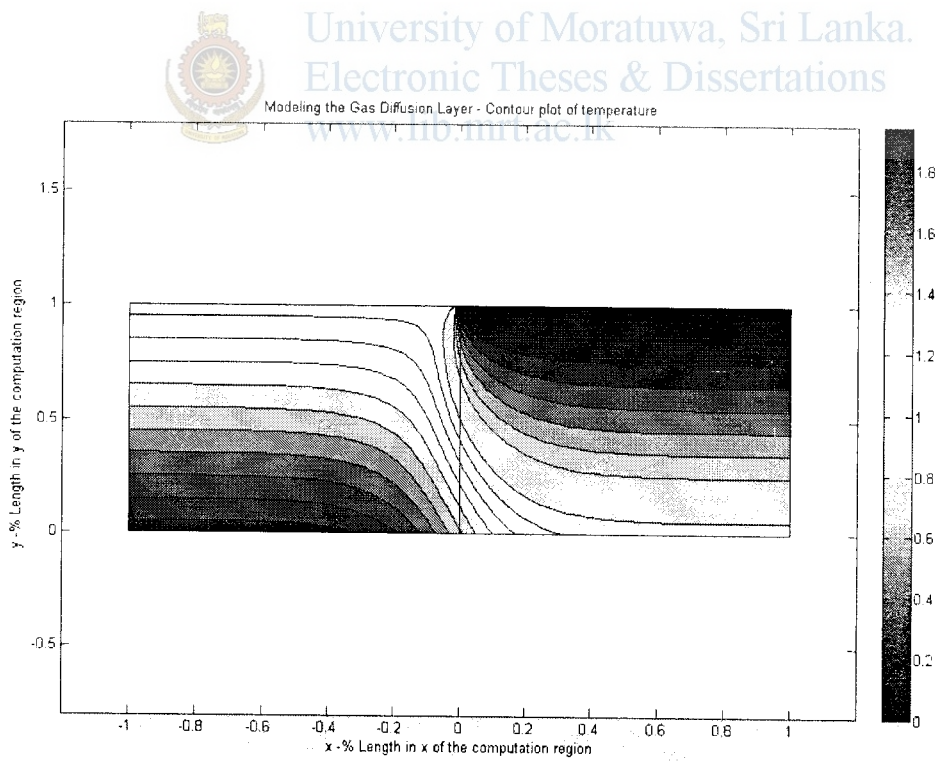


Figure 4.7- Temperature variance in Gas Diffusion Layer

4.5 Pressure Drop in Flow Channels

In many fuel cell types, the flow fields are usually arranged as a number of parallel flow channels; therefore, the pressure drop along a channel is also the pressure drop in the entire flow field. In a typical flow channel, the gas moves from one end to the other at a certain mean velocity. The pressure difference between the inlet and outlet drives the fluid flow. By increasing the pressure drop between the outlet and inlet, the velocity is increased. The flow through bipolar plate channels is typically laminar, and proportional to the flow rate. The pressure drop can be approximated using the equations for incompressible flow in pipes

$$\Delta P = f \frac{L_{chan}}{D_H} \rho \frac{\bar{V}^2}{2} + \sum K_L \rho \frac{\bar{V}^2}{2} \quad (4.14)$$

Where f is the friction factor, L_{chan} is the channel length, m, D_H is the hydraulic diameter, m, ρ is the fluid density, kg/m³, \bar{V} is the average velocity, m/s, and K_L is the local resistance. The hydraulic diameter for a circular flow field can be defined by:

$$D_H = \frac{4 \times A_c}{P_{cs}} \quad (4.15)$$

Where A_c is the cross-sectional area, and P_{cs} is the perimeter. For the typical rectangular flow field, the hydraulic diameter can be defined as:

$$D_H = \frac{2 w_c d_c}{w_c + d_c} \quad (4.16)$$

Where w_c is the channel width, and d_c is the depth. The channel length can be defined as:

$$L_{chan} = \frac{A_{cell}}{N_{ch}(W_c + W_L)} \quad (4.17)$$

where A_{cell} is the cell active area, N_{ch} is the number of parallel channels, w_c is the channel width, m, and W_L is the space between channels, m. The friction factor can be defined by:

$$f = \frac{56}{Re} \quad (4.18)$$

The velocity at the fuel cell entrance is:

$$v = \frac{Q_{stack}}{N_{cell} N_{ch} A_{ch}} \quad (4.19)$$

where v is the velocity in the channel (m/s), Q_{stack} is the air flow rate at the stack entrance, m³/s, N_{cell} is the number of cells in the stack, N_{ch} is the number of parallel channels in each cell, and A_{ch} is the cross-sectional area of the channel.

The total flow rate at the stack entrance is:

$$Q_{stack} = \frac{1}{4F} \frac{S_{O_2}}{r_{O_2}} \frac{RT_{in}}{P_{in} - \Phi P_{sat}(T_{in})} N_{cell} \quad (4.20)$$

where Q is the volumetric flow rate (m³/s), I is the stack current, F is the Faraday's constant, S_{O_2} is the oxygen stoichiometric ratio, r_{O_2} is the oxygen content in the air, R is the universal gas constant, T_{in} is the stack inlet temperature, P_{in} is the pressure at the stack inlet, Φ is the relative humidity, P_{sat} is the saturation pressure at the given inlet temperature, and N_{cell} is the number of cells in the stack. By combining the previous equations, the velocity at the stack inlet is:

$$v = \frac{1}{4F} \frac{S_{O_2} (W_c + W_L) l_{chan}}{r_{O_2} W_c d_c} \frac{RT}{P - \phi P_{sat}} \quad (4.21)$$

Liquid or gas flow confined in channels can be laminar, turbulent, or transitional and is characterized by an important dimensionless number known as the Reynold's number (Re). This number is the ratio of the inertial forces to viscous forces and is given by:

$$Re = \frac{\rho v_m D_{ch}}{\mu} = \frac{v_m D_{ch}}{\nu} \quad (4.22)$$

Where V_m is the characteristic velocity of the flow (m/s), D_{ch} is the flow channel diameter or characteristic length (m), r is the fluid density (kg/m³), μ is the fluid viscosity [kg/(m * s or N * s/m²)], and ν is the kinematic viscosity (m²/s). When Re is small (<2300), the flow is laminar.

The flow rate at the stack outlet is usually different than the inlet. If it is assumed that the outlet flow is saturated with water vapor, the flow rate is:

$$Q_{stack} = \frac{1}{4F} \left(\frac{S_{O_2}}{r_{O_2}} - 1 \right) \frac{RT_{out}}{P_{in} - \Delta P - \phi P_{sat}(T_{out})} N_{cell} \quad (4.23)$$

Fuel cell gas streams are rarely composed of a single species. Usually, they are gas mixtures, such as oxygen and nitrogen from the air. The following expression provides a good estimate for the viscosity of a gas mixture:

$$\mu_{max} = \sum_{i=1}^N \frac{X_i \mu_i}{\sum_{j=1}^N X_j \phi_{ij}} \quad (4.24)$$

Where ϕ_{ij} is a dimensionless number obtained from

$$\phi_{ij} = \frac{1}{\sqrt{8}} \left(1 + \frac{M_i}{M_j} \right)^{-1/2} \left[1 + \left(\frac{\mu_i}{\mu_j} \right)^{1/2} \left(\frac{M_i}{M_j} \right)^{1/4} \right]^2 \quad (4.25)$$

Where N is the total number of species in the mixture, x_i and x_j are the mole fractions of species i and j, and M_i and M_j are the molecular weight (kg/mol) of species i and j. For porous flow fields, the pressure drop is determined by Darcy's law:

$$\Delta P = \mu \frac{Q_{cell}}{k A_c} L_{chan} \quad (4.26)$$

Where μ is the viscosity of the fluid, Q_{cell} is the geometric flow rate through the cell, m³/s, K is the permeability, m², A_c is the cross-sectional area of the flow field, m², and L_{chan} is the length of the flow field.

The modeling of pressure drop through a PEM fuel cell cathode flow field of a single graphite plate with 100-cm² cell area. The stack operates at 3 atm at 60 °C with 100% saturated air. The flow field consists of 24 parallel serpentine channels 1 mm wide, 1 mm deep, and 1 mm apart. The cell operates at 0.7 A/cm² at 0.65 V. the result output is given as shown in Appendix C-C-7.

Chapter 5

PEM Fuel cell special Features

5.1 Comparison between batteries and fuel cells for photovoltaic system backups

The energy storage devices, batteries continue to be applied to electric power utilities for drawing benefits of peak shaving and load leveling. Battery energy storage facilities provide the utilities additional dynamic benefits such as voltage and frequency regulation, load following, spinning reserve, and power factor correction [25] [26]. Applications of the storage batteries to power systems are predicted to grow in the future due to those benefits coupled with the ability to provide peak power.

Fuel cell power generation is another attractive option for providing power for electric utilities and commercial buildings because of its high efficiency and environmentally benign feature. This type of power production is especially economical (i) where potential users are faced with high cost in electric power generation from coal or oil, (ii) where environmental constraints are stringent, or (iii) where load constraints of transmission and distribution systems are so tight that their new installations are not possible.

Photovoltaic power outputs vary depending mainly upon solar insolation and cell temperature. Since control of the ambient weather conditions is beyond human beings' capability, it is almost impossible for human operators to control the PV power itself. Thus, a PV power generator may sometimes experience sharp output power fluctuations owing to intermittent weather conditions, which causes control problems such as load frequency control, generator voltage control and even system stability analysis. There is, therefore, a need for backup power facilities in the PV power generation. Batteries and fuel cells are the most likely technologies to provide the PV system with backup power because these two backup power sources contain some distinct features in common. Those characteristics are listed below.

- A. Fast Load-Response Capability
- B. Modularity in Production
- C. Highly Reliable Sources
- D. Flexibility in Site Selection (Environmental Acceptability)

Comparison between battery backup and fuel cell backup for PV power supplement is made in the following sections.

1. Efficiency

Power generation in fuel cells directly convert available chemical free energy to electrical energy rather than going through heat exchange processes. Thus, it can be said that fuel cells are a more efficient power conversion technology than the conventional steam-applying power generations. Electricity, the conventional power generator has several steps for electricity generation and each step requires a certain amount of energy loss. Fuel cell power systems have around 40-60% efficiencies depending on the type of electrolytes and independent of size. Battery power systems themselves have high energy efficiencies, but their overall system efficiencies from raw fuel (mostly coal or nuclear) through the batteries

to converted ac power are reduced to below 30%. This is because energy losses take place whenever one energy form is converted to another.

2. Capacity Variation

As the battery discharges, its terminal voltage gradually decreases. The fall of the terminal voltage on discharge is due to its internal resistance. However, the internal resistance of a battery varies with its cell temperature and state of discharge. Fuel cell systems have a greater efficiency at full load and this high efficiency is retained as load diminishes, so inefficient peaking generators may not be needed.

3. Flexibility in Operation

Fuel cells have an advantage over storage batteries in the respect of operational flexibility. Batteries need several hours to be taken for recharging after they are fully discharged. During discharge the batteries' electrode materials are lost to the electrolyte, and the electrode materials can be recovered during the recharging process. Fuel cells, on the other hand, do not undergo such material changes. The fuel stored outside the cells can quickly be replenished, so they do not run down as long as the fuel can be supplied.

4. Cost

The history of fuel cell equipment costs has shown that the price of fuel cells has dropped significantly as the commercial market grows and the manufacturing technology becomes mature.

5.2 Efficiency and hydrogen consumption Efficiency

The efficiency of a fuel cell system is defined as the percentage of the fuel that is converted to electric energy. This is made by comparing the output electric energy with the consumed chemical energy. The common value of chemical energy is the lower heating value (LHV) of the fuel. High efficiency means low hydrogen consumption. A fuel cell system that delivers 1000 W net power will consume hydrogen according to the table

$$Efficiency = \frac{Electricity}{Fuel} \tag{5.1}$$

Table 5.1 - Efficiency and hydrogen consumption

Efficiency-%	Hydrogen(nl/min)	Hydrogen (g/h)
35	17.1	86.0
40	14.9	75.3
45	13.3	66.9
50	11.9	60.2

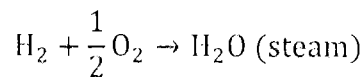
Previously shown that it was the 'Gibbs free energy' that is converted into electrical energy. This energy would be converted into electrical energy, and the efficiency could be said to be 100%. However, this is the result of choosing one among several types of 'chemical energy' and can be indicated the following that it also changes with pressure and other factors. All in all, to define efficiency as

$$Efficiency = \frac{Electrical\ energy\ produced}{Gibbs\ free\ energy\ change} \tag{5.2}$$

This is not very useful, and is rarely done, as whatever conditions are used the efficiency limit is always 100%. Since a fuel cell uses materials that are usually burnt to release their energy, it would make sense to compare the electrical energy produced with the heat that would be produced by burning the fuel. This is sometimes called the *calorific value*, though a more precise description is the change in ‘enthalpy of formation’. Its symbol is $\Delta\bar{h}_f$. As with the Gibbs free energy, the convention is that $\Delta\bar{h}_f$ is negative when energy is released. So to get a good comparison with other fuel-using technologies, the efficiency of the fuel cell is usually defined as 2.3

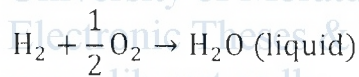
$$\text{Efficiency} = \frac{\text{Electrical energy produced per mole of fuel}}{-\Delta\bar{h}_f} \quad (5.3)$$

However, even this is not without its ambiguities, as there are two different values that we can use for $\Delta\bar{h}_f$. For the ‘burning’ of hydrogen



$$-\Delta\bar{h}_f = -241.83 \text{ kJmol}^{-1}$$

Whereas if the product water is condensed back to liquid, the reaction is



$$\Delta\bar{h}_f = -285.84 \text{ kJmol}^{-1}$$

The difference between these two values for $\Delta\bar{h}_f$ (44.01 kJ mol⁻¹) is the molar enthalpy of vaporization of water. The higher figure is called the *higher heating value* (HHV), and the lower, quite logically, the ‘lower heating value’ (LHV). Any statement of efficiency should say whether it relates to the higher or lower heating value. If this information is not given, the LHV has probably been used, since this will give a higher efficiency figure. It is clear that there is a limit to the efficiency as defined it as in equation 2.3. The maximum electrical energy available is equal to the change in Gibbs free energy, so

$$\text{Maximum Efficiency possible} = \frac{\Delta\bar{g}_f}{\Delta\bar{h}_f} \times 100\% \quad (5.4)$$

This maximum efficiency limit is sometimes known as the ‘thermodynamic efficiency’. Table 5.2 gives the values of the efficiency limit, relative to the HHV, for a hydrogen fuel cell.

Table-5.2 Efficiency Limits for PEMFC

Form of water product	Temperature C	$\Delta\bar{g}_f$ kJmol ⁻¹	Max EMF - V	Efficiency limit %
Liquid	25	-237.2	1.23	83
Liquid	80	-228.2	1.18	80
Gas	100	-225.2	1.17	79
Gas	200	-220.3	1.14	77
Gas	400	-210.3	1.09	74
Gas	600	-199.6	1.04	70
Gas	800	-188.6	0.98	66
Gas	1000	-177.4	0.92	62

$\Delta\bar{g}_f$, maximum EMF (or reversible open circuit voltage), and efficiency limit(HHV basic) for hydrogen fuel cells

5.3 Efficiency and the Fuel Cell Voltage

It is clear from Table 2.2 that there is a connection between the maximum EMF of a cell and its maximum efficiency. The operating voltage of a fuel cell can also be very easily related to its efficiency. This can be shown by adapting equation 5.5.

$$E = \frac{-\Delta\bar{g}_f}{2F} \quad (5.5)$$

If all the energy from the hydrogen fuel, its 'calorific value', heating value, or enthalpy of formation, were transformed into electrical energy, then the EMF would be given by

$$E = \frac{-\Delta\bar{h}_f}{2F} = 1.48 \text{ V if using the HHV or } 1.25 \text{ if using the LHV} \quad (5.6)$$

These are the voltages that would be obtained from a 100% efficient system, with reference to the HHV or LHV. The actual efficiency of the cell is then the actual voltage divided by these values, or

$$\text{Cell Efficiency} = \frac{V_c}{1.48} 100\% \text{ (with reference to HHV)} \quad (5.7)$$

However, in practice it is found that not all the fuel that is fed to a fuel cell can be used, for reasons discussed later. Some fuel usually has to pass through un-reacted. A fuel utilization coefficient can be defined as

$$\mu_f = \frac{\text{mass of fuel reacted in cell}}{\text{mass of fuel input to cell}} \quad (5.8)$$

This is equivalent to the ratio of fuel cell current and the current that would be obtained if all the fuel were reacted. The fuel cell efficiency is therefore given by

$$\text{Efficiency, } \eta = \mu_f \frac{V_c}{1.48} 100\% \quad (5.9)$$

5.4 Why is the efficiency not 100%

All energy conversions will lead to a certain amount of degradation of energy quality. All input energy will not come out as output. Some of the energy will be lost as heat. Fuel cell development work aims to maximize the output by minimizing the losses. The losses could be traced to either the stack or the components of system. The fuel cell stack converts the chemical energy to electric energy. The electrochemical process and the conductance of current will however lead to losses and heat generation. These losses always increase at high current outtake. Stack design and operating conditions could be optimized to reduce the losses. There are two kinds of losses at system level: Fuel losses and electric losses. The fed hydrogen will be converted to electricity in the stack. Small amounts of hydrogen will however be purged out of the system. This fuel will represent a minor loss that must be considered when establishing the efficiency. The last thing to consider is the internal components of the system. They will consume some of the power delivered from the stack. Components like the air blower, cooling pump, cooling fans, valves and control circuits will support the stack and consume electric power. The net power delivered from the system will be slightly lower than the gross power from the stack, because of the internal consumption. The overall efficiency of the system takes all these losses into account.

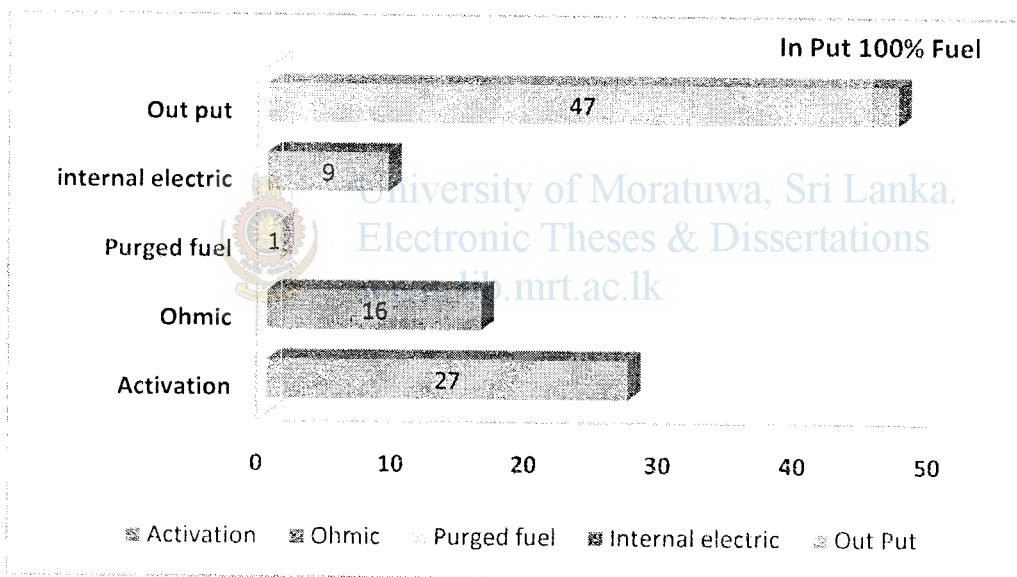


Figure-5.1 The overall losses in PEMFC system

5.6 Implementation of PEMFC system

5.6.1 Solar Hydrogen PEM Fuel cell system for a home

The development of a hydrogen economy can have many benefits for the environment. It could play a role in reducing global warming and air quality problems in and around major cities. A large percentage of the pollution that contributes to these issues is easily traced to the power demands of buildings and the emissions of vehicles. Provided hydrogen can be produced from renewable resources at reasonable costs, the use of hydrogen fuel cell technology in buildings and vehicles would effectively eliminate a major contribution to air pollution problems and global warming.

Table-5.3 The Properties of Fuel cells

Fuel Cell	Electrolyte	Operating Temperature	Electrical Efficiency	Fuel Oxidant
Alkaline FC AFC	Potassium hydroxide(KOH) solution	Room temperature to 90C	60-70%	H ₂ , O ₂
Proton Exchange Membrane FC PEMFC	Proton Exchange membrane	Room temperature to 80C	40-60%	H ₂ , O ₂ , Air
Direct Methanol FC DMFC	Proton exchange membrane	Room temperature to 130C	20-30%	CH ₃ OH, O ₂ , Air
Phosphoric acid FC PAFC	Phosphoric acid	160-220C	55%	Natural gas, biogas, H ₂ , O ₂ , Air
Molten Carbonate FC MCFC	Molten mixture of alkali metal carbonates	620-660	65%	Natural gas, biogas, Coal Gas, H ₂ , O ₂ , Air
Solid Oxide FC SOFC	Oxide ion conducting ceramic	800-1000C	60-65%	Natural gas, biogas, Coal Gas, H ₂ , O ₂ , Air

The cost of solar hydrogen production needs to be competitive with similar hydrogen production processes for it to be successful in the hydrogen market. As a prototype, constructing a system today is relatively expensive. However, efficient and cost effective design and mass production can significantly reduce future production costs. The projected cost for such a system will be evaluated and compared to similar hydrogen production systems. Table 5.4 shows the cost analysis of solar hydrogen PEM fuel cell system for a single home.

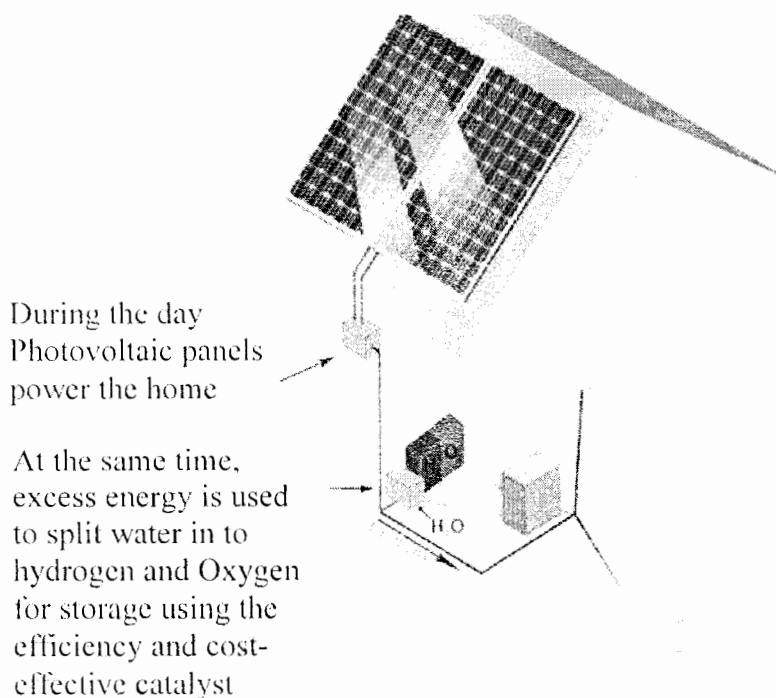


Figure 5.2- Solar hydrogen Fuel cell system for a Home

Table 5.4- Cost analysis of a solar hydrogen Fuel cell system for a Home

Power needed	1200	kwh/yr
Fraction coverage	98	%
AC output needed	0.75	kw
Module area	15.00	sqft
Area needed	183	sqft
Modules	12	
Power per module	65	watts
DC power	793	watts
Inverter efficiency	94	%
AC power	746	watts
Module cost rate	\$2.10	watt
Module Cost	\$1,666	
Inverter cost rate	\$0.50	watts
Inverter cost	\$397	
Installation cost rate	\$1.00	per watt
Installation cost	\$793	
Fuel backup days	2	day
Fuel storage needed	7	kwh
Fuel cell cost rate	\$125	kwh
Fuel cell cost + Gas St'ge + relifef valves+ tubings	\$3,500	
FC replacement time	15	yr
Total cost	\$6,356	
Capacity factor	18	%
CA equiv array	1576.8	kwh/year/kw
Output per year	1176	kwh
Degradation rate	-0.10	%/yr
Maintenance cost per year per kw	\$10.00	
Maintenance cost per year FC	\$233.33	
Maintenance cost per year	\$7	yr
Maintenance cost per year w/ FC	\$241	yr

Output after year:	25	50	75	100
%	97.5	95.1	92.8	90.5
Total power delivered - kwh	29037	57356	84977	111914
Cost w/ maint w/out FC	\$6,543	\$6,729	\$6,916	\$7,102
Cost per kwh amortized w/out FC	\$0.23	\$0.12	\$0.08	\$0.06
Cost including maintenance w/ FC	\$12,376	\$18,396	\$24,416	\$30,435
Cost per kwh amortized w/ FC	\$0.43	\$0.32	\$0.29	\$0.27
Typical CO2 emission from oil	583	kg/MWh		
Power per lifetime per MW of PV (MWh)	39420	78840	118260	157680
Emissions saved (kg)	16928	33439	49541	65246
Typical gas consumption per MWh	125	gal		
Gas saved (gal)	3630	7170	10622	13989

5.6.2 Solar Hydrogen PEM Fuel cell Basic model

The solar hydrogen FC set contains two fuel storage cylinders, reversible PEMFC unit and the load(motor).Reversible PEMFC can act as both electrolyzer mode and Fuel cell mode. The solar module converts radiant energy into electrical energy to power the electrolyser. The electrolyser breaks water into its basic constituents of hydrogen and oxygen. These gases are stored in the graduated cylinders. When electrical power is required, the PEM fuel cell recombines the stored gases to form water, and release heat and electricity. The systematic fuel cell unit is shown in figure 5.3.

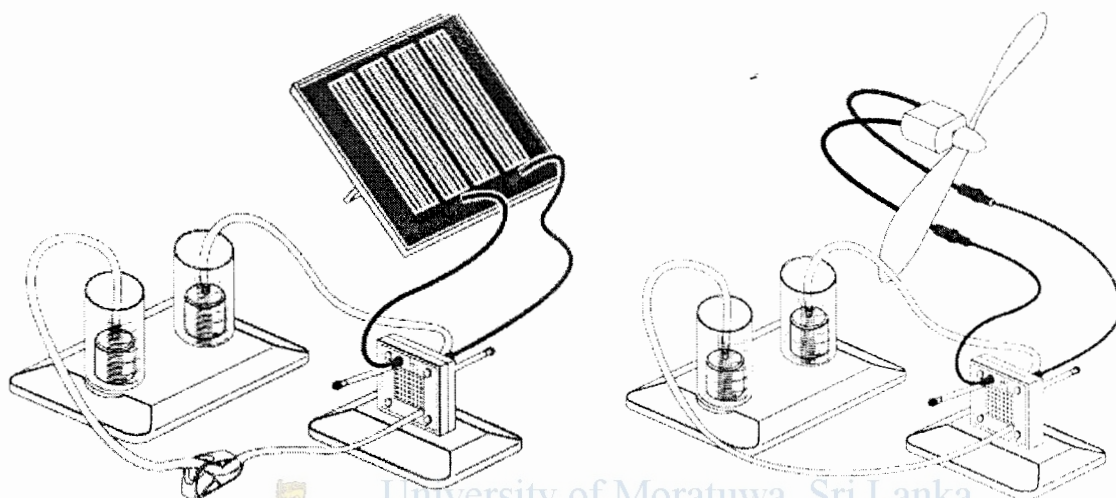


Figure 5.3- Fuel cell basic model; Electrolyzer mode -Left and FC mode-right

5.6.2 PEMFC Stack principle

Table 5.5- PEMFC Experimental data

Len gth	Heig ht	Area cm ²	Current		No of Stacks	Voltage		Power=VI	
				Amp			Volts		Watt
1	1	1	0.5	Amp	1	0.03	Volts	0.015	Watt
1	2	2	1	Amp	1	0.06	Volts	0.06	Watt
2	2	4	2	Amp	1	0.12	Volts	0.24	Watt
4	4	16	8	Amp	1	0.48	Volts	3.84	Watt
5	5	25	12.5	Amp	1	0.75	Volts	9.375	Watt
6	6	36	18	Amp	1	1.08	Volts	19.44	Watt
5	6	30	15	Amp	1	0.9	Volts	13.5	Watt
4	6	24	12	Amp	1	0.72	Volts	8.64	Watt
3	3	9	4.5	Amp	1	0.27	Volts	1.215	Watt

According to the table 5.5, the fuel cell dimensions and its corresponding power output is given. In the third column it shows the fuel cell stack area depending on its length and height. According to the stack principle the data is calculated. The standard stack principle is given as "Once cell (anode +membrane cathode) can deliver 0.6 voltages. To get enough power out of the fuel cell, several calls are piled in a stack. Gas plates are placed between the cells to distribute the hydrogen and oxygen gas to the membranes. The area of the membrane gives the current.1 cm² delivers 0.5 Amp".

Table 5.6 shows the experimental data of PEM electrolyzer outputs. Table shows the Hydrogen and oxygen production due to the water electrolyzing. Also it shows the comparison between reversible actions of PEMFC.

Table 5.6- Electrolyzer Output Data

<i>Elec 'zer Pow er-W</i>	<i>Char geing Time Mins</i>	<i>No of cells in Elzr</i>	<i>Produ ced O2- cm3</i>	<i>Prod uced H2 - cm3</i>	<i>FC out put</i>		<i>Wor king time- min</i>	<i>Ele'zer I/P- Wmin</i>	<i>FC O/P Wmin</i>
1	2	1	7.5	15	500	mW	8	2	4
1	1	1	3.75	7.5	500	mW	8	1	4
1	4	1	15	30	500	mW	8	4	4
3	1	3	11.25	22.5	1500	mW	24	3	36
2	2	2	15	30	1000	mW	16	4	16
50	10	50	1875	3750	25000	mW	400	500	10000

5.6.3 Fuel cell Concept model Vehicle

The Model of a hydrogen car with a regenerative fuel cell shows in figure 5.12. The Fuel Cell Car works with a regenerative fuel cell. The cell can both be a Fuel Cell and electrolyser cell. This system contains following components as shown in figure 5.12.

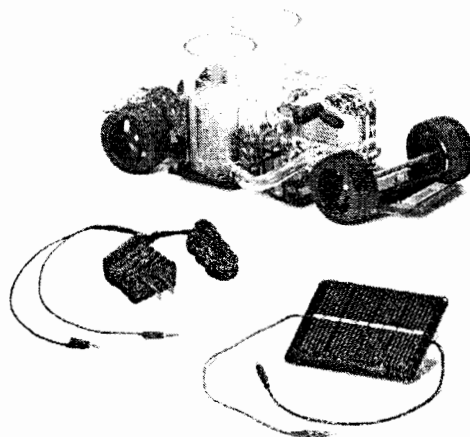


Figure 5.4-Fuel cell Concept car

- 1) Two cylinders with fuel storing containers
- 2) Reversible fuel cell
- 3) Controlling system with motor
- 4) Solar module
- 5) Connecting tubes and connectors

Once the solar module converts radiant energy into electrical energy to power the electrolyzer, it starts to produce hydrogen and oxygen in the storages. Reversing of the electrolyzer is a Fuel cell which converts both fuels in to electricity.

Technical data:

Power 1 W (electrolyzer mode), 500 mW (fuel cell mode), Gas storage 15 cm³ H₂; 15 cm³ O₂. HxWxD 75x90x200 mm (3"x3 1/2"x7 5/6"), Weight: 260 g, This system has Approximately 2 minutes charging time and 8 minutes running time.



University of Moratuwa, Sri Lanka.
Electronic Theses & Dissertations
www.lib.mrt.ac.lk

Chapter 6

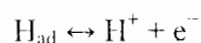
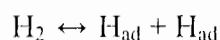
Conclusion

While fuel cell is a unique and fascinating system, the accurate system selection, design, and modeling for prediction of performance are needed to obtain optimal performance and design. In order to make strides in performance, cost, and reliability, one must possess an interdisciplinary understanding of electrochemistry, materials, manufacturing, and mass and heat transfer. Accurately modeling the PEM layer can help improve the properties of future membrane materials.

There are many types of PEM models, and choosing the right one depends upon the end goals and resources available. In order to have an accurate model, mass, energy, and charge balances must be written for the fuel cell membrane layer. In addition to these, using an empirical relationship for membrane water content may save time when creating a model. The requirements for the membrane include high ionic conductivity, adequate barrier to the reactants, and chemically and mechanically stable and low electronic conductivity. There are many choices for the PEM in the fuel cell, and the decision regarding the type chosen must depend upon many factors including, most importantly, cost and mass manufacturing capabilities. Understanding the reactions at the fuel cell anode and cathode is critical when modeling fuel cells.

Usage of a mathematical model to define the useful terms of fuel cell and its components helps one to derive the use full modeling foundation. According the research which is done on hydrogen and fuel cell describes under three sections as given below.

- 1) The chapter 3 covered the basic electrochemistry needed to predict electrode kinetics, activation losses, currents, and potentials in a fuel cell. The electrochemical reactions control the rate of power generation and are the main cause of activation voltage losses. The activation overvoltage is the voltage loss due to overcoming the catalyst activation barrier in order to convert products into reactants. The equations presented in this chapter help to predict how fast the reactants are converted into electric current, and how much energy loss occurs during the actual electrochemical reaction.
 - I. Accordingly derived here are the following issues for designing of improved and better fuel cells. Basically electrolysis of water effectively any and efficiently into H₂ and O₂ at low cost is specific. It was so justified here.
 - II. Basic electro kinetic concepts have been established. Here the actual reactions proceed through many steps and intermediate species. Anodic reaction is specific.



III. Activation loss, Ohmic Loss and Voltage losses are next important factors established.

$$V_{act} = -b * \log\left(\frac{i}{i_0}\right) \quad \text{where } b = \frac{R * T}{2 * \alpha * F}$$

$$V_{Ohmic} = -(i * r)$$

$$V = E_{Nernst} + V_{act} + V_{ohmic} + V_{conc}$$

Accordingly simulation was carried out for the given real time data as shown in Example 3.1 in page 33. According to the above situation, its useful to study about the electrochemistry of fuel cell as it helps to identify the electrical behavior of Fuel cell. The simulated polarization curve of FC voltage loss describes how the electrical energy is drawn from the fuel cell, the actual cell voltage drops from the theoretical voltage due to several irreversible loss mechanisms such as activation polarization, ohmic polarization and concentration polarization. Therefore, the operating voltage of the cell can be represented as the departure from ideal voltage caused by these polarizations. To develop the better and efficient output, the gap between operating voltage and ideal voltage should be reduced.

Modeling catalyst layer is also established (Table 3.2), together with the following parameters and the steps are given below. Likewise, reliable parameters were established for the modeling of catalyst layer. Thus, assumptions are also satisfied

- The first step is to calculate the Nernst voltage and voltage losses
- The partial pressure of hydrogen and Oxygen
- The voltage losses will now be calculated
- The ohmic losses (see Chapter 4) are estimated using Ohm's law
- The Nernst voltage can be calculated using the following equation

$$E_{Nernst} = -\frac{G_{f,liq}}{2 * F} - \frac{R * T_k}{2 * F} * \ln\left(\frac{P_{H_2O}}{P_{H_2} * P^{1/2}_{O_2}}\right)$$

- The actual voltage is the addition of the Nernst voltage plus the voltage losses

$$V = E_{Nernst} + V_{act} + V_{ohmic} + V_{conc}$$

- The calculation of effectiveness factor is extracted as a justification of the search

$$E = \frac{1}{3\phi^2} (3\phi \coth(3\phi) - 1)$$

Modeling of Effectiveness factor due to the mass transfer and reaction of H₂ and O₂ versus current density also shows how the behavior of effectiveness of H₂ and O₂ with reference to the current density is. The effectiveness factor deals with the actual rate of reaction of particular fuel with the rate of reaction with losses as mentioned above. To normalize the effectiveness factors of fuel cell the modeling and simulation are highly helpful. In the meanwhile the power curve represents the abnormal behavior in the increase in current density. That is also due to the several irreversible mechanisms in fuel cell. It was clearly demonstrated here.

Voltage loss as a function of cell area clearly shows how important the fuel cell membrane area is. According to the graph, it is clear that voltage loss is directly proportional to the area of the membrane. To avoid the voltage loss the less area of fuel cell membrane can be used to gain high output.

2) The study of thermodynamics and its relation to fuel cells is very important for predicting fuel cell performance. The determination of fuel cell potential and efficiency depends heavily on the evaluation of thermodynamic properties. Some of the important properties explored in the chapter 4 include the enthalpy, specific heat, entropy, Gibbs free energy, reversible voltage, net output voltage, and the fuel cell efficiency. The following factors for modeling were searched and established were as follows with the heat transfer calculations given in the Table 4.1.

1. Entropy of H₂, O₂, and water in the PEM cell
2. Heat transfer of fuel cell
3. Energy balances for fuel cell layers

The geometrical model for Gas Diffusion layer (GDL) is extremely helpful for modeling of interior heat distribution. These thermodynamic concepts allow one to predict states of the fuel cell system, such as potential, temperature, pressure, volume, and moles in a fuel cell. Learning and applying these concepts are the bases of all fuel cell modeling and analysis, and is essential for understanding the remainder of this thesis.

The basic behavior of heat inside the fuel cell is very complicated to understand as the heat produced in FC reaction is negligible. But when the FC system comes as a large, the heat behavior is considerable. In such a situation the modeling of heat transfer inside the fuel cell is highly valuable. In FC technology the only output which can be considered as non environmental friendly is heat. Therefore the simulation of FC interior is helpful to eliminate the heat distribution inside it. In such a situation external cooling systems or self-cooling agents can be introduced for better output.

3) In many fuel cell types, the flow fields are usually arranged as a number of parallel flow channels; therefore, the pressure drop along a channel is also the pressure drop in the entire flow field. In a typical flow channel, the gas moves from one end to the other at a certain mean velocity. The pressure difference between the inlet and outlet drives the fluid flow. By increasing the pressure drop between the outlet and inlet, the velocity is increased. In such a situation the modeling of FC channel properties, the pressure drop can be simulated to identify the flow fields. Fuel flowing manner inside the channel is highly important in FC output. In such a situation the external pressure controlling unit can be introduced to control and regulate the fuel flow.

The pressure drop calculation as a justification is done with the following equation extracted, with the help of relevant parameters.

$$\Delta P = f \frac{L_{chan}}{D_H} \rho \frac{\bar{v}^2}{2} + \sum K_L \rho \frac{\bar{v}^2}{2}$$

- 4) The chapter 5 highlights the real world applications and experimental data. Under this chapter basic proton exchange membrane fuel cell stack principle is discussed with the real time experimental details along with the solar hydrogen FC basic model and Fuel cell concept model vehicle. Cost estimation for solar hydrogen fuel cell basic model for home is discussed.

The basic FC concept is new to the Srilanka as well as to the southern region of Asia. It is really important to identify the reasons why the FC technology is not absorbed by this region. According to the nature of environmental condition in southern region of Asia, it is obvious that the input resource can be generated easily. The major input resource: hydrogen can be easily electrolyzed by using the solar power or wind power. Therefore the only impossible target is the membrane material (Nifion). As the Nifion is a chemical polymer it is so costly to produce or buy. Other than to that the developer can turn in to the possible substitute for the said material. Established here are the following factors for the comparison between batteries and fuels cells

- Fuel cell power systems have around 40-60% efficiencies depending on the type of electrolytes and independent of size. Battery power systems themselves have high energy efficiencies, but their overall system efficiencies from raw fuel (mostly coal or nuclear) through the batteries to converted ac power are reduced to below 30%. The actual efficiency of the cell is then the actual voltage divided by these values, or

$$\text{Cell Efficiency} = \frac{V_c}{1.48} 100\% \text{ (with reference to HHV)}$$

The Figure 5.1 shows why the Fuel cell efficiency does not reach 100%.

- Fuel cells have an advantage over storage batteries in the respect of operational flexibility. Batteries need several hours to be taken for recharging after they are fully discharged. Fuel cells, on the other hand, do not undergo such material changes. The fuel stored outside the cells can quickly be replenished, so they do not run down as long as the fuel can be supplied
- The history of fuel cell equipment costs has shown that the price of fuel cells has dropped significantly as the commercial market grows and the manufacturing technology becomes mature.

Basing on the above issues mathematically, the practical model was designed basically to justify that the fuel cell system is possible partially as a substitute for fuel crisis in world.

References:

- [1] Committee on Alternatives and Strategies for Future Hydrogen Production and Use, National Research Council.2004, '*The Hydrogen Economy: Opportunities, Costs, Barriers, and R&D Needs.*' The National Academy Press. Washinton D C.
- [2] International Energy Agency, and Organization for Economic Co-operation and Development.2008.World Energy Outlook.
- [3] Elena, C. and Ene, H. 1996, '*computational fluid dynamics analysis of a PEM fuel cell system for power generation*' National Research Institute for Isotopic & Cryogenic Technologies, Rm Valcea, Romania Mathematical Institute, Romanian Academy of Sciences, Bucharest, Romania.
- [4] Piergiorgio, A. Massimo G. and Federico, M. 2005, '*A coupled electro-chemical model of a direct methanol fuel cell for portable electronic devices*' Dipartimento di Ingegneria Elettrica, Universita' di Padova, Padova, Italy.
- [5] Energy Information Administration, International Energy Outlook 2008, Washington DC. (No. DOE/EIA-0484). Retrieved January 25, 2009.
- [6] Hydrogen – Facts Sheet,2008, '*Mini hydrogen*' Denmark.
- [7] Bates, B. C. Kundzewicz, Z. W. Wu S. and Palutikof, J. P. 2008, '*Climate Change and Water*' Technical Paper of the Intergovernmental Panel on Climate Change, IPCC Secretariat, Geneva, 210 pp. Retrieved February 8, 2009.
- [8] Hegerl, G. C. Zwiers F. W. Braconnot, P. Gillett,N. P. Luo,Y. J.A. Marengo, O. Nicholls,N. and Stott, P.A. 2007, '*Understanding and Attributing Climate Change*' In:Climate Change , New York.
- [9] Spiegel, C.S. 2007, '*Designing and Building Fuel Cells*' McGraw-Hill, New york .
- [10] Spiegel, C.S. 2008. '*PEM Fuel Cell Modeling and Simulation Using MATLAB*' Elsevier Science, New york.
- [11] Zawodzinski, T.A. Derouin, C. Radzinski, S. Sherman, R. J. Smith, V.T. Springer, E. and Gottesfeld, S. 1993, 'Water uptake by and transport through Nafion 117 membranes,' *Journal of the Electrochemical Society*' **140**(4), 1041–1047.
- [12] Barbir, F.1999, Fuel cell powered utility vehicles. *Proceedings of the European Fuel Cell Forum Portable Fuel Cells Conference*, Lucerne.
- [13] Chase, M. W. 2002, '*JANAF Thermochemical Tables*' 3rd ed, American Chemical Society and the American Institute for Physics, '*J. Physical and Chemical Reference Data*' Vol. 14, Supplement 1.
- [14] Chen, R. and Zhao, T. S. 2005, Mathematical modeling of a passive feed DMFC with heat transfer effect.' *J. Power Sources.*' Vol. 152.

- [15] Faghri, A. and Guo, Z. 2005, Challenges and opportunities of thermal management issues related to fuel cell technology and modeling. *Int. J. Heat Mass Transfer*, Vol. 48.
- [16] Samuel, T. D. M. A. 1991, Estimation of Global Radiation for Sri Lanka. *Solar Energy* 47(5): 333-337.
- [17] Samuel, T. D. M. A. and Srikanthan, R. Solar Radiation Estimation for Sri Lanka. 1982. *Transactions of the Institution of Engineering, Sri Lanka*.
- [18] Maxwell, E.L. 1998, METSTAT -The solar radiation model used in the production of the NSRDB. *Solar Energy*.
- [19] Marion, W. and George, R. Calculation of solar radiation using a methodology with worldwide potential. 2001 *Solar Energy*
- [20] Marion, W. and Urban, K. 1995, User's manual for TMY2s—typical meteorological years derived from the 1961-1990 National Solar Radiation Data Base. NREL/SP-463-7668. National Renewable Energy Laboratory, Golden, Colorado.
- [21] *Sri Lanka Wind Resource Atlas* NREL/TP-500-34518, National Renewable Energy Laboratory, Golden, Colorado, 2003.
- [22] *Feasibility Study for a 3 MW Pilot Wind Farm in Sri Lanka* RLA Consulting, Inc., Bothell, Washington, March 1997.
- [23] Fernando K.S. Kariyawasam P. L. G. Alwis A M A. 2002, *Wind Energy Resource Assessment – Puttalam and Central Regions of Sri Lanka*, Ceylon Electricity Board, Colombo, Sri Lanka.
- [24] *Long Term Transmission Development Studies 2002 – 2011* Ceylon Electricity Board, Colombo, Sri Lanka, August 2002.
- [25] Hurwitch, J. W. and Carpenter, C. A. 1999, 'Technology and Application Options for Future Battery Power Regulation', *IEEE Transactions on Energy Conversion*, Vol. 6, No. 1, pp. 216-223.
- [26] Kottick, D. Blau, M. and Edelstein, D. 1993, 'Battery Energy Storage for Frequency Regulation in an Island Power System', *IEEE Transactions on Energy Conversion*, Vol. 8, No. 3, pp. 455-458.

APPENDIX- A : GDL (gas diffusion layer) Modeling

The pressure, P , temperature, T , oxygen concentration, u , water vapor concentration, v , and liquid-water volume fraction, θ , will be calculated. All of the variables will be functions of θ . Since the physical process exhibited is the same as in the transport of groundwater in unsaturated porous media, the governing equation is Richard's equation, which gives the moisture velocity (V_θ) of liquid and vapor in porous media. The general form of the equation is:

$$V_\theta = -K_\theta(\theta)\nabla\psi \quad \text{A-1}$$

where K_θ is the hydraulic conductivity of the GDL to the liquid water, and ψ is the moisture potential. Since the non hysteretic case is considered, θ will be a single-valued function of ψ only ($\psi = \psi(\theta)$). Assuming incompressibility (the density of water is constant), the conservation equation becomes:

$$\nabla \cdot V_\theta = \Sigma \quad \text{A-2}$$

where Σ is the source term introduced to incorporate condensation and evaporation

$$\nabla \cdot (-K_\theta(\theta)\nabla\psi) = \Sigma \quad \text{A-3}$$

The diffusion coefficient of water can be defined by:

$$D_\theta(\theta) = K_\theta(\theta) \frac{d\psi}{d\theta} \quad \text{A-4}$$

Evaporation is a temperature-dependent process and is modeled using Arrhenius' law:

$$\text{Evaporation} \propto \exp\left[\frac{-E_A}{RT}\right] \theta \quad \text{A-5}$$

Introducing the constant of proportionality, β_θ , for evaporation and β_v for condensation:

$$\beta_\theta \exp\left[\frac{-E_A}{RT}\right] \theta + \beta_v \hat{v} = \Sigma \quad \text{A-6}$$

Therefore, this becomes:

$$\nabla \cdot [D_\theta(\theta)\nabla\psi] - \beta_\theta \exp\left[\frac{-E_A}{RT}\right] \theta + \beta_v \hat{v} = 0 \quad \text{A-7}$$

For the gases (oxygen), either Fickian diffusion, or the Stefan-Maxwell equation can be used to describe the diffusion processes. Fick's equation for diffusion and transport is:

$$\nabla \cdot [D_u(\theta)\nabla_{\tilde{u}} - \tilde{u}\tilde{V}_g] = 0 \quad \text{A-8}$$

where \tilde{V}_g is the velocity of the gas phase, and D_u is the diffusion coefficient of oxygen. In order to model the vapor transport, the evolution of the vapor phase of water must include convection:

$$\nabla \cdot [D_u(\theta)\nabla_{\tilde{u}} - \tilde{u}\tilde{V}_g] + \nu_1 \left[\beta_\theta \exp\left[\frac{-E_A}{RT}\right] \theta + \beta_v \right] = 0 \quad \text{A-9}$$

where D_u is the diffusion coefficient of the water vapor, and ν_1 is a normalization factor. The evaporation term produces vapor and the condensation term removes it.

No Liquid Governing Equations

In the case that there is no liquid, all of the terms due to q are neglected. Also, condensation and evaporation terms drop out of the equations. If the gas phase convects, the velocity is governed by Darcy's law:

$$\vec{V}_g = \frac{-K_g(\theta)}{\mu} \nabla \bar{P} \quad \text{A-10}$$

where k_g is the permeability of the GDL to gases and μ is the viscosity of the gas. The permeability k_g depends upon q because liquid water will remove the available pore space for the gas. In order to solve for pressure, the continuity equation can be used:

$$\nabla \cdot \vec{V}_g = 0, \quad \nabla \cdot \left[\frac{-K_g(\theta)}{\mu} \nabla \bar{P} \right] = 0 \quad \text{A-11}$$

Since q has been dropped, $k_g(\theta)$ is a constant:

$$\frac{K_g(\theta)}{\mu} \nabla \cdot \nabla \bar{P} = 0 \quad \text{A-12}$$

Equation A-13 now becomes:

$$D_u \cdot \nabla \cdot (\nabla \tilde{u}) - \nabla \cdot (\tilde{u} \vec{V}_g) = 0 \quad \nabla \cdot \tilde{u} + \frac{K_g(\theta)}{\mu D_u} \left[\frac{\partial \tilde{u}}{\partial \tilde{x}} \cdot \frac{\partial \bar{P}}{\partial \tilde{x}} + \frac{\partial \tilde{u}}{\partial \tilde{y}} \cdot \frac{\partial \bar{P}}{\partial \tilde{y}} \right] = 0 \quad \text{A-13}$$

The condensation and evaporation term is dropped because of the no liquid assumption.

$$\nabla \cdot \tilde{v} + \frac{K_g(\theta)}{\mu D_v} \left[\frac{\partial \tilde{v}}{\partial \tilde{x}} \cdot \frac{\partial \bar{P}}{\partial \tilde{x}} + \frac{\partial \tilde{v}}{\partial \tilde{y}} \cdot \frac{\partial \bar{P}}{\partial \tilde{y}} \right] = 0 \quad \text{Equation A-16 becomes: } \nabla^2 \cdot \tilde{T} = 0 \quad \text{A-14}$$

The governing equations and boundary conditions motivate the following dimensionless parameters:

$$X = \frac{\tilde{x}}{d}, \quad Y = \frac{\tilde{y}}{d}, \quad u = \frac{\tilde{u}}{u_1}, \quad v = \frac{\tilde{v}}{v_1}, \quad T(X,Y) = \frac{T(\tilde{X},\tilde{Y}) - T_m}{T_1 - T_m}, \quad P(x,y) = \frac{2\bar{P}(\tilde{X},\tilde{Y}) - (P_1 + P_r)}{P_1 + P_r} \quad \text{A-15}$$

Substituting these into the previous equations:

$$Pe_u = \frac{K_g U_1 (P_1 + P_r)}{2\mu D_u} \quad \text{A-16}$$

Where Pe is the Peclet number for the oxygen. When v is replaced with u , then:

$$Pe_v = \frac{K_g U_1 (P_1 + P_r)}{2\mu D_v}, \quad \frac{(T_1 - T_m)}{d^2} \frac{\partial^2 y}{\partial x^2} + \frac{(T_1 - T_m)}{h^2} \frac{\partial^2 r}{\partial y^2} = 0, \quad \frac{h^2}{d^2} \frac{\partial^2 y}{\partial x^2} + \frac{\partial^2 r}{\partial y^2} = 0 \quad \text{A-17}$$

Substituting into:

$$\varepsilon^2 \frac{\partial^2 T}{\partial x^2} + \frac{\partial^2 T}{\partial y^2} = 0 \quad \text{A-18}$$

No Liquid, No Convection, Constant Flux

For the case of no liquid, no convection and constant flux, the transport will now just be Fickian, and the pressure is constant. Therefore:

$$\varepsilon^2 \frac{\partial^2 u}{\partial x^2} + \frac{\partial^2 u}{\partial y^2} = 0, \quad \varepsilon^2 \frac{\partial^2 v}{\partial x^2} + \frac{\partial^2 v}{\partial y^2} = 0 \quad \text{A-19}$$

When examining the boundary conditions with constant pressure, the regions of positive and negative x are symmetric about $x = 0$. If the region from $-2 \leq x \leq 0$ is used, the boundary conditions are as follows:

$$\frac{\partial T^m}{\partial X}(0, Y) = 0 \quad , \quad \frac{\partial u^m}{\partial X}(0, Y) = 0 \quad , \quad \frac{\partial v^m}{\partial X}(0, Y) = 0 \quad \text{A-20}$$

At the cathode catalyst layer interface, constant flux is assumed. Oxygen flow out of the gas diffusion layer, therefore The water vapor and temperature fluxes are given by:

$$D_u \frac{\partial \tilde{u}}{\partial n} = -\tilde{q}_u \quad , \quad D_v \frac{\partial \tilde{v}}{\partial y}(\tilde{X}, 0) = -\tilde{q}_v \quad , \quad \tilde{k}_c \frac{\partial \tilde{T}}{\partial y}(\tilde{X}, 0) = -\tilde{q}_T \quad \text{A-21}$$

Substituting Equation A-18 into Equations A-29 through A-31:

$$D_u \frac{u_1}{h} \frac{\partial u}{\partial Y}(X, 0) = \tilde{q}_u \quad , \quad \frac{\partial u}{\partial Y}(X, 0) = q_u \varepsilon^2 \quad , \quad q_u \varepsilon^2 = \frac{q_u h}{D_u u_1} \quad \text{A-22}$$

$$D_u \frac{v_1}{h} \frac{\partial v}{\partial Y}(X, 0) = -\tilde{q}_v \quad , \quad \frac{\partial v}{\partial Y}(X, 0) = -q_v \varepsilon^2 \quad , \quad q_v \varepsilon^2 = \frac{q_v h}{D_u v_1} \quad \text{A-23}$$

$$\tilde{k}_c \frac{T_1 - T_m}{h} \frac{\partial T}{\partial Y}(X, 0) = -\tilde{q}_T \quad \text{A-24}$$

Using $\varepsilon = 0.2$ as the perturbation parameter, the dependent variable can be written as:

$$\Gamma(X, Y, \varepsilon) = T_0(X, Y) + 0(\varepsilon) \quad \text{A-25}$$

Now substituting Equation A-23 into A-38

$$\varepsilon^2 \frac{\partial^2 T}{\partial X^2} + \frac{\partial^2 T}{\partial Y^2} + 0(\varepsilon) = 0 \quad , \quad \frac{\partial^2 T}{\partial Y^2} = 0 \quad \text{A-26}$$

Using the following boundary conditions:

$$\frac{\partial T^m}{\partial X}(0, Y) = 0 \quad , \quad \frac{\partial T}{\partial Y}(X, 0) = -q_T \quad , \quad \frac{\partial T^1}{\partial X}(-2, Y) = 0 \quad \text{A-27}$$

Integrating and using the boundary conditions:

$$T_0 = -q_T Y + f(X) \quad , \quad F'(-2) = f'(0) = 0 \quad \text{A-28}$$

Now the problem has two different regions:

$$T_0^1(X, Y) = q_T(1 - Y) + 1 \quad -2 \leq X \leq -1 \quad \text{A-29}$$

$$T_0^m(X, Y) = q_T(1 - Y) \quad -1 \leq X \leq 0 \quad \text{A-30}$$

An interior layer variable is introduced to account for the discontinuity at

$$x = 0: \quad Z = \frac{X+1}{\varepsilon} \quad , \quad T(X, Y) = q_T(1 - Y) + T^i(Z, Y) \quad \text{A-31}$$

where T^i is the interior temperature. Substituting A-50 into A-23, A-37, and

$$\frac{\partial^2 T^i}{\partial Z^2} + \frac{\partial^2 T^i}{\partial Y^2} = 0 \quad , \quad T^i(Z, 1) = 1 \quad Z < 0 \quad , \quad T^i(Z, 1) = 0 \quad Z > 0 \quad \text{A-32}$$

Now matching the outer solution:

$$q_T(1 - Y) + T^i(-\infty, Y) = T^1(-1^-, Y) = q_T(1 - Y) + 1 \quad \text{A-34}$$

$$T^i(-\infty, Y) = 1$$

$$q_T(1 - Y) + T^i(-\infty, Y) = T^m(-1^+, Y) = q_T(1 - Y) \quad \text{A-35}$$

$$T^i(-\infty, Y) = 0$$

A set of transformations are now introduced:

$$f_1 = Z + iY \quad , \quad f_2 = \exp(u \cdot f_1) \quad , \quad f_3 = \frac{f_2 - 1}{f_2 + 1} \quad , \quad f_4 = \frac{1}{2} + \frac{1}{\pi} \text{Si}^{-1}(f_3) \quad \text{A-36}$$

The solution is then:

$$T^i = \Re f_4 \quad \text{A-37}$$

Modeling the diffusion layer

The derivation of the oxygen concentration is analogous to the temperature derivation

$$\frac{\partial^2 u_0}{\partial y^2} = 0 \quad \text{A-38}$$

For the left region:

$$\frac{\partial u^1}{\partial Y}(X, 0) = q_u \varepsilon^2 \quad \text{A-39}$$

Integrating once:

$$\frac{\partial u_0}{\partial y} = f(X) \quad \text{A-40}$$

Now the problem has two different regions:

$$T^1(X, Y) = 1 - q_u \varepsilon^2 (1 - Y) \quad -2 \leq X \leq -1 \quad \text{A-41}$$

$$u^m(X, Y, \varepsilon) = u_0^m(X, Y) - \varepsilon^2 u_2^m(X, Y) + o(1) \quad -1 \leq X \leq 0$$

$$\varepsilon^2 \frac{\partial^2 (u_0^m + u_2^m)}{\partial X^2} + \frac{\partial^2 (u_0^m + u_2^m)}{\partial Y^2} = 0 \quad , \quad \frac{\partial^2 (u_0^m)}{\partial Y^2} = 0 \quad , \quad \frac{\partial^2 (u_2^m)}{\partial Y^2}(X, 0) = q_u \quad \text{A-42}$$

Now matching the outer solution:

$$u_2^m(-1, Y) = 1 \quad , \quad u_0^m = f(X) \quad \text{A-43}$$

The boundary conditions are:

$$f_0(-1) = 1, f_0'(0) = 0$$

$$\frac{\partial^2 u_2^m}{\partial Y^2} = -f_0''(X) \quad , \quad \frac{\partial u_2^m}{\partial Y} = -f_0''(X)(Y - 1), \quad \frac{\partial u_2^m}{\partial Y}(X, 0) = f_0''(X) = q_u \quad \text{A-44}$$

Continuing to simplify:

$$f_0' = q_u X \quad , \quad u_0^m(X, Y) = f_0 = 1 - q_u \left(\frac{1 - X^2}{2} \right) \quad \text{A-45}$$

Substituting after integrating:

$$u_2^m(X, Y) = q_u \left(Y - \frac{Y^2}{2} \right) + f_2(X) \quad \text{A-46}$$

where $f_2(x)$ is determined from the next order in the perturbation expansion. If $\varepsilon \rightarrow 0$ in the solutions, then:

$$u(X, Y) = 1 + \varepsilon u^i(Z, Y) \quad \text{A-47}$$

Taking $\varepsilon \rightarrow 0$, and substituting A-72 into A-24 and A-33:

$$\frac{\partial^2 u^i}{\partial Z^2} + \frac{\partial^2 u^i}{\partial Y^2} = 0 \quad \text{A-48}$$

Now matching the outer solution:

$$\frac{\partial u^i}{\partial z}(z, Y) = -q_u$$

A-49

The solutions for water vapor concentration are again analogous to those computed for T and u:

$$V^1(X, Y) = 1 + q_u \varepsilon^2 (1 - Y) \quad -2 \leq X \leq -1$$

$$V^m(X, Y, \varepsilon) = V_0^m(X, Y) + V_2^m(X, Y) + O(1) \quad -1 \leq X \leq 0$$

$$v_0^m(X, Y) = 1 - q_v \left(\frac{1 - X^2}{2} \right) \quad \text{A-50}$$

$$v_2^m(X, Y) = q_v \left(Y - \frac{Y^2}{2} \right) + g_2(X)$$

$$V(X, Y) = 1 + \varepsilon V^1(Z, Y)$$

$$\frac{\partial^2 v^i}{\partial z^2} + \frac{\partial^2 v^i}{\partial Y^2} = 0$$

A-51

$$\frac{\partial v^i}{\partial Y}(z, 0) = 0$$

A-52

To determine the regions that are oversaturated, the following variable needs to be defined:

If

$S > 0$, liquid water will be present.

$$S(v, T) = \frac{v - v_{sat}(T)}{v_{sat}(T)}$$

A-53



University of Moratuwa, Sri Lanka.
Electronic Theses & Dissertations
www.lib.mrt.ac.lk

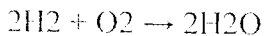
APPENDIX – B : Useful Fuel Cell Equations

B1.1 Introduction

In this appendix, many useful equations are derived. They relate to

- Oxygen usage rate
- Air inlet flow rate
- Air exit flow rate
- Hydrogen usage, and the energy content of hydrogen
- Rate of water production
- Heat production.

In many of the sections that follow, the term *stoichiometric* is used. Its meaning could be defined as 'just the right amount'. So, for example, in the simple fuel cell reaction



exactly two moles of hydrogen would be provided for each mole of oxygen. This would produce exactly $4F$ of charge, since two electrons are transferred for each mole of hydrogen. Note that either or both the hydrogen and oxygen are often supplied at greater than the stoichiometric rate. This is especially so for oxygen if it is being supplied as air. If it was supplied at exactly the stoichiometric rate, then the air leaving the cell would be completely devoid of oxygen. Note also that reactants cannot be supplied at *less* than the stoichiometric rate. This stoichiometry can be expressed as a variable, and the symbol λ is normally used. Its use can be put like this. If the rate of *use* of a chemical in a reaction is n moles per second, then the rate of *supply* is λn moles per second. To increase the usefulness of the formulas, they have been given in terms of the electrical power of the whole fuel cell stack P_e , and the average voltage of each cell in the stack V_c . The electrical power will nearly always be known, as it is the most basic and important information about a fuel cell system. If V_c is not given, it can be assumed to be between 0.6 and 0.7 V, as most fuel cells operate in this region. If the efficiency is given, then V_c can be calculated using equation 2.5. If no figures are given, then using $V_c = 0.65\text{V}$ will give a good approximation. Estimate somewhat higher if the fuel cell is pressurised.

B1.2 Oxygen and Air Usage

From the basic operation of the fuel cell, we know that four electrons are transferred for each mole of oxygen.

So charge = $4F \times$ amount of O_2

Dividing by time, and rearranging

$$\text{O}_2 \text{ usage} = I / 4F \text{ moles s}^{-1}$$

This is for a single cell. For a stack of n cells

$$\text{O}_2 \text{ usage} = In / 4F \text{ moles s}^{-1}$$

B -1

However, it would be more useful to have the formula in kg s^{-1} , without needing to know the number of cells, and in terms of power, rather than current. If the voltage of each cell in the stack is V_c , then

$$\text{Power, } P_e = V_c \times I \times n$$

So,

$$I = P_e / V_c \times n$$

Substituting this into equation A2.1 gives

$$\text{O}_2 \text{ usage} = Pe / 4 \cdot V_c \cdot F \text{ moles s}^{-1} \quad \text{B-2}$$

Changing from moles s⁻¹ to kg s⁻¹

$$\begin{aligned} \text{O}_2 \text{ usage} &= 32 \times 10^{-3} \cdot Pe / 4V_cF \text{ kg s}^{-1} \\ &= 8.29 \times 10^{-8} \times Pe / V_c \text{ kg s}^{-1} \end{aligned} \quad \text{B-3}$$

This formula allows the oxygen usage of any fuel cell system of given power to be calculated. If V_c is not given, it can be calculated from the efficiency, and if that is not given, the figure of 0.65V can be used for a good approximation. However, the oxygen used will normally be derived from air, so we need to adapt equation A2.2 to air usage. The molar proportion of air that is oxygen is 0.21, and the molar mass of air is 28.97×10^{-3} kg mole⁻¹. So, equation A2.2 becomes

$$\begin{aligned} \text{Air usage} &= 28.97 \times 10^{-3} \times Pe / 0.21 \times 4 \times V_c \times F \text{ kg s}^{-1} \\ &= 3.57 \times 10^{-7} \times Pe / V_c \text{ kg s}^{-1} \end{aligned}$$

However, if the air was used at this rate, then as it left the cell it would be completely devoid of any oxygen – it would all have been used. This is impractical, and in practice the airflow is well above stoichiometry, typically twice as much. If the stoichiometry is λ , then the equation for air usage becomes,

$$\text{Air usage} = 3.57 \times 10^{-7} \times \lambda \times Pe / V_c \text{ kg s}^{-1} \quad \text{B-4}$$

The kilogram per second is not, in fact, a very commonly used unit of mass flow. The following conversions to 'volume at standard conditions related' mass flow units will be found useful. The mass flow rate from equation A2.4 should be multiplied by

- 3050 to give flow rate in standard m³ h⁻¹
- 1795 to give flow rate in SCFM (or in standard ft³ min⁻¹)
- 5.1×10^4 to give flow rate in slm (standard Lmin⁻¹)
- 847 to give flow rate in sls (standard L s⁻¹)

APPENDIX- C: MAT-Lab Programs for Modeling and simulation of PEMFC

C-1 Calculating the Voltage Losses for a Polarization Curve

```
Inputs
R = 8.314;           % Ideal gas constant (J/molK)
F = 96487;          % Faraday's constant (Coulombs)
Tc = 80;            % Temperature in degrees C
P_H2 = 3;           % Hydrogen pressure in atm
P_air = 3;          % Air pressure in atm
A_cell=100;         % Area of cell
N_cells=90;        % Number of Cells
r = 0.19;           % Internal Resistance (Ohm-cm^2)
Alpha = 0.5;        % Transfer coefficient
Alpha1 = 0.085;    % Amplification constant
io = 10^-6.912;     % Exchange Current Density (A/cm^2)
il = 1.4;           % Limiting current density (A/cm2)
Gf_liq = -228170;   % Gibbs function in liquid form (J/mol)
k = 1.1;           % Constant k used in mass transport

% Convert degrees C to K
Tk = Tc + 273.15;

% Create loop for current
loop = 1;
i = 0;
for N = 0:150
    i = i + 0.01;

    % Calculation of Partial Pressures
    % Calculation of saturation pressure of water
    x = -2.1794 + 0.02953 .*Tc-9.1837 .* (10.^-5) .* (Tc.^2) + 1.4454 .* (10.^-7) .* (Tc.^3);
    P_H2O = (10.^x)
    % Calculation of partial pressure of hydrogen
    pp_H2 = 0.5 .* ((P_H2)./(exp(1.653 .* i ./ (Tk.^1.334)))) - P_H2O;
    % Calculation of partial pressure of oxygen
    pp_O2 = (P_air ./ exp(4.192 .* i / (Tk.^1.334))) - P_H2O;
    % Activation Losses
    b = R .* Tk ./ 2 .* Alpha .* F;
    V_act = -b .* log10(i./io); % Tafel equation
    % Ohmic Losses
    V_ohmic = -(i .* r);
    % Mass Transport Losses
    term = (i - (i./il));
    if term > 0
        V_conc = Alpha1 .* (i.^k) .* log(1 - (i./il));
    else
        V_conc = 0;
    end

    % Calculation of Nernst voltage
    E_nernst = -Gf_liq ./ (2 .* F) - ((R .* Tk) .* log(P_H2O ./ (pp_H2 .* (pp_O2.^0.5)))) ./ (2 .* F)
    % Calculation of output voltage
    V_out = E_nernst + V_ohmic + V_act + V_conc;
    if term < 0
        V_conc = 0;
    break
end
if V_out < 0
    V_out = 0;
    break
end

figure(1)
title('Fuel cell polarization curve')
xlabel('Current density (A/cm^2)');
ylabel('Output voltage (Volts)');
plot(i,V_out,'*')
grid on
hold on
disp(V_out)
% Calculation of power
P_out = N_cells .* V_out .* i .* A_cell;
```

```

figure(2)
title('Fuel cell power');
xlabel('Current density (A/cm^2)');
ylabel('Power (Watts)');
plot(i,P_out,'*');
grid on
hold on
disp(P_out);
end

```

C-2 Modeling the Catalyst Layer

```

% Handling homogeneous reactions
% Parameters
F = 96487; % Faraday's constant
R = 8.31434; % Ideal gas constant
E0 = 83.1434; % Ideal gas constant
T = 340.15; % Temperature (K)
Tc = T - 273.15; % Temperature (degrees C)
Psi_O2_agg = 1.5e-11; % O2 permeation in agglomerate
Psi_H2_agg = 2e-11; % H2 permeation in agglomerate
R_agg_an = 110e-5; % Agglomerate radius in anode
R_agg_cat = 110e-5; % Agglomerate radius in cathode
P_gas = 1; % Total gas pressure
P_H2 = 1; % Hydrogen pressure in atm
P_air = 1; % Air pressure in atm
S = 0.6e-12; % Saturation
x_O2_g = 0.21; % Mole fraction of O2 in the gas phase
x_H2_g = 1; % Mole fraction of H2 in the gas phase
alpha_a = 1; % Anode transfer coefficient
alpha_c = 0.9; % Cathode transfer coefficient
R_ohm = 0.02; % Constant ohmic resistance (ohm-cm^2)
I_l = 1.4; % Limiting current density (A/cm2)
k = 1.1; % Constant k used in mass transport
Alpha1 = 0.085; % Amplification constant
S1_liq = -228170; % Gibbs function in liquid form (J/mol)
a1Fv = 10000; % Electrode specific interfacial area (1/cm)
v01 = 0.01:1:2; % Voltage
i = 0:0.01:1.2; % Current Density (A/cm^2)

% Calculation of Partial Pressures
% Calculations of saturation pressure of water
P_H2O = (10.^x);
P_H2O = (10.^x);

% Calculation of partial pressure of hydrogen
p_H2 = 0.5 .* ((P_H2)./(exp(1.653 .* 1./(T.^1.334)))-P_H2O);
% Calculation of partial pressure of oxygen
p_O2 = (P_air./exp(4.192 .* 1/(T.^1.334)))-P_H2O;

% Reaction 1: H2O generation as liquid
% Exchange current density (A/cm^2)
i_0r = 1.0e-7 .* exp((73269./R) .* ((1./303)-(1./T)));
% Kinetic portion of the Thiele modulus
k_O2 = a120 .* i_0r ./ (4 .* F) .* exp(((1-alpha_c) .* F) ./ (R .* T)) .* (-volt));
% Thiele modulus
phi_O2 = R_agg_cat .* sqrt(k_O2 ./ Psi_O2_agg);
% Effectiveness factor due to mass transfer & reaction
E_O2 = 3 ./ phi_O2.^2 .* (phi_O2 ./ tanh(phi_O2) - 1);
% Reaction rate of liquid water at cathode catalyst layer
rate_rx_H2O1 = k_O2 .* x_O2_g .* P_gas .* (1 - S) .* E_O2;

% Reaction 2: Hydrogen oxidation
% Exchange current density (A/cm^2)
i_0h = 1e-3 .* exp((9500./R) .* ((1./303)-(1./T)));
% Kinetic portion of the Thiele modulus
k_h = a120 .* i_0h ./ (2 .* F) .* exp((alpha_a .* F) ./ (R .* T) .* volt);
% Thiele modulus
phi_H2 = R_agg_an .* sqrt(k_h ./ Psi_H2_agg);
% Effectiveness factor due to mass transfer & reaction
E_H2 = 3 ./ phi_H2.^2 .* (phi_H2 ./ tanh(phi_H2) - 1);
i_h = exp(-(alpha_c .* F) ./ (R .* T)) .* exp((alpha_a .* F) ./ (R .* T) .* volt);
% Reaction rate of hydrogen at anode catalyst layer
rate_rx_H2 = k_h .* (x_H2_g .* P_gas - i_h) .* (1 - S) .* E_H2;

% Calculate activation losses from Butler-Volmer equation
% Activation loss at the anode

```

```

% Activation loss at the anode
V_act_anode = log(i./(-alpha_a .* alpha_a)) .* E0 .* log(i./(-beta_a .* alpha_a .* (1 - S) .* x_H2_g .* P_gas));
% Activation loss at the cathode
V_act_cathode = log(i./(-alpha_c .* (1 - S) .* i_ox .* (x_O2_g .* P_gas))) .* ((R .* T)/(-alpha_c .* F));
% Total activation loss
V_act = V_act_anode + V_act_cathode;
% Ohmic losses
V_ohmic = -i .* R_ohm;
% Mass Transport Losses
term = (1-(i./i1));
if term > 0
V_loss = Alpha .* (L.*R) .* log(1-(i./i1));
else
V_loss = 0;
end
% Calculation of Neinst voltage
E_neinst = -Gf_liq./(2 .* F)-((R .* T) .* log(P_H2O./(pp_H2 .* (pp_O2.^0.5))))./(2 .* F)
% Calculation of output voltage
V_out = E_neinst + V_ohmic + V_act + V_loss;
if term < 0
V_out = 0;
end
if V_out < 0
V_out = 0;
end
% Plot the cell current versus the effectiveness factor
figure1 = figure('Color',[1 1 1]);
subplot(1,E_O2,1,E_H2);
title('Cell Current vs. Effectiveness Factor','FontSize',14,'FontWeight','Bold');
xlabel('Cell Current (A/cm^2)','FontSize',12,'FontWeight','Bold');
ylabel('Effectiveness Factor','FontSize',12,'FontWeight','Bold');
set(hdip,'LineWidth',1.5);
hold on;
% Plot the cell current versus voltage
figure2 = figure('Color',[1 1 1]);
subplot(1,V_act);
title('Cell Current vs. Voltage','FontSize',14,'FontWeight','Bold');
xlabel('Cell Current (A/cm^2)','FontSize',12,'FontWeight','Bold');
ylabel('Voltage (Volts)','FontSize',12,'FontWeight','Bold');
set(hdip,'LineWidth',1.5);
hold on;
% Plot the polarization curve
figure3 = figure('Color',[1 1 1]);
subplot(1,V_out);
title('Cell Current vs. Voltage','FontSize',14,'FontWeight','Bold');
xlabel('Cell Current (A/cm^2)','FontSize',12,'FontWeight','Bold');
ylabel('Voltage (Volts)','FontSize',12,'FontWeight','Bold');
set(hdip,'LineWidth',1.5);
hold on;
% Plot the flux density of hydrogen
figure4 = figure('Color',[1 1 1]);
subplot(1,rate_rx_H2);
title('Superficial flux density of hydrogen','FontSize',14,'FontWeight','Bold');
xlabel('Cell Current (A/cm^2)','FontSize',12,'FontWeight','Bold');
ylabel('Flux density of H2 (mol/cm^2-s)','FontSize',12,'FontWeight','Bold');
set(hdip,'LineWidth',1.5);
hold on;

```

C-3 The Ohmic Voltage Loss with Different Fuel Cell

```

% Inputs
i = 0.1; % Current Density (A/cm^2)
A1 = 10; % Area 1 (cm^2)
R1 = 0.05; % Resistance (ohms)
A2 = 40; % Area 2 (cm^2)
R2 = 0.02; % Resistance (ohms)
% Part a: Ohmic voltage losses for first fuel cell size
ASR1 = R1 .* A1;
% Calculate the ohmic voltage loss
V_ohm1 = i .* ASR1;
% Calculate the total current
I1 = i .* A1;

```

```

    Calculate the ohmic voltage loss
    V_ohm1a = i .* R1
    Part b: Ohmic voltage losses for second fuel cell size
    ASR2 = R2 .* A2;
    Calculate the ohmic voltage loss
    V_ohm2 = i .* ASR2;
    Calculate the total current
    I2 = i .* A2;
    Calculate the ohmic voltage loss
    V_ohm1b = I2 .* R1
    Part c:
    A = 1:100;
    ASR = R1 .* A;
    Calculate the ohmic voltage loss
    V_ohm = i .* ASR;
    Calculate the total current
    I = i .* A;
    Calculate the ohmic voltage loss
    V_ohm = I .* R1

    Plot of the ohmic losses as a function of fuel cell area
    figure1 = figure('Color',[1 1 1]);
    hold on;
    plot(A,V_ohm);
    title('Ohmic Loss as a Function of Fuel Cell Area','FontSize',14,'FontWeight','Bold');
    xlabel('Fuel Cell Area (cm^2)','FontSize',12,'FontWeight','Bold');
    ylabel('Ohmic Loss (V)','FontSize',12,'FontWeight','Bold');
    set(h,'LineWidth',1.5);
    grid on;

```

C-4 The Entropy of H₂, O₂, and Water

```

% Inputs
R = 8.314 % Ideal Gas Constant
T = 300 : 50 : 1000 % Temperature range from 300 K to 1000 K with increments of 50

% Create Temperature Loop
i = 0; % Initialization of loop variable
for T = 300 : 50 : 1000; % Temperature range from 300 K to 1000 K with increments of 50
    i = i + 1; % Loop variable

    % Enthalpy Calculations
    % hydrogen entropy calculations
    sf_h = 130.57;
    st_h = log(24.42) + 22.26E-3 * (T - 298) - 24.2E-6 * (T^2 - 298^2) + 15.3E-9 * (T^3 - 298^3)
    + 3.78E-12 * (T^4 - 298^4);
    S_hydrogen = (sf_h + st_h);

    % oxygen entropy calculations
    sf_o = 205.03;
    st_o = log(30.15) - 15.6E-3 * (T - 298) + 29.33E-6 * (T^2 - 298^2) - 18.7E-9 * (T^3 - 298^3)
    + 4.48E-12 * (T^4 - 298^4);
    S_oxygen = (sf_o + st_o);

    % water entropy calculations
    sf_w = 188.72;
    st_w = log(33.84) - 9.216E-3 * (T-298) + 17.26E-6 * (T^2-298^2) - 8.21E-9 * (T^3-298^3) +
    1.67E-12 * (T^4-298^4);
    S_water = (sf_w + st_w);

    % Create new variables to save the new calculated values for hydrogen, oxygen and water
    % entropy at each temperature increment
    Hydrogen_Entropy(i) = S_hydrogen;
    Oxygen_Entropy(i) = S_oxygen;
    Water_Entropy(i) = S_water;
    Temperature(i) = T;
end % End Loop

```

The following MATLAB code can be used to plot the hydrogen and oxygen enthalpy as a function of temperature:

```

figure1 = figure('Color',[1 1 1]);
hold on;
plot(Temperature,Hydrogen_Entropy,Temperature,Oxygen_Entropy,Temperature,Water_Entropy);
title('Hydrogen, Oxygen and Water Entropies','FontSize',12,'FontWeight','Bold');
xlabel('Temperature (K)','FontSize',12,'FontWeight','Bold');
ylabel('Entropies (KJ/kgK)','FontSize',12,'FontWeight','Bold');

```

```
set(halp,'linewidth',1.5);
axis on;
```

C-5 FUELCELLHEAT Fuel cell stack heat transfer model

```
function [t,T] = fuelcellheat
% Best viewed with a monospaced font with 4 char tabs.
% Constants
const.tfinal = 60; % Simulation time (s)
const.N = 7; % Number of layers
const.T_0 = 350; % End plate temperature
const.T_end = 350; % End plate temperature
const.T_in = 298.15; % Initial temperature (K)
const.h_surr = 17; % Convective loss from stack
% Layers
% 1 ? Left end plate
% 2 ? Rubber gasket
% 3 ? Anode Flow Field (Stainless steel)
% 4 ? MEA
% 5 ? Cathode Flow Field (Stainless steel)
% 6 ? Rubber gasket
% 7 ? Right end plate
% Layer parameters
% 1 2 3 4 5 6 7
% Number of temperature slices within layer (can be changed to as many slices as necessary)
param.M = [10, 4, 2, 2, 2, 4, 10]; % Density (kg/m^3)
param.Sen = [1300, 1400, 8000, 1300, 9000, 1400, 1300]; % Area (m^2)
param.A = [0.0064, 0.001704, 0.003385, 0.0016, 0.003385, 0.001704, 0.0064]; % Thickness (m)
param.thick = [0.011, 0.001, 0.0005, 0.001, 0.0005, 0.001, 0.011]; % Thermal Conductivity (W/m-K)
param.k = [0.2, 1.26, 65, 26, 65, 1.26, 0.2]; % Specific heat capacity (J/Kg-k)
param.Cp = [1200, 1000, 500, 864, 500, 1000, 1200];

% Create 1D temperature slices (M temps per layer).
% The temperatures are at the center of each slice.
% x is at the edge of each slice (like a stair plot).
x = 0;
layer = [];
for i=1:const.N,
x = [x, x(end) + (1:param.M(i)) * param.thick(i)/param.M(i)]; % Boundary Points
layer = [layer, i * ones(1,param.M(i))];
end
x = [-x(1), x]; % Add left hand heating block position (same width as first slice)
% Last point x(end) is the position of the right hand heating block
% Slice thicknesses
dx = diff(x); % Gives approximate derivatives between x's

% Heat transfer parameter (W/m^2-K)
left = 2:length(dx)-1;
center = 3:length(dx);
right = 3:length(dx);
layer = [0, layer];
param.U_left = [0, 1 ./ (dx(center) ./ (1* param.k(layer(center))) + dx(left) ./ (1* param.k(layer(left))))];
param.U_right = [ 1 ./ (dx(center-1) ./ (1* param.k(layer(center-1))) + dx(right) ./ (1* param.k(layer(right)))) , 0];
param.U_left(1) = 1 ./ (dx(1) ./ (1* param.k(1)) + 1/const.h_surr);
param.U_right(end) = 1 ./ (dx(end) ./ (1* param.k(end)) + 1/const.h_surr);
layer = layer(2:end);

% Define temperature matrix
T = const.T_in * ones(size(x)); % Preallocate output
T(1) = const.T_0; % Left hand end plate temperature
T(end) = const.T_end; % Right hand end plate temperature
options = odeset('OutputFcn',@(t,y,opt) heatplot(t,y,opt,x));
[T,T] = ode45(@(t,T) heat(t,T,x,layer,param,const), [linspace(0,const.tfinal,100)], T,options);
end % of function

function dTdt = heat(t,T,x,layer,param,const)
% Heat transfer equations for fuel cell
% Make a convenient place to set a breakpoint
if (t > 30)
n = 1;
```

```

end

d1 = diff(T); % Gives approximate derivatives between T's
dx = diff(x); % Gives approximate derivatives between x's
Q_left = -dT(1:end-1);
Q_right = dT(2:end);
dx = dx(2:end);

% Choose energy balance terms
Q_right = param.U_right .* param.A(layer) .* dT_right';
Q_left = param.U_left .* param.A(layer) .* dT_left';
mass = param.den(layer) .* param.A(layer) .* param.Cp(layer) .* dx;

% Combine into rate of change of T
dTdt = (Q_left + Q_right) ./ (mass);
dTdt = [0;dTdt(:);0];
end % of function

function status = heatplot(t,y,opt,x)
if isempty(opt)
stairs(x,y), title(['t = ',num2str(t)])
status = 0;
drawnow
end % of function

```

C-6 Modeling the Temperature in the Interior Layer

```

% UnitSystem SI
% use all
% use
format rat

% Define the parameters
eps = 0.5; % Perturbation Parameter
% Define the number of grid points in x and y direction
nx = number of grid points in x direction
ny = number of grid points in y direction
Lx = 10;
Ly = 20;

% Define the dimension of the domain
Lx = 1.0; % Length in x of the computation region
Ly = 1.0; % Length in y of the computation region

% Calculate the mesh size
hx = Lx/(nx-1); % Grid spacing in x
hy = Ly/(ny-1); % Grid spacing in y

% Generate the mesh/grid
x(1) = -1.8;
y(1) = 0.0;
for k = 2:nx
x(k) = x(k-1)+hx;
end
for j = 2:ny
y(j) = y(j-1)+hy;
end
% Inner Layer Variable
z = (x+1.0)/eps;
[Z,Y] = meshgrid(z,y);

% Now determine the functions
f1 = complex(Z,Y);
f2 = exp(pi * f1);
f3 = (f2-1.0)/(f2+1.0);
f4 = (1.0/2.0)-(1.0/pi) * (asin(f3));

% Inner Variable
t1 = real(f4);
% Make a 3D plot of T1
figure
surf(Z,Y,t1,'EdgeColor','none')
set(gca,'DataAspectRatio',[1 1 1])
axis([-4.0 4.0 0 1 0 1])
zaxis('z')
xlabel('x')
ylabel('y')

```

```

    subplot(2,1,1)
    print -djpeg Tinteriorlayer

```

Modeling the Gas Diffusion Layer

```

UnitSystem SI
all
clear all
format long e

% Define the parameters
eps = 0.1; % Perturbation Parameter
% Define the number of grid points in x and y direction
nx = number of grid points in x direction
ny = number of grid points in y direction
nx = 101;
ny = 65;

% SOR parameters
omega = 1.4; % SOR parameter
t = (2.0 * cos(pi/(nx * ny)))^2;
% Calculate a optimum value of SOR parameter
omega1 = (16.0+sqrt((256.0-(64.0 * t))))/(2.0 * t);
omega2 = (16.0-sqrt((256.0-(64.0 * t))))/(2.0 * t);
lopt = min(omega1,omega2)
if (lopt <= 1.0) || (lopt >= 2.0 )
    lopt = 1.0;
end
omega = lopt;

% Define the dimension of the domain
lx = 2.0; % Length in x of the computation region
ly = 1.0; % Length in y of the computation region
% Calculate the mesh size
hx = lx/(nx-1); % Grid spacing in x
hy = ly/(ny-1); % Grid spacing in y

% Generate the mesh/grid
x(1) = 0.0;
x(2) = 0.0;
for i = 1:nx
    x(i) = x(i-1)+hx;
end
for j = 1:ny
    Y(j) = y(j-1)+hy;
end

% Solve the Temperature equation
% Initialize the temperature field as zero
T = zeros(nx,ny);
% Max-Norm on Error (L-inf Error) Initialized
Error = 1.0;
iteration = 0;
while (Error > 1.0e-5)
    iteration = iteration+1;
    % Store the old values of T in Told
    Told = T;
    % Apply the boundary conditions
    for i = 1:nx
        % BC for the bottom boundary
        T(i,1) = T(i,2)+hy;
        % BC for the top boundary
        if (x(i) <= 0 )
            T(i,ny) = 1;
        else
            T(i,ny) = 0;
        end
    end
    for j = 1:ny
        % BC for the Left boundary
        T(1,j) = T(2,j);
        % BC for the Right boundary
        T(nx,j) = T(nx-1,j);
    end

    % Now compute the interior domain using 2nd order finite difference
    for i = 2:nx-1
        for j = 2:ny-1
            term1 = ((eps/hx)^2) * (T(i-1,j)+T(i+1,j));
            term2 = ((1.0/hy)^2) * (T(i,j-1)+T(i,j+1));

```



```

uold = zeros(nx,ny);
u = 2.0 * ((eps/hx)^2 * ((1.0/hy)^2));
num = num/den;
T(i,j) = (omega * Tgs) + ((1.0-omega) * Told(i,j));
end
end

% Calculate the error
err = abs(T-Told);
Linf = norm(err,2);

% Print the convergence history every 100 iterations
fprintf('round(iteration/100)-(iteration/100);
if (iteration == 1) || (ccheck == 0)
fprintf(' %d \t %e \n', iteration, Linf)
end
end

% Plot the solutions
figure
[X,Y] = meshgrid(x,y);
clevel = [-1 -0.005 0 0.053 0.152 0.252 0.352 0.451 0.551 0.65 0.75 0.949 1.049 1.148 1.248
1.348 1.447 1.547 1.646 1.746 1.848 1.945 2.0 3.0];
contourf(X',Y',T,clevel)
colorbar
axis([-1.2 1.2 -0.8 1.8])
xlabel(' x ')
ylabel(' y ')
zlabel(' T(x,y) ')
hold on
ys = [0:0.01:1];
xs = zeros(length(ys));
plot(xs,ys,'black');
print -djpeg figures\chap4\temperature4

% Save data to a file
save data\chap4\Temp.dat T -ASCII -DOUBLE

% Solve the Oxygen concentration equation
omega = 1.0; % SOR parameter
% Initialize the oxygen concentration field as zero
u = zeros(nx,ny);
% Max-Norm on Error (l1-inf Error) initialized
Linf = 1.0;
iteration = 0;
while (Linf > 1.0e-5)
iteration = iteration+1;
% Store the old values of T in Told
uold = u;
% Apply the boundary conditions
for i = 1:nx
% BC for the bottom boundary
u(i,1) = u(i,2) - (1.81 * (eps^2) * hy);
% BC for the top boundary
if (x(i) <= 0)
u(i,ny) = 1;
else
u(i,ny) = u(i,ny-1);
end
end
for j = 1:ny
% BC for the Left boundary
u(1,ny-j) = 1;
% BC for the Left boundary
u(nx,j) = u(nx-1,j);
end

% Now compute the interior domain using 2nd order fi nite difference
for i = 2:nx-1
for j = 2:ny-1
term1 = ((eps/hx)^2) * (u(i-1,j)+u(i+1,j));
term2 = ((1.0/hy)^2) * (u(i,j-1)+u(i,j+1));
num = term1+term2;
den = 2.0 * ((eps/hx)^2)+((1.0/hy)^2);
u(i,j) = (omega * ugs) + ((1.0-omega) * uold(i,j));
end
end

% Calculate the error
err = abs(u-uold);
Linf = norm(err,2);

```



```

    Plot the convergence history every 100 iterations
    check = round(iteration/100)-(iteration/100);
    if ( iteration == 1 )
        handle = figure;
        hold on;
    end
    if (check == 0)
        title('Plot of T vs \n', iteration, Linf)
        plot(iteration,Linf,'b-',iteration,Linf,'r.')
        hold on;
    end
    axis([0,100,0,1]);
    xlabel('Iteration');

    Plot the solutions
    hold on;
    [X,Y] = meshgrid(x,y);
    clevel = [-1 -0.5 -0.087 -0.031 0 0.025 0.08 0.136 0.192 0.247 0.303 0.359 0.415 0.47 0.526
              0.583 0.638 0.693 0.749 0.805 0.86 0.916 0.972 1 3.0];
    contour(X',Y',u,clevel)
    hold on;
    [xi, yi] = mesh(-1.2:1.2,-0.6:1.8);
    xlabel('x');
    ylabel('y');
    title('u(x,y)');
    hold on;
    [xi, yi] = mesh(-10:10,0:1);
    [v] = zeros(length(yi));
    plot(xi,yi,'black');
    print -djpeg figures\chap4\oxygen-concentration4
    Save data to a file save data\chap4\oxygen.dat u -ASCII -DOUBLE
    Solve the Water vapor concentration equation
    Initialize the water vapor concentration field as zero
    [nx,ny] = zeros(nx,ny);
    Max-Norm on Error (L-inf Error) Initialized
    [err] = 1.0;
    iteration = 0;
    while (Linf > 1.0e-5)
        iteration = iteration+1;
        Store the old values of T in Told
        [vold] = v;
        Apply the boundary conditions
        [v] = vold;
        % For the bottom boundary
        [v(i,2)] = (0.755 * (eps^2) * hy);
        % For the top boundary
        [v] = vold;
        [v] = vold;
        [v] = vold;
        % For the left boundary
        [v(2,j)] = vold(2,j);
        % For the right boundary
        [v(nx,j)] = vold(nx,j);
    end

    Now compute the interior domain using 2nd order finite difference
    for i = 2:nx-1
        for j = 2:ny-1
            term1 = ((eps/hx)^2) * (v(i-1,j)+v(i+1,j));
            term2 = ((1.0/hy)^2) * (v(i,j-1)+v(i,j+1));
            num = term1+term2;
            den = 2.0 * ((eps/hx)^2)+((1.0/hy)^2);
            vgs = num/den;
            [v(i,j)] = (omega * vgs)+((1.0-omega) * vold(i,j));
        end
    end

    Calculate the error
    [err] = abs(v-vold);
    [Linf] = norm(err,2);

    Plot the convergence history every 100 iterations
    check = round(iteration/100)-(iteration/100);
    if ( iteration == 1 )
        handle = figure;

```



```

clear all
close all
figure('Name','Iteration', iteration, Linf)
title('Iteration,Linf','b-',iteration,Linf,'c. ');
axis on
hold off
hold on
axis(figurehandle);

%Plot the solutions
figure
[X,Y] = meshgrid(x,y);
clevel = [0. 1. 1.012 1.035 1.058 1.082 1.105 1.128 1.152 1.175 1.198 1.222 1.245 1.268
1.291 1.315 1.338 1.361 1.385 1.408 1.431 3.0];
contourf(X',Y',v,clevel)
colorbar
axis([-1.2 1.2 -0.8 1.8])
xlabel('x ')
ylabel('y ')
zlabel(' v(x,y) ');
hold on
yi = [0:0.01:1];
xi = zeros(length(yi));
plot(xi,yi,'black')
print -djpeg fi gures\chap4\watervapor-concentration4
% Save data to a file
save data\chap4\watervapor.dat v -ASCII -DOUBLE
% Calculate the water vapor saturation
% and the S variable from equation 4.40
for i = 1:nx
for j = 1:ny
term1 = 710.0/((2.0 * T(i,j))+353.0);
term2 = (7.87e-2) * T(i,j);
term3 = (5.28e-4) * (T(i,j)^2);
term4 = (2.65e-6) * (T(i,j)^3);
wsat(i,j) = term1 * (exp((-0.869+term2-term3+term4)));
S(i,j) = (v(i,j)-wsat(i,j))/wsat(i,j);
end
end
%Plot the solutions
figure
[X,Y] = meshgrid(x,y);
clevel = [-1. 0 0.045 0.07 0.105 0.134 0.167 0.2 0.233 0.266 0.299 0.332 0.365 0.397 0.43
0.468 0.498 0.529 0.562 0.595 0.628 0.661 0.694 0.711 1.0];
contourf(X',Y',S,clevel)
colorbar
axis([-1.2 1.2 -0.8 1.8])
xlabel('x ')
ylabel('y ')
zlabel(' S(v,T) ');
hold on
yi = [0:0.01:1];
xi = zeros(length(yi));
plot(xi,yi,'black')
print -djpeg fi gures\chap4\saturation4

```



C-7 Out put of the Pressure drop in FC channel

```

P = (Pascal)
1.0e+004 *
Columns 1 through 9
    8.2308    2.6577    0.9145    0.5144    0.3292    0.2286    0.1680    0.1286    0.1016
Columns 10 through 18
    0.0823    0.0680    0.0572    0.0487    0.0420    0.0366    0.0322    0.0285    0.0254
Columns 19 through 27
    0.0228    0.0206    0.0187    0.0170    0.0156    0.0143    0.0132    0.0122    0.0113

```

Columns 26 through 36

0.0105	0.0098	0.0091	0.0086	0.0080	0.0076	0.0071	0.0067	0.0064
--------	--------	--------	--------	--------	--------	--------	--------	--------

Columns 37 through 45

0.0060	0.0057	0.0054	0.0051	0.0049	0.0047	0.0045	0.0043	0.0041
--------	--------	--------	--------	--------	--------	--------	--------	--------

Columns 46 through 50

0.0039	0.0037	0.0036	0.0034	0.0033
--------	--------	--------	--------	--------

P_atm = Converted from Pa to atm

1.0e+004 *

Columns 1 through 9

8.1232	2.0308	0.9026	0.5077	0.3249	0.2256	0.1658	0.1269	0.1003
--------	--------	--------	--------	--------	--------	--------	--------	--------

Columns 10 through 18

0.0812	0.0671	0.0564	0.0481	0.0414	0.0361	0.0317	0.0281	0.0251
--------	--------	--------	--------	--------	--------	--------	--------	--------

Columns 19 through 27

0.0225	0.0203	0.0184	0.0168	0.0154	0.0141	0.0130	0.0120	0.0111
--------	--------	--------	--------	--------	--------	--------	--------	--------

Columns 28 through 36

0.0104	0.0097	0.0090	0.0085	0.0079	0.0075	0.0070	0.0066	0.0063
--------	--------	--------	--------	--------	--------	--------	--------	--------

Columns 37 through 45

0.0059	0.0056	0.0053	0.0051	0.0048	0.0046	0.0044	0.0042	0.0040
--------	--------	--------	--------	--------	--------	--------	--------	--------

Columns 46 through 50

0.0038	0.0037	0.0035	0.0034	0.0032
--------	--------	--------	--------	--------



University of Moratuwa, Sri Lanka.
Electronic Theses & Dissertations
www.lib.mrt.ac.lk